View metadata, citation and similar papers at core.ac.uk
brought to you by CORE
provided by ScholarBank@NUS

ASSOCIATION CONTROL IN WIRELESS MESH NETWORKS

YU JINQIANG

(*B.Eng*.(*1st Class Hons*.), *NUS*)

A THESIS SUBMITTED

FOR THE DEGREE OF DOCTOR OF PHILOSOPHY

NUS GRADUATE SCHOOL FOR INTEGRATIVE SCIENCES AND ENGINEERING

NATIONAL UNIVERSITY OF SINGAPORE

2015

DECLARATION

I hereby declare that the thesis is my original work

and has been written by me in its entirety.

I have duly acknowledged all the sources of information

which have been used in the thesis.

This thesis has also not been submitted for any

degree in any university previously.

Yu Jinqiang

Yu Jinqiang

3 February 2015

Acknowledgements

First and foremost, I would like to express my heartfelt gratitude to my supervisor Prof. Wong Wai-Choong, Lawrence, for his continuous guidance and support during my PhD study. His insights, suggestions, and valuable feedback have helped me shape my research skills and extended my dimensions of thinking. His enthusiasm, encouragement, patience, and faith in me throughout have been extremely inspiring and helpful. He was always available for my questions and has generously devoted his time and efforts to this thesis, without which its completion would not be possible.

I would also like to thank my thesis advisory committee (TAC) members, Prof. Hari Krishna Garg and Prof. Akkihebbal L. Ananda, for their time and efforts in assessing my research work, for their valuable suggestions and critical yet beneficial comments in our TAC meetings.

I would like to thank NUS Graduate School for Integrative Sciences and Engineering for financially supporting my study through NGS Scholarship.

I would like to thank my friends in IDMI Ambient Intelligence Lab for all the great times we have shared. I am thankful to Mr Song Xianlin and Ms Guo Jie, for providing assistance in carrying out my research.

I am deeply thankful to my family for their love, support, and sacrifices. I dedicate this thesis to my parents, Yu Liming and Wang Shulian, who have devoted unparalleled love and care to me. Most importantly, my very special thanks and love go to my dear wife He Yanran, who has made the days with her the best of my life.

Contents

Summary

The Wireless Mesh Network (WMN) is quickly emerging as a promising solution for low-cost ubiquitous network access. Due to its special characteristics, existing wireless network resource management algorithms need to be redesigned to fully release WMN's potential. Association control is one of them. In this thesis, we investigate association control mechanisms for WMNs from various aspects. In WMNs, a mobile station (STA) associates with one of the nearby mesh access points (MAPs) that are connected to a wireless multi-hop backhaul. Unlike the wired backhaul in the conventional Wireless Local Area Networks (WLANs), the wireless backhaul enables easy network deployment, but at the expense of limitations such as limited capacity, inter-flow and intra-flow interferences, and unfairness in the backhaul contention, etc. The association between MAPs and STAs determines the network logical topology and has significant impact on load distribution, aggregate throughput, and user fairness. The state-of-the-art association metrics proposed for WMNs still adopt the design methodology from WLANs and cannot make good use of the network resource. In addition, there are very few previous works on optimal association in WMNs. Therefore, in this thesis, we propose several innovative association control schemes including both distributed association-metric-based heuristics and centralized optimization-based algorithms, to improve network performance of WMNs.

We first propose two practical heuristic schemes: a cross-layer heuristic association scheme that is able to effectively allocate more STAs to the good-backhaul MAPs and at the same time avoid over-congestion at these MAPs, and a

mobility-aware reassociation control scheme that is able to prolong mobile STAs' association time with the good-backhaul MAPs and discover network dynamics in a smart and timely way without interrupting normal communication too much. Then we formulate the problem of optimal joint association and bandwidth allocation in WMNs, considering three types of fairness objectives: max-min fairness, proportional fairness, and utility-based fairness. We propose two approximation algorithms for the optimization problems and analyse the theoretical approximation ratios as well as the corresponding ratio improvement algorithms. As association control, MAP channel assignment, and STA bandwidth allocation are closely related to each other, we propose a resource management framework that jointly considers the three subjects and further improves WMNs performance. In the framework, we propose an efficient local-clique based network modeling method whose performance is almost identical to that of the exponential-time optimal algorithms. We demonstrate the superior performance of the proposed schemes against the state-of-the-art schemes via simulations using ns-3 simulator as well as our customized simulator.

List of Tables

List of Figures

List of Abbreviations

AC	Association Control
AP	Access Point
A.R.	Approximation Ratio
ARI	Approximation Ratio Improvement
BA	Bandwidth Allocation
BGR	Bipartite Graph Rounding
CA	Channel Assignment
CAETT	Contention Aware Expected Transmission Time
CCA	Clear Channel Access
CFP	Contention-Free Period
CSMA/CA	Carrier Sense Multiple Access with Collision Avoidance
dBm	Decibel-milliwatts
DCF	Distributed Coordination Function
ETT	Expected Transmission Time
GAP	Generalized Assignment Problem
HWMP	Hybrid Wireless Mesh Protocol
JABA	Joint Association and Bandwidth Allocation
JCaBa	Joint Channel assignment and Bandwidth allocation
JCBA	Joint Channel assignment, Bandwidth allocation, and Association control
LAETT	Load Aware Expected Transmission Time
LFR	Largest Fraction Rounding

MAC	Multiple Access Control
MARA	Mobility Aware ReAssociation control
MAP	Mesh Access Point
MM	Max-Min fairness
MUMP	Maximum Utility Matching Problem
PF	Proportional Fairness
QoS	Quality of Service
RSSI	Received Signal Strength Indicator
S.D.	Standard Deviation
SNR	Signal-to-Noise Ratio
SS	Strongest Signal
STA	Mobile station
TDMA	Time Division Multiple Access
UDP	User Datagram Protocol
VC	Vertex Coloring
WLAN	Wireless Local Area Network
WMN	Wireless Mesh Network

List of Symbols

Symbol	Semantics
α	The parameter that controls the priority of fairness.
α_{LFR}	The approximation ratio of JABA-LFR algorithm.
α_{BGR}	The approximation ratio of JABA-BGR algorithm.
λ_i	The channel idleness ratio of MAP *i*.
λ_t	The channel idleness ratio threshold.
ω_A	The weight assigned to the access link cost.
ω_{Max}	The maximum access weight.
ω_{Min}	The minimum access weight.
AC_{ij}	The access link airtime cost between MAP *i* and STA *j*.
$AppRatio(i)$	The approximation ratio of MAP *i*.
b_{ij}	The bandwidth allocated to STA *j* to communicate with MAP *i*.
b_j	The bandwidth of STA *j*.
b_{min}	The minimum STA bandwidth in a feasible bandwidth allocation.
B	A STA bandwidth allocation vector $\{b_i\}$.
B_i	The bandwidth allocated to MAP *i*.
B_{lower}	The parameter controlling the lower bound of STA bandwidth.
B_{upper}	The parameter controlling the upper bound of STA bandwidth.
BC_i	The backhaul airtime cost of the multi-hop path from MAP *i* to the portal.
BCG	A backhaul conflict graph.
$BG(X')$	A bipartite graph constructed according to the fractional association *X'*.

C	A channel assignment vector $\{c_i\}$.
CH	The set of all non-overlapping channels $\{ch_1, ch_2, \ldots, ch_{N\text{-}CH}\}$.
$D_{i,t}$	The distance to MAP i measured by a STA in a scan t.
D_{th}	The distance threshold above which a STA is considered moving towards a MAP.
F	Jain's fairness index.
$f_{utility}(B)$	The utility objective function value of the bandwidth allocation B.
$f_{AP}(X,B)$	The objective function value of iAP and fAP with input (X,B).
i	A MAP.
$IntR$	Interference range.
j	A STA.
k	A clique.
$k(i)$	The set of local access cliques at MAP i.
$k(l)$	the set of local maximal cliques at link l.
K_A	The set of access link cliques.
K_B	The set of all backhaul link cliques.
$K_{cfl}(l)$	All maximal cliques among the links in $L_{cfl}(l)$.
L_B	The set of the backhaul links.
$L_{cfl}(l)$	The set of links that are conflict with link l.
l_{ij}	The access link between MAP i and STA j.
$LinkRateRatio$	The ratio of the backhaul link rate over the access link rate.
$load_{itf}(i,i')$	The traffic that is carried by MAP i' and interferes with MAP i.
$load_{self}(i)$	The total traffic to be carried by MAP i for its associated STAs.
$load_{t\text{-}self}(i)$	The total self-load of MAP i and its interfering MAPs in $M_{ifi}(i)$.
$load_{t\text{-}w\text{-}itf}(i)$	The metric of total weighted interference for MAP i.

M	The set of all MAPs $\{i\}$.
$M(j)$	The set of MAPs that have fractional association with STA j.
$M_{IR}(i)$	The set of MAPs that are within the interference range of MAP i.
$M_{itf,1}(i)$	The set of MAPs that are within the interference range of MAP i.
$M_{itf,2}(i)$	The set of MAPs that are outside the interference range of MAP i, but have access links interfering with i.
$M_{itf}(i)$	The set of MAPs that have access links interfering with MAP i on the same channel.
MC_A	The optimal set of all maximal cliques of the access links.
MC_B	The optimal set of all maximal cliques of the backhaul links.
N_0	The receiver noise in dBm.
$P_l(d)$	The path loss in dB for path length d.
P_{Rx}	The received power in dBm.
P_{Tx}	The transmitting power in dBm.
$path(i)$	The set of links on the routing path between MAP i and the portal.
$Q_{itf}(i)$	The set of all maximal cliques of MAPs that interfere with MAP i and mutually interfere with each other.
r_{ij}	The access link rate between MAP i and STA j.
r_{ki}	The effective backhaul link rate for MAP i in backhaul clique k.
r_{ij}^a	The estimated achievable data rate between MAP i and STA j.
S	The set of all STAs $\{j\}$.
$S(i)$	The set of STAs that are fractionally associated with MAP i.
$S_{IR}(i)$	The set of STAs that are within the interference range of MAP i.
$S_{TR}(i)$	The set of STAs that are within the transmission range of MAP i.
$scv(i,j)$	The sorting criteria variable used by MAP i to sort the STAs $j \in S(i)$.
$T_{Interval}$	The STA scan interval.

$T_{Interval\_Max}$	The maximum scan interval allowed.
$T_{Interval\_Min}$	The minimum scan interval allowed.
T_{TC}	The total association cost improvement threshold.
T_{TC_Low}	The *TC* improvement threshold when a STA is moving towards good-backhaul MAPs.
T_{TC_Middle}	The *TC* improvement threshold when a STA is static.
T_{TC_High}	The *TC* improvement threshold when a STA is moving towards poor-backhaul MAPs.
TC_{ij}	Total association cost between MAP *i* and STA *j*.
TransR	Transmission range.
$U_\alpha(b_j)$	The utility of STA *j*'s allocated bandwidth.
X	A STA-MAP association matrix $\{x_{ij}\}$.
(X', B')	An optimal fractional JABA solution.
$(\hat{X}', \hat{B}')$	An approximated integral JABA solution.
$(\hat{X}^*, \hat{B}^*)$	An optimal integral JABA solution.
x_{ij}	The association between MAP *i* and STA *j*.
y_{ki}	Indicating whether backhaul clique *k* is on MAP *i*'s backhaul path.

Chapter 1: Introduction

1.1. Association Mechanisms in WLANs

IEEE 802.11 Wireless Local Area Networks (WLANs) support infrastructure mode and ad hoc mode. The predominant deployment of WLANs is in infrastructure mode, where an access point (AP) and its associated mobile stations (STAs) form a Basic Service Set (BSS). Several APs are connected to a Distribution System (DS) via wired backhaul links such as Ethernet to form an Extended BSS (EBSS) which is a single MAC domain to facilitate auto hand off for mobile users. Traffic between the Internet and WLANs is handled by gateway nodes in a DS [7].

In infrastructure WLANs, a STA must associate with one of the APs in the vicinity to enable data communication. The association in the 802.11 standard is a 3-stage procedure. First, the STA discovers available APs in range by active scan or passive scan. In active scan, the STA broadcasts a probe request frame and listens for probe response frames from the nearby APs. In passive scan, the STA waits for periodic AP beacon frames. Because APs may operate in different frequency channels, the scan process should be conducted in each channel in order to discover all the available APs. The second stage is association decision making. Based on the AP information carried by probe response frames or beacon frames in addition to STA's local measurements, the STA chooses the best AP to associate with. There are different association metrics to measure the goodness of an AP. The one used in the current IEEE 802.11 standards is Received Signal Strength Indicator (RSSI), i.e. the STA associates with the AP from which the strongest signal is received. At the last stage, the STA sends an Association Request to the best AP and waits for an Association Response. If the STA receives the Association Response indicating a successful association, the association procedure is finished and the STA proceeds with the authentication procedure, after which the STA has joined the network successfully [7].

Nowadays, as more and more APs are deployed to support the fast growing Wi-Fi enabled mobile devices, the overlapping of neighbouring AP cells becomes more and more significant and it is often the case for a STA to discover several available APs in the vicinity. The association between STAs and APs determines the logical network topology; therefore has significant impact on the load distribution and the performance of the whole network. So it is important for a STA to select the most suitable APs to associate with, not only for its own benefit, but also for the sake of the other users.

The simple RSSI based association in the current IEEE 802.11 standard is incapable of load balancing among APs and may lead to poor performance, such as low throughput, unfairness among users, and congestion at hot spot areas, etc. It has been shown in [17] that load balancing in WLANs is beneficial and improves the overall system performance. In the past decade, the association problem in WLANs has been studied a lot and many new association schemes have been proposed. These schemes can be classified into two categories: distributed AP selection [13]-[23] and centralized association control [24]-[35]. Distributed AP selection normally uses heuristic methods where a STA chooses the best AP based on network condition estimated by local measurements (non-intrusive) or information carried by the AP or other STAs' frames (intrusive). Heuristic methods have the advantage of light load, easy deployment and good scalability, but hardly achieve global optimum. On the other hand, in centralized association control, a central network control server calculates the optimal association and distributes it to APs and STAs. As the optimization problem is always NP-hard, approximation techniques have been used to get solutions as close to the optimal as possible. Centralized methods suffer from scalability and adaptability problems, as the central server must be aware of the entire network condition such as node locations, link rate, current associations, etc. The offline optimization algorithm can be triggered periodically or when the network condition has significantly changed, while some online heuristic algorithms take care of light network changes such as a few STAs joining/leaving the network.

1.2. Wireless Mesh Network Architecture

1.2.1. The General WMNs

The Wireless Mesh Network (WMN) is quickly emerging as a promising solution for last few miles access network. Attractive qualities of WMNs include low-cost deployment, robustness and its inheritance of useful characteristics from both the ad-hoc networking paradigm and the traditional wired infrastructure paradigm [2]. The fundamental objective of mesh deployment has been low-cost Internet access. Application scenarios of WMNs include broadband home/community/enterprise networking, building automation, public area surveillance, remote medical care, traffic control system, public services, and integration with sensor monitoring systems, etc.

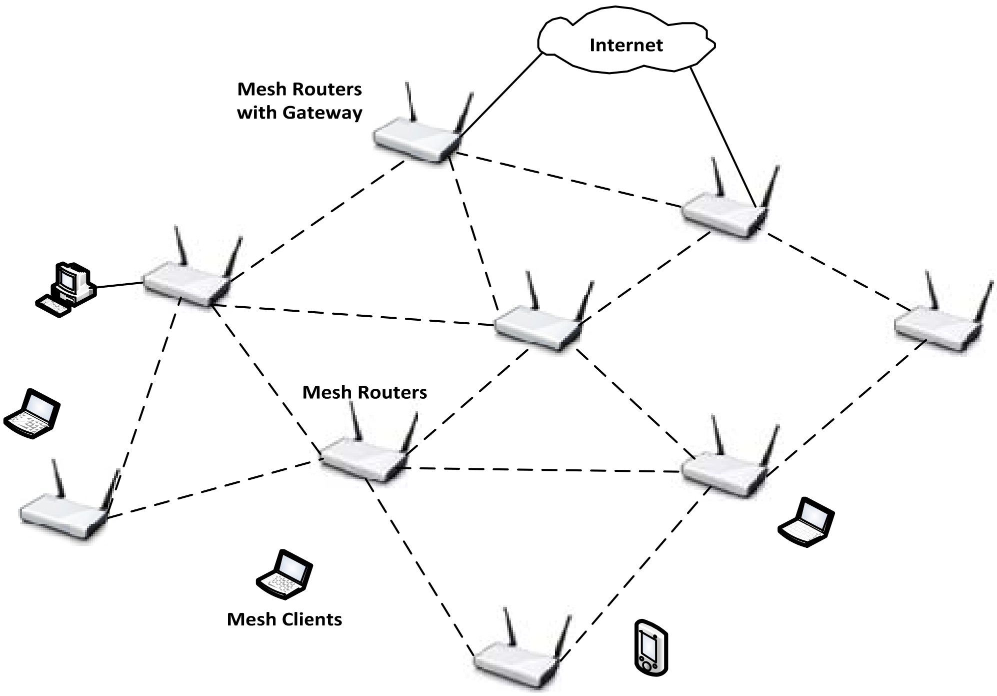

Figure 1.1: Wireless mesh architecture.

Generally WMNs comprise two types of nodes: mesh routers and mesh clients (See Fig. 1.1). Mesh routers have minimal mobility and form a relatively stable multi-hop wireless mesh backbone for mesh clients. Certain mesh routers with the gateway/bridge functionalities enable integration of WMNs with other networks such as the Internet. Mesh clients connect to mesh routers via wireless or wired links. This general form of WMNs can be visualized as an integration of two planes where the access plane provides connectivity to the clients while the forwarding plane relays traffic between the mesh routers. Though WMNs inherit almost all characteristics of the more general ad-hoc network paradigm, such as decentralized design, distributed communications etc., there are a few differences. Mesh routers are quasi-stationary and have no energy consumption limitation. Also the traffic pattern between routers is assumed fairly stable over time.

Based on whether mesh clients participate in mesh forming, WMNs can be broadly classified into two types [1]: infrastructure mesh and hybrid mesh. Infrastructure mesh is the most common form of WMNs. Like the STAs in the infrastructure WLAN mode, mesh clients communicate with mesh routers only without forwarding data for any other nodes. Hybrid mesh is an emerging vision for the future of WMNs, where clients may relay packets for others.

WLAN mesh has been standardized in the IEEE 802.11s amendment [8], which has been published in the latest standard IEEE 802.11-2012 [7]. 820.11s has specified the mesh backhaul mechanisms that are necessary for WLAN mesh networking, such as the frame structure, the mesh backhaul formation and management, the media access control, the path selection, etc [9], [10].

1.2.2. The WMNs in the Thesis

Next we introduce the WMN architecture considered in this thesis. We work on 802.11 based infrastructure mesh WLANs. The network consists of three types of nodes. Following the convention of the 802.11 standards, we name the nodes: client station (STA), mesh access point (MAP), and portal. The STA is the mesh client, and may also be called end user or mobile station. The STA is equipped with a single 802.11 wireless interface and must associate with one of the MAPs to access the network. The MAP has two interfaces: one is the access interface that performs the same functionality as AP in an infrastructure WLAN; the other is the backhaul interface that operates as a mesh router forming the multi-hop wireless backhaul. The portal is the mesh router with gateway functionality enabling Internet access. Each MAP accesses the Internet through one portal only. Each portal and its associated MAPs form an individual cluster in the WMN.

A WMN can be viewed as an integration of two types of network: access networks formed by MAP access interfaces and their associated STAs, and backhaul network formed by MAP backhaul interfaces. Adjacent access network may operate in orthogonal channels to minimize interference, while the backhaul network operates in the same channel to maintain backhaul connectivity, i.e. the backhaul is a single-interface single-channel mesh network. Access links and backhaul links do not interfere with each other, which can be realized by adopting different 802.11a/b/g standards or operating on non-overlapping channels. As for the traffic pattern, we consider Internet traffic only where all STAs send and receive packets to and from the Internet, as low-cost Internet access is the most common usage of a WMN.

1.3. Motivation and Objectives

Association control in WMNs has attracted some research interest in recent years. Noticing the backhaul difference between WLANs and WMNs, researchers have proposed such association metrics for WMNs that takes into consideration the network condition at not only the access network but also the wireless backhaul [36]-[41]. However, their association metrics still adopt the design methodology from WLANs and cannot make good use of the scarce network resource. In addition, there are very few good quality optimization-based association control schemes, e.g. [42] and [43] formulate optimal association problems in WMNs without giving general approximation solutions. Therefore, in this thesis, by taking account of the special features of WMNs, we aim to improve network performance of WMNs through advanced association control schemes including both association metric based heuristics and centralized optimization based approaches.

1.3.1. Heuristic Association

In a conventional WLAN, the APs are connected to a wired backhaul that normally has abundant bandwidth. Therefore, STAs only consider the access link condition when making association decisions, and load balance among APs is preferred. However, in

WMNs, MAPs are connected to a wireless multi-hop backhaul which enables easy network deployment, but at the same time may easily become saturated and become the bottleneck of the whole network due to limitations such as limited capacity compared to the access networks, inter-flow and intra-flow interferences, and unfairness among MAPs. When the backhaul is saturated, a lot of packets would be dropped at the backhaul, even though they have got through their associated access networks. Therefore, in WMN association control, the backhaul plays an important role and should be considered together with the access network conditions, and a certain degree of load unbalance among MAPs is preferred.

We can generally classify MAPs into two classes: good-backhaul MAPs and poor-backhaul MAPs. The good-backhaul MAPs are those with good backhaul conditions such as higher backhaul link rate and shorter backhaul path. On the contrary, the poor-backhaul MAPs are those with poor backhaul condition and low backhaul capacity. A successful packet delivery from the good-backhaul MAPs requires a smaller number of relays and retransmissions, less transmission time, and therefore consumes less network resource compared to transmitting the same packet from the poor-backhaul MAPs. In IEEE 802.11 based WMNs, the poor-backhaul MAPs are even more unfavourable due to the unfairness in multi-hop network contention as shown in [6] that the MAPs with more hops away from the portal yield much lower effective bandwidth.

Therefore, higher aggregate throughout as well as higher resource utilization efficiency can be achieved by allowing more STAs to associate with the good-backhaul MAPs and at the same time allocating more network resource (e.g. transmission time, orthogonal channels) to those MAPs. However, that must be done properly. Otherwise, if too many STAs associate with the good-backhaul MAPs, the access network of these

MAPs could be over-congested; in addition, the STAs associated with the poor-backhaul MAPs may easily get starved, and severe unfairness may occur.

In this thesis, we aim to propose innovative association metric based heuristic association and reassociation schemes such that more STAs can associate with good-backhaul MAPs for better network resource utilization and at the same time avoid over-congestion at the good-backhaul MAPs.

1.3.2. Optimal Association

We can get optimal association by jointly considering association control and user bandwidth allocation, as shown in [32], [34], [35]. Both association control and bandwidth allocation have significant impact on load distribution, aggregate throughput and user fairness, and should be essential components of any resource management framework. Optimization-based joint association control and bandwidth allocation has been studied for WLANs. Previous works on optimal association control schemes for WMNs only gave problem formulation without providing general approximation solutions. In our optimal association control algorithms, we would not only formulate the optimization problems, but also propose approximation algorithms with theoretical analysis on the approximation ratios.

Besides the aggregate throughput, which is determined by resource utilization efficiency, user fairness in bandwidth is also an important consideration factor in resource management. However, these two objectives usually conflict with each other [57]-[60]. For example, as discussed above, we can achieve very high throughput by allocating all the transmission opportunities to the good-backhaul MAPs, which is obviously extremely unfair to the STAs associated with the other MAPs.

There are two commonly used fairness criteria for bandwidth allocation objectives: max-min fairness (MM) [61] and proportional fairness (PF) [62]. By MM, the bandwidth of any STA cannot be increased without decreasing the allocation of a STA with smaller or equal bandwidth. PF is achieved when the sum of the logarithm of each STA's bandwidth is maximized. MM tries to allocate the bandwidth of all STAs as equal as possible; on the other hand, PF increases network throughput by sacrificing fairness, exploiting the trade-off between the two.

The IEEE802.11 MAC protocols implicitly enforce max-min throughput fairness among users in the long term, i.e. each user gets equal transmission opportunity and achieves equal throughput. That would drop the throughput of all the STAs associated with one AP to approximately the lowest link rate of the STAs in the cell, resulting in network resource under-utilization [4]. Therefore researchers have proposed the concept of time-based fairness [60], where all the STAs associated with one AP get equal transmission time. It has been shown in [35] that, for a single WLAN cell, time-based fairness is equivalent to the proportional fairness.

In this thesis, we aim to propose centralized optimization based association control schemes that find optimal association and bandwidth allocation achieving not only MM or PF fairness but also any degree of the trade-off between resource utilization efficiency and user fairness.

Previous works on optimal association, no matter for WLANs or for WMNs, assumed careful frequency planning such that no inter-cell interference is considered. In this thesis, we would like to propose a centralized algorithm that jointly considers MAP channel assignment, association control and user bandwidth allocation.

1.4. Contributions and Organization of the Thesis

In Chapter 2, we do a comprehensive literature review on association control schemes for WLANs and WMNs.

In Chapter 3, we propose a cross-layer heuristic association scheme that takes the multi-hop wireless backhaul property into consideration and is able to effectively allocate more STAs to the good-backhaul MAPs and at the same time avoid over-congestion at these MAPs. We demonstrate the benefit of unbalanced loading in WMNs and the improved end-to-end performance of the proposed scheme via simulations using ns-3 simulator.

In Chapter 4, we propose a mobility-aware reassociation control scheme, named MARA, which takes the wireless backhaul and STAs mobility into consideration. By prolonging mobile STAs' association time with the good-backhaul MAPs, MARA improves the network resource utilization. By dynamically adjusting the scan interval, MARA is able to discover network dynamics in a smart and timely way without interrupting normal communication too much. We demonstrate the improved end-to-end performance via ns-3 simulation.

In Chapter 5, we formulate and propose approximation algorithms for the problem of optimal joint association and bandwidth allocation in WMNs, considering max-min fairness and proportional fairness objectives. We first relax the integral association constraint and get an optimal fractional association solution. Then we propose two rounding algorithms to get an integral association solution. We do theoretical analysis on the approximation ratios of the proposed rounding algorithms, which reflect the gap between the produced solution and the optimal one. To let the theoretical approximation ratio more closely reflect the true performance gap, we propose two approximation ratio improvement algorithms. We demonstrate via simulations that the proposed algorithm achieves nearly optimal performance and outperforms popular heuristic algorithms.

In Chapter 6, we formulate an optimal joint association and bandwidth allocation problem that achieves a utility fairness objective in WMNs. Utility fairness is more general than max-min fairness and proportional fairness and more flexible in controlling the trade-off between resource utilization efficiency and user fairness. We introduce a user bandwidth boundary constraint to make the trade-off more controllable and at the same time prevent extreme unfairness. We demonstrate through simulations how to control the trade-off between efficiency and fairness to achieve the desired performance by tuning the control parameters.

In Chapter 7, we propose a network resource management framework for WMNs that improves the network performance by jointly managing MAP channel assignment, user association, and user bandwidth allocation. The proposed framework is composed of three components: a utility-fairness-based bandwidth allocation algorithm, a channel assignment algorithm that effectively increases the network capacity by reducing the interference at the good-backhaul MAPs, and an optimization based association control algorithm. In addition, to model the concurrent transmission constraints in WMNs, we propose an efficient local-clique based network modeling method whose performance is almost identical to that of the exponential-time optimal algorithms.

In Chapter 8, we conclude the thesis and discuss about future works.

Chapter 2: Literature Review

2.1. WLAN Association Schemes

AP selection or association control problem in WLANs has drawn a lot of research interest in the past decade. Although the metrics, techniques, and methodologies proposed in the WLAN association schemes may not suit the association requirements in WMNs, due to the backhaul difference, they provide valuable insights and inspire new ideas.

2.1.1. Distributed Approaches for WLANs

In [13], to balance load, overloaded APs force some stations to handoff to under-loaded APs. The architecture is completely distributed but requires AP load information broadcasting in the backhaul. In [14], stations quickly associate with each available AP and run a battery of tests to estimate the quality and usability of each AP's connection to the Internet. In our work, we assume all APs are usable and no restriction on Internet access. In [15], a queue-based user association management is proposed to handle heavy loads in WLANs. Approaches to manage heavily loaded WLANs can be categorized into: over-provisioning, selective dropping, load balancing, and traffic shaping. Load balancing is of limited help when the total load is high enough to overwhelm all APs. The proposed management controls the frequency and duration of user associations with the network by using a queue of users requesting network access. In [16], each STA locally makes association decision according to an association transition probability that is computed based on an annealed Gibbs sampler technique. Assuming a saturated network and only downlink traffic, the aggregate transmission delay (inverse of transmission rate) of all STAs is minimized when the algorithm converges. [17] surveys and summarizes load balancing approaches according to station based load distribution and network based load distribution. They measure the AP's load and effectiveness of load balancing by AP's effective throughput and show experimentally that effectively balancing AP traffic load can increase overall system throughputs. [18] proposes a practical online AP association strategy that maximizes minimal throughput for all clients. The authors use a weighted congestion game model to prove the superiority of the online strategy over the selfish strategy, in terms of convergence and competitive ratio. In the selfish strategy, every user keeps moving to associate with the AP that could offer it the best throughput until Nash Equilibrium is reached. In the online strategy proposed, a new client will irrevocably associate with the AP that will minimize the loads on all the APs within its transmission range.

Various association metrics that estimate the available bandwidth of APs have been proposed in [19]-[23]. In [19], the bandwidth a station is likely to receive if it were to associate with an AP is estimated based on measurements of delay of beacon frames. The scheme assumes beacon frames are transmitted with the same priority as the data frames, which is rarely the case in real WLANs. In [20], instead of RSSI, the authors use Signal-to-Noise Ratio (SNR) as the association metric, which can reflect the link quality more realistically and achieve good performance in a network with high interference. But the metric is incapable of load balancing. [21] proposes an association metric that takes account of both achievable throughput and the impact of the new STA's association on already associated STAs. The achievable throughput calculation considers channel access overhead and transmission failure due to packet error, but does not consider packet collision. The "impact" value is computed by comparing the average channel occupancy time per STA before and after a new STA association. The authors have also proposed to dynamically enlarge or shrink the scan interval so as to avoid unnecessary scanning for dynamic reassociation. In [22], stations estimate the available residual bandwidth of a WLAN by calculating the RTS collision probability and channel idle ratio based on channel state assessment. This method requires a long observing period to get a relatively accurate estimation. In [23], the achievable throughput is approximated by the metric that takes account of contention from one-hop (associated and non-associated) and interference from two-hop neighbours (hidden nodes). Each node has to broadcast its lists of neighbours and activity factor introducing large overhead.

2.1.2. Centralized Approaches for WLANs

In [24]-[27], a central control server is aware of the network conditions and makes the association decisions for STAs. In [24], an admission control server maintains all per-cell and per-user state and controls use of the wireless bandwidth in the entire network. The server instructs the station to associate or roam to the AP that satisfies its QoS requirement. In [25], a user senses and delivers the network conditions, such as AP traffic loads, to APs; then each AP estimates and returns the potential throughput for the user. The user associates with the AP with the maximum potential throughput. The authors demonstrated the performance of the proposed method for a single user rather than the whole network. [26] proposes a centralized coordination system such that only a set of non-interfering APs is activated during any given time of the contention-free period (CFP). The number of slots allocated to each AP in the CFP is proportional to its load and the system's performance is optimized by employing efficient scheduling algorithms. In [27], the STA activity factor is considered when estimating the average throughput of a STA.

In [28]-[31], the association is controlled through the AP transmission power control. [28] and [29] propose cell-breathing techniques for load balancing in WLANs with continuous-power and discrete-power assignment respectively. Cell breathing is implemented by controlling the transmission power of an AP's beacon frames, and does not require any change to the client or to the standard. In [28] the association problem is modelled as a minimum weighted perfect matching problem by assuming STAs with unit demand and rejecting new STAs when the AP capacity has been reached, which makes the model less realistic. [29] targets at the long-term inter-AP fairness with no effort in improving the network throughput. The authors give an optimal solution to a variant of the NP-hard min-max load balancing problem, where each AP is given a unique priority or weight. In [31], an AP power control algorithm is proposed for proportional fairness in multi-rate WLANs. It is assumed that all APs operate on the same channel which is rarely the case in a real network deployment.

The power control based association control methods are good at easy implementation. However, they achieve sub-optimal performance compared to the optimization based association control methods such as [32]-[35]. In [32], max-min fairness is achieved through min-max AP load balancing. The optimal association problem is formulated as an integer linear programming problem, which is solved by a relaxation-then-rounding algorithm that achieves a constant approximation factor of 2. [33] proposes to evaluate the quality of an association by the utilities of throughputs, where the utility is the logarithm of the throughput. The authors solve a linear relaxation of the utility maximizing problem in two simple cases without giving a general solution to the optimization problem. In [34], the optimal association for proportional fairness in WLANs is modelled as an integer nonlinear programming problem (NLP). The NLP is then relaxed to a discretized linear program (DLP) by discretizing the scheduling period of each AP into discrete slots that are as many as the number of STAs. As there are too many variables in DLP, solving DLP would be very time consuming if this method is applied in WMNs. [35] shares the same problem formulation as [34]; they differ in how the optimization problem is relaxed, yielding different approximation ratios. Both [34] and [35] adopt the same rounding procedure that is first proposed for the generalized assignment problem [65].

2.2. WMN Association Schemes

The association problem in WMNs has attracted researchers' attention in recent years as various aspects of WMNs are intensively studied.

2.2.1. Heuristic Approaches for WMNs

[36]-[41] have proposed association metrics for WMNs that comprise access link cost and backhaul link cost. They are different in the association factors considered in the metric. Luo et al. propose Contention Aware Expected Transmission Time (CAETT) in [36] and the Load Aware Expected Transmission Time (LAETT) in [37] as the access link cost. CAETT is equal to the sum of the Expected Transmission Time (ETT) of the already associated stations and the associating station. LAETT metric improves CAETT by estimating the effective bit rate of an access link more accurately based on the channel idleness ratio. When the idleness ratio is large, the network is lightly loaded and LAETT equals to the associating station's ETT. When the idleness ratio is smaller than a threshold, the network is considered saturated and LAETT is similar to CAETT. The authors only demonstrate the performance of LAETT in a lightly loaded network. It is not clear how the metric performs in heavy load situations.

In [38], an end-to-end airtime metric is proposed as the association metric. The airtime metric is similar to ETT except that it incorporates channel access overhead and protocol overhead that are standard-specific constant values. The authors also propose a load balancing scheme where a STA increases the weight of the access metric when it finds the AP load unbalanced based on the current load balance index as well as the threshold value carried in beacons. It proposes a hybrid scheme that incorporates airtime metric and SNR metric to handle light load and heavy load respectively. In [39], the association metric is the end-to-end delay of one packet including packet transmission time as well as protocol and physical overhead, but not considering network load, contention or packet error. In the backhaul metric calculation, long-hop routes are given more weight to favour short-hop routes, which is preferred by small-sized packets. In [40], dynamic association and reassociation oscillation avoidance mechanisms are investigated; the channel idle ratio is calculated based on per channel observation. [41] extends LAETT by including the uplink and downlink backhaul metric and demonstrates the implementation of a cross-layer association scheme on a Linux-based test-bed.

The state-of-the-art cross-layer association schemes [37], [38], [41] are similar in association metric calculation. In particular, they estimate access link available bandwidth by distinguishing access network saturation using a pre-defined channel idleness ratio threshold. The problem with this method is that the association metric of the MAPs that are estimated as saturated are much larger than those that are not estimated as saturated. This may prevent incoming STAs associating with the good-backhaul MAPs and result in network resource under-utilization.

2.2.2. Optimization Approaches for WMNs

There are very few papers on optimization based association in WMNs, possibly because research attention has been focusing on either single-hop WLANs or multi-hop backhaul network, but not the interaction between the two networks. In [42], a joint user association, backhaul routing and max-min bandwidth allocation problem is formulated for WMNs. Instead of approximating the optimal solution, association and routing are constructed via a heuristic approach, which makes the algorithm much less optimal. In [43], load balancing is done by minimizing the variance of the MAP load, where the load is defined as the number of STAs by assuming that STAs have equal data rate and demand. Instead of providing sub-optimal solutions to the NP-hard problem, the authors compute the optimal solution by enumerating all the possible associations.

Chapter 3: A Cross-Layer Association Control Scheme for WMNs

In this chapter, we propose a network resource aware cross-layer association control scheme that takes access and backhaul link quality, network load, and backhaul contention into consideration. Our simulation results in the context of IEEE 802.11 based WMN show that the proposed association scheme is able to achieve improved end-to-end performance as well as improved network resource utilization efficiency.

3.1. Introduction

As discussed in Section 1.3.1, due to the characteristics of the wireless multi-hop backhaul of WMNs, we can make better use of the scarce backhaul network resource by associating more STAs with the good-backhaul MAPs, i.e. a certain degree of load unbalance among MAPs is preferred. However, as discussed in the literature review on heuristic association control schemes for WMNs in Section 2.2.1, the state of the art cross-layer association schemes tend to realize load balancing among MAPs, resulting in network resource underutilization, because they tend to judge a MAP's access network as saturated and prevent new STAs associating with it.

In the 802.11 based WMNs, MAPs do not receive fair backhaul bandwidth due to multi-hop contention. In [6] it is shown that MAPs with more hops from the gateway yield much lower effective bandwidth. In our proposed network resource aware association control scheme, unfairness in backhaul contention is taken into consideration and more STAs are associated with the MAPs of higher backhaul capacity. We also investigate the benefit of unbalanced loading in WMN.

3.2. The Cross-layer Association Control Scheme

Our proposed association control scheme comprises four components: Load Aware Airtime metric (LAA), Link Quality Aware airtime metric (LQA), access weight adjustment, and load balancing among MAPs of similar backhaul cost. Metrics similar to the LAA metric have been studied in [37], [38], [41], while the other three features are new.

3.2.1. Association Metrics

We adopt an airtime metric as the association metric that reflects the amount of channel resource (time) consumed by a successful transmission. The total airtime cost of STA j associating with MAP i is calculated as:

$$TC_{ij} = \omega_A \cdot AC_{ij} + (1 - \omega_A) \cdot BC_i \tag{3.1}$$

where AC_{ij} is the access link airtime cost between i and j ; BC_i is the backhaul airtime cost of the multi-hop path from MAP i to the portal; ω_A is the weight assigned to the access link cost and its value has impact on the throughput and MAP load balancing. The access link airtime cost is calculated as:

$$AC_{ij} = (O_{ca} + O_p + \frac{p}{r_{ij}^a}) \frac{1}{1 - e_j} \tag{3.2}$$

where O_{ca} is the channel access overhead; O_p is the protocol overhead; O_{ca} + O_p is a constant value determined by the adopted 802.11 standard, e.g. for the 802.11b standard the value is 1.25 microseconds; p is the expected dominant packet size in bits; e_j is the estimated packet error rate that can be estimated through techniques such as observing past frame loss, sending overhead testing frame, or calculated based on the Signal-to-Noise Ratio (SNR) measurement; r_{ij}^{a} is the estimated achievable data rate and can be calculated in two ways as in (3.3) and (3.4).

$$r_{ij}^{a} = r_{ij} \tag{3.3}$$

$$r_{ij}^{a} = \begin{cases} \lambda_i r_{ij} & \lambda_i \geq \lambda_t \\ \dfrac{1}{\sum_{j' \in S(i)} \dfrac{1}{r_{ij'}} + \dfrac{1}{r_{ij}}} & \lambda_i < \lambda_t \end{cases} \tag{3.4}$$

In (3.3), r_{ij} is the physical link rate between MAP i and STA j. In (3.4), $r_{ij'}$ is the physical link rate of STA j' that has already associated with i; λ_i is the channel idleness ratio of i and λ_t is the channel idleness ratio threshold below which the access network of i is considered saturated. The MAP keeps track of the channel idleness ratio by monitoring the time the channel state is idle during a monitoring window.

We name the total airtime metric where the achievable data rate r_{ij}^{a} is calculated using (3.3) as Link Quality Aware airtime metric (LQA). On the other hand, if r_{ij}^{a} is calculated using (3.4), we name the corresponding total airtime metric as Load Aware Airtime metric (LAA). The access link cost calculated using the LQA metric is smaller than that calculated using the LAA metric. The LQA metric in effect lowers the weight of the access link cost in the total association cost. As a result, with the LQA metric, more STAs would associate with the MAPs with smaller backhaul cost, and the load distribution among MAPs is more unbalanced.

The backhaul airtime cost of i is calculated using (3.5), which is the accumulated airtime cost on each hop along the backhaul path. r_k is the physical link rate between MAP k and its next hop MAP.

$$BC_i = \sum_{k=1}^{hopcount} (O_{ca} + O_p + \frac{p}{r_k}) \frac{1}{1-e_k} \tag{3.5}$$

3.2.2. Access Weight Adjustment Scheme

With LQA metric, more STAs would associate with the MAPs with better backhaul conditions, i.e. lower backhaul cost. However, as more and more STAs join the network, the good-backhaul MAPs will be overloaded. To avoid congestion at these MAPs, we propose an access weight adjustment scheme:

$$\omega_A = \begin{cases} \omega_{Min} & \lambda_i \geq \lambda_t \\ \omega_{Max} - (\omega_{Max} - \omega_{Min}) \cdot \dfrac{\lambda_i}{\lambda_t} & \lambda_i < \lambda_t \end{cases} \tag{3.6}$$

where λ_i and λ_t are the same channel idleness ratio and threshold as in (3.4); ω_{Min} is the minimum access weight; ω_{Max} is the maximum access weight. The equation is chosen such that when there are few STAs in the network and the channel idleness ratio is high, the access weight is set to the minimum value, and therefore the backhaul cost of a MAP contributes more in the total association cost. As a result, more STAs would associate with the good-backhaul MAPs, which would increase the backhaul network capacity as well as the aggregate network throughput. As more and more STAs join the network and the channel idleness ratio decreases, the access weight will be increased, so that the newly joined STAs will be distributed more evenly among the MAPs. As a result, congestion at the good-backhaul MAPs could be relieved. The access weight approaches the maximum value as the channel idleness ratio approaches zero.

Combining the LQA metric with the access weight adjustment scheme, we get an improved scheme, which is named LQAW. We will see from the simulation results that LQAW effectively associates more STAs with the good-backhaul MAPs and at the same time avoids overloading these MAPs.

The message overhead for cost calculations is the following information element fields in MAP access network beacon frames.

- IeRoutingCost: 4 bytes (backhaul routing airtime cost)
- IeAccessMetric: 4 bytes (total access link airtime cost of the associated STAs)
- IeIdleRatio: 2 bytes (access network channel idleness ratio)

The access network beacon interval is 0.1 second and beacons are transmitted at 1Mbps data rate. So the overhead in time caused by association scheme in access network is 800 microseconds per second (0.08%), which is very small. Therefore, the overhead has negligible effect on performance.

3.2.3. Procedure of the Proposed Association Scheme

The procedure of the cross-layer network resource aware association scheme is as follows:

1) MAPs broadcast access beacon frames every beacon interval. The modified beacons carry additional information elements such as access network load, access channel idleness ratio, and backhaul airtime cost.
2) The STA passively scans each channel. Upon receiving a beacon, the STA records the information and calculates the link rate and packet error rate based on the SNR of the received beacon.
3) After scanning the last channel, the STA has gathered information from all the available MAPs. Then it calculates the access weight using (3.6) based on the smallest channel idleness ratio received.
4) The STA calculates the total airtime cost of the available MAPs using the LQA metric and LAA metric.

5) If the function of load balancing among MAPs of similar backhaul cost is disabled, the STA associates with the least LQA metric MAP. Otherwise, the STA picks up the two MAPs with the least LQA metric and checks whether they have similar backhaul cost. If the two MAPs do not have similar backhaul cost, the STA associates with the least LQA metric MAP. Otherwise, the STA associates with the least LAA metric MAP.
6) Finally, the STA switches to the channel of the chosen MAP and exchanges Association Request frame and Association Response frame with it. Then the association process ends successfully.

3.3. Performance Evaluation

We have implemented the proposed association scheme in network simulator ns-3 [11]. In our experiments, we simulate a WMN that consists of 12 MAPs, 1 portal, and 10-80 STAs in a rectangular field of 280m×210m. The portal is located at the centre. In this section we present and discuss the simulation results of two experiments. In the first experiment, the MAPs are located in a 4×3 grid topology. With known MAP location and association details of each MAP, we investigate how the access weight affects the network performance and clearly demonstrate why our proposed scheme outperforms the benchmark association metrics. As the grid topology may not be always feasible in a real network deployment, in the second experiment, MAPs are randomly placed in the field.

We choose the 802.11s mesh module in ns-3 as the backhaul protocol. Its default routing protocol, Hybrid Wireless Mesh Protocol (HWMP), constructs a routing tree rooted at the portal for the wireless multi-hop backhaul. A WiFi physical model named *yans* [44] and ideal rate controller are used. Backhaul links and access links adopt 802.11a and 802.11g standards respectively so that they do not interfere with each other.

STAs are randomly located in the field and remain at the same location throughout the experiment. After all STAs have joined the network, the simulator starts to record performance data. Each STA sends UDP packets to the Internet, with a packet size of 800 bytes, and data generation rate of 150 Kbps. The experimental results are averaged over 20 runs.

We compare the performance of our proposed association schemes, LQA, LQAW, and LQAWLB, against the benchmark metrics SNR and LAA. SNR, like RSSI, can only reflect access link quality. LAA is the state-of-the-art cross-layer association metric that still adopts the load balancing design methodology from the conventional WLANs. LQAW is the LQA airtime metric combined with the access weight adjustment scheme. LQAWLB is LQAW with load balancing function enabled.

3.3.1. Experiment 1: Grid Topology

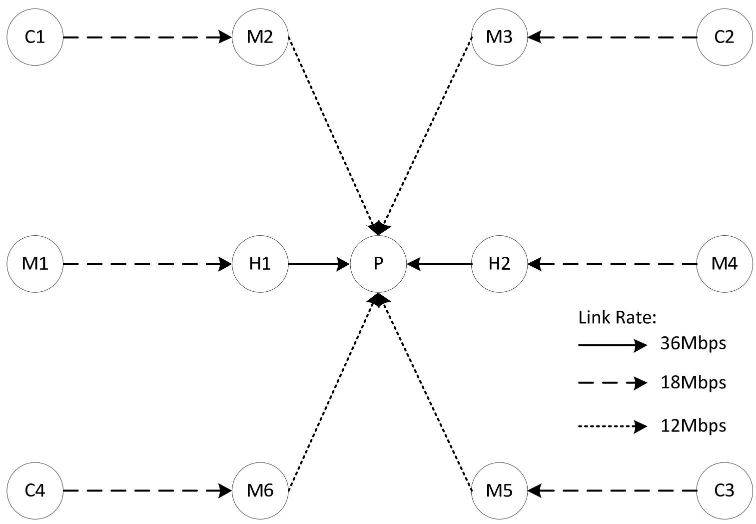

Figure 3.1: 12-MAP grid topology.

The location of the MAPs is depicted in Fig. 3.1. According to the different backhaul conditions, we categorize the MAPs into three categories: *H1* and *H2* in the middle are A-class MAPs as they have the best backhaul condition (the fewest hop, the fastest link rate, and the highest backhaul capacity); *M1* to *M6* are B-class MAPs; *C1* to *C4* at the corners are C-class MAPs as they have the poorest backhaul condition and the smallest effective bandwidth. Node *P* in the centre is the portal.

A. Effect of the Access Weight

Fig. 3.2 shows the association results and performance of 70 STAs using the LQA metric under different access weights. In Fig. 3.2 (a), with bigger access weight, the load distribution is more even among all MAPs (load balanced), while with smaller access weights, the A-class MAPs are more crowded (load unbalanced). In Fig. 3.2 (b), the left bar at each access weight is the aggregate end-to-end throughput, which shows that neither too much load balance nor too much load unbalance is good and the highest end-to-end throughput is achieved at an access weight of 0.25. The network bottleneck resides in the access network when the access weight is small and in backhaul when the access weight is large. For access weights larger than 0.25, although all offered load from STAs can get through the access network, a lot of packets are dropped at the MAPs. The reason is that contention from the poor-backhaul MAPs (B-class and C-class) decreases the transmission opportunities of the good-backhaul MAPs (A-class), resulting in lower backhaul capacity and lower resource utilization efficiency.

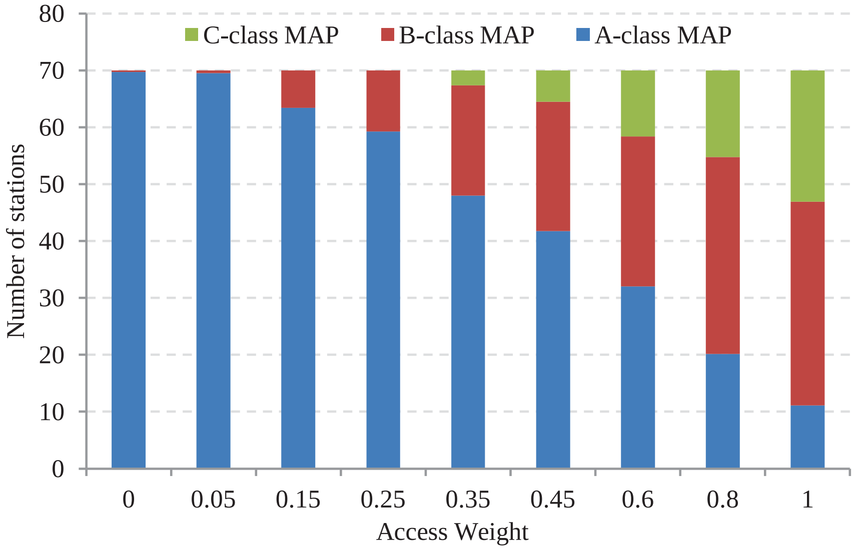

(a) Association Results

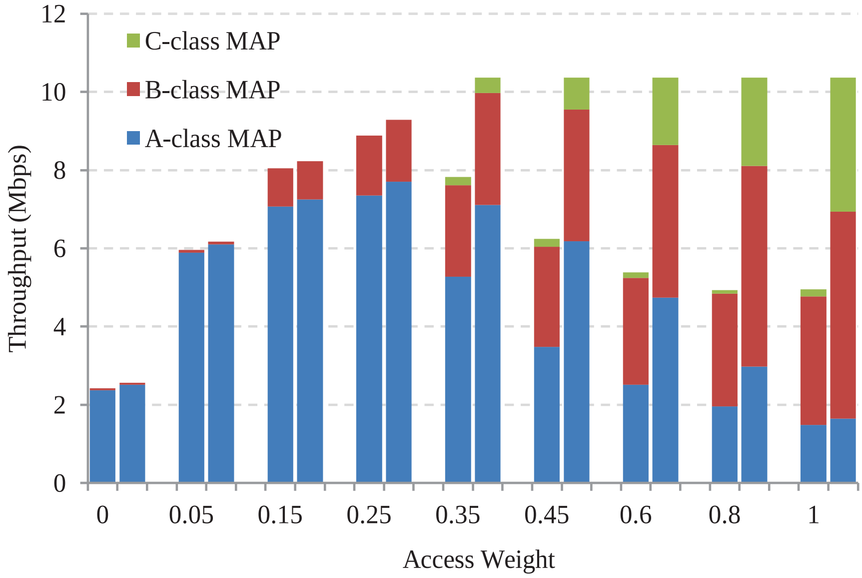

(b) End-to-end throughput (left bar) & access network throughput (right bar)

Figure 3.2: Effect of the access weight.

B. Performance of LQAW

From Fig. 3.3, Fig. 3.4, and Fig. 3.5 we compare the performance of SNR, LAA, LQA and LQAW schemes. In the experiments, the channel idleness ratio threshold for LAA and LQAW is 0.6. The access weight for LAA is 0.25, while for LQA is 0.25 or 0.4. The ω_{Min} and ω_{Max} in LQAW is 0.25 and 0.45 respectively. The 95% confidence interval range looks a bit large in the figures because the total number of simulation runs is 20. The confidence interval would be smaller when the number of runs is larger.

Fig. 3.3 depicts the association results of 70 STAs under different metrics. We can see that more STAs are associated with the A-class MAPs under LQA and LQAW, compared to SNR and LAA. The association result under LQAW is in between LQA with access weight 0.25 and LQA with access weight 0.4, which is as expected because the changing access weight in LQAW falls between 0.25 and 0.4. Under the uniform user topology, the SNR metric evenly distributes the STAs to the MAPs. Therefore, in Fig. 3.3 we see that, for SNR, the number of STAs associated with different MAP classes matches the number of the MAPs in the MAP classes (A-class:B-class:C-class=2:6:4).

We can see from Fig. 3.4 that LQA and LQAW achieve higher aggregate throughput than SNR and LAA because of less contention from the poor-backhaul MAPs. From Fig. 3.5 we see that LQA0.4 and LQAW achieve the lowest end-to-end average packet delay. Comparing LQA0.4 and LAA, the access airtime cost calculated by LQA0.4 is lower, resulting in more STAs associated with the A-class MAPs and less STAs associated with the C-class MAPs. Due to less contention from the poor-backhaul MAPs, LQA0.4 achieves higher network capacity, higher aggregate throughput, and lower end-to-end packet delay. For the LQA metric without the access weight adjustment function, when the access weight is further decreased from 0.4 to 0.25, more STAs are associated with the good-backhaul MAPs resulting in even higher aggregate throughput. However, packet delay in LQA0.25 is much longer due to heavy congestion at the access links of the good-backhaul MAPs. LQAW achieves throughput performance that is comparable to that of LQA0.25 because the access weight of LQAW almost equals 0.25 when the network load is low, resulting in a large number of STAs associated with the good-backhaul MAPs. LQAW achieves low packet delay because the weight of the access airtime cost is increased when the network load increases, resulting in more balanced load distribution.

In Fig. 3.4, for SNR, LQA0.4, and LAA, the throughput starts decreasing when the number of stations increases beyond a certain value. This is because the wireless backhaul is the bottleneck of the whole network. The aggregate throughput performance is determined by the backhaul capacity. When the number of STAs increases beyond a certain value, there would be many STAs associated with the poor-backhaul MAPs (they are located far from the portal and can hear from poor-backhaul only) and there would be a lot of competition in the backhaul from the poor-backhaul MAPs, which will reduce the backhaul resource utilization efficiency and lower the backhaul capacity. Therefore, we see the aggregate throughput decreases

From Fig. 3.4 and Fig. 3.5 we find that LQAW achieves the best overall performance because it successfully takes advantage of the backhaul contention property and makes better use of the backhaul network resource, while at the same time it is able to avoid over congestion at the good-backhaul MAPs.

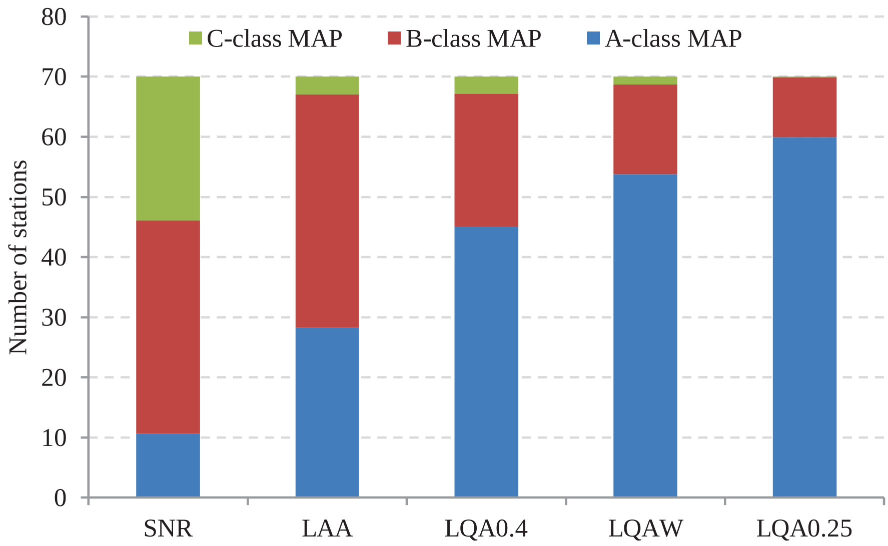

Figure 3.3: Association results under different association metrics.

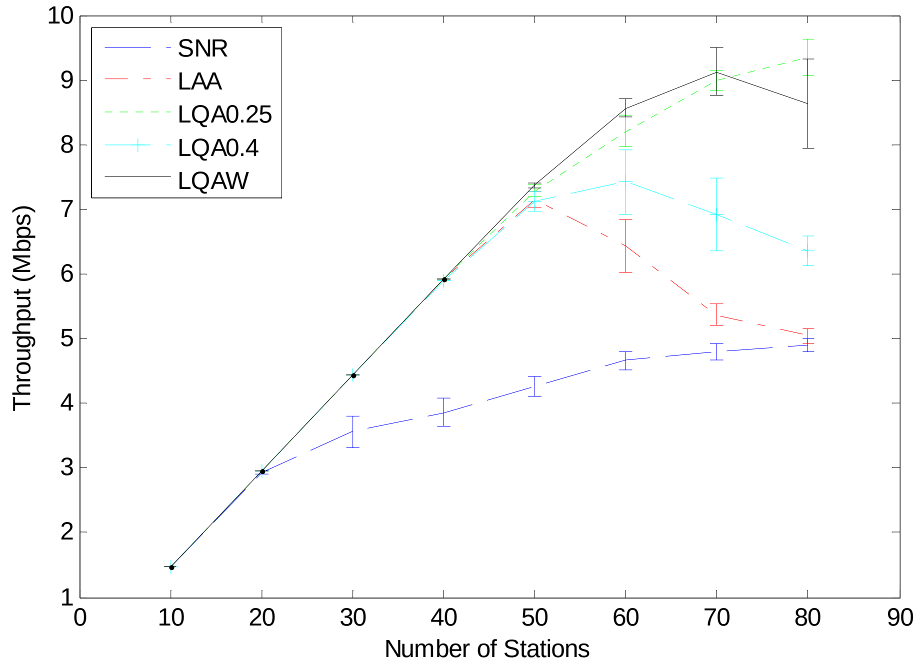

Figure 3.4: Aggregate throughput in the grid MAP topology.

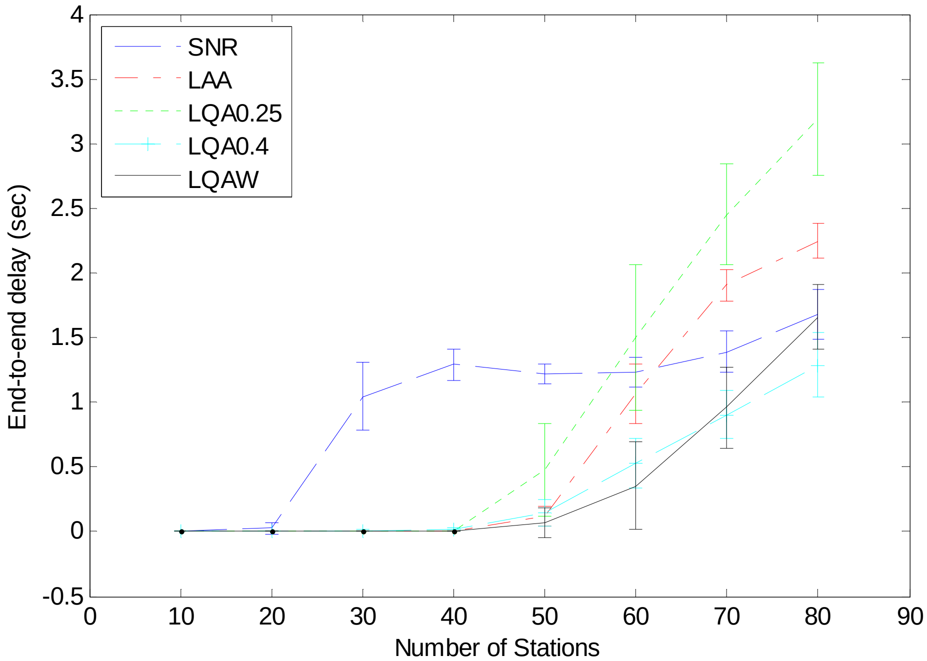

Figure 3.5: Average packet delay in the grid MAP topology.

3.3.2. Experiment 2: Random Topology

In a random placement MAP topology, the good-backhaul MAPs are those closer to the portal and having fewer hops on the backhaul path, similar to the A-class MAPs in the grid topology. Associating more STAs with the short-path MAPs can make better use of the network resource, and the simulation results depicted in Fig. 3.6 and Fig. 3.7 are as expected showing that LQAW achieves much higher throughput and lower end-to-end delay than SNR and LAA. For the same reason as in the grid topology, LQAW is able to associate more STAs with the good-backhaul MAPs and less STAs with the poor-backhaul MAPs and at the same time avoid over-congestion at the good-backhaul MAPs. From Fig. 3.7 we see that adding the load balancing function to LQAW can slightly improve the delay performance which means the load balancing function is able to find some load balancing opportunities among the MAPs with similar backhaul cost. More balanced load distribution results in less access network contention and less packet delay. For the load balancing is done only among MAPs with similar backhaul condition, the network throughput is not sacrificed by the load balancing.

The throughput shown in Fig. 3.6 is the aggregate throughput of all STAs in the network. Sometimes the aggregate throughput can be improved by giving much more transmission opportunities to the STAs with fast links, which is unfair to the other STAs. We use Jain's fairness index [12] to measure the fairness among STAs. The fairness index F is calculated using (3.7), where b_j is the end-to-end throughput of STA j and n is the total number of STAs. The index equals to 1 when all STAs achieve the same throughput. From Fig. 3.8 we see that the fairness index of LQAWLB is the highest, which means its throughput advantage does not sacrifice the user fairness. In SNR and LAA, the STAs associated with the poor-backhaul MAPs receive very little bandwidth due to the unfairness in the wireless multi-hop backhaul contention. In LQAWLB, more STAs are associated with the good-backhaul MAPs, resulting in fewer STAs associated with the poor-backhaul MAPs being starved. In addition, contention among STAs associated with the same MAP is much fairer. As a result, LQAWLB achieves higher fairness index.

$$F = \left(\sum b_j\right)^2 \Big/ \left(n \cdot \sum b_j^2\right) \tag{3.7}$$

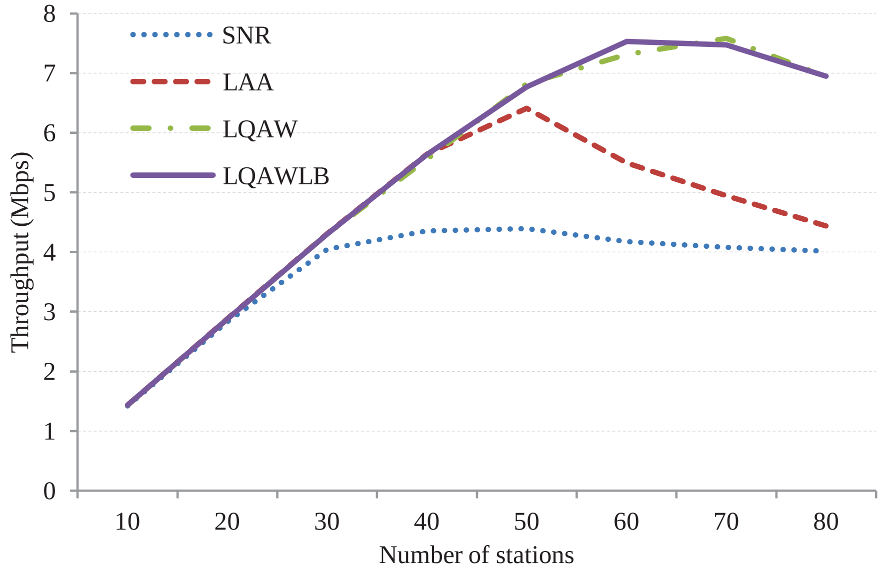

Figure 3.6: Aggregate throughput in the random MAP topology.

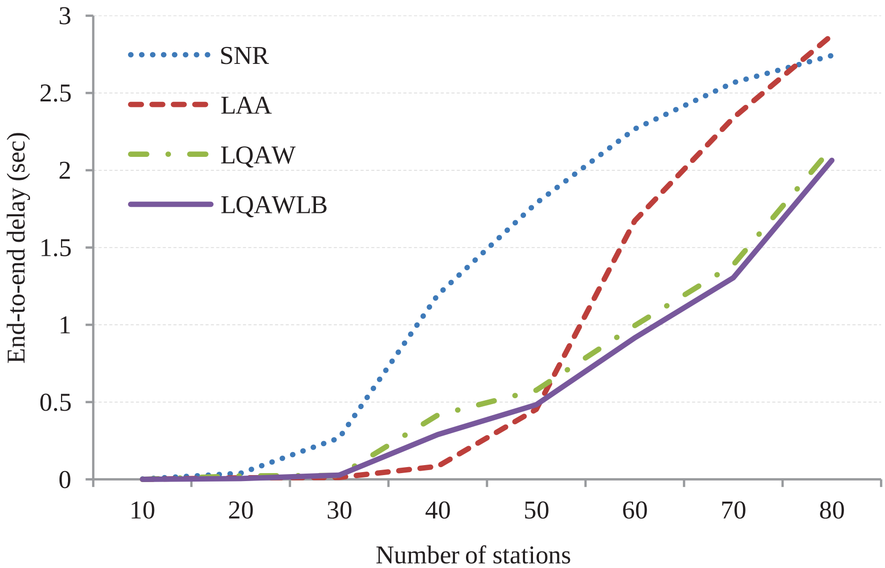

Figure 3.7: Average packet delay in the random MAP topology.

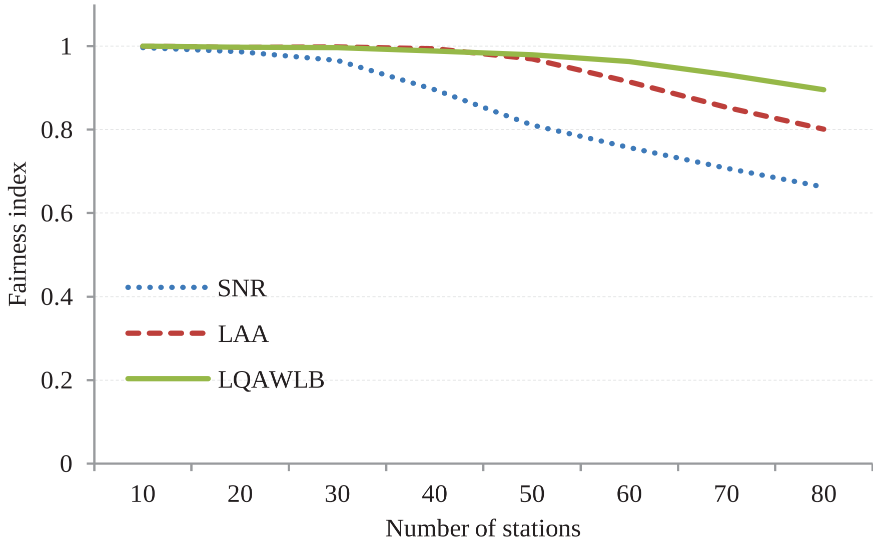

Figure 3.8: Fairness index in the random MAP topology.

3.4. Conclusion

Unlike in the conventional WLANs, where the wired backhaul provides abundant bandwidth and load balance among APs is preferred, in a WMN, the wireless multi-hop backhaul encounters the network bottleneck and properly allocating more loads to the MAPs with good backhaul condition can make better use of the backhaul network resource and improve network performance. Our proposed association schemes LQAW and LQAWLB take the multi-hop wireless backhaul property into consideration and are able to effectively allocate more loads to the good-backhaul MAPs and at the same time avoid over-congestion at these MAPs. Simulation results have demonstrated the improved performance of our schemes.

Chapter 4: Mobility-aware Reassociation Control in WMNs

In the previous chapter, we consider static STAs and network condition is not rapidly changing. In this chapter, we propose a Mobility-Aware Reassociation (MARA) control scheme for dynamic networks where the STAs are mobile. MARA makes better use of the network resource by prolonging mobile stations' association period with the good-backhaul MAPs. In MARA, STAs adjust their scan intervals and make association decisions based on the estimated moving directions and the association cost of the nearby MAPs. Our simulation results show that the proposed scheme achieves improved end-to-end performance consistently under different network scenarios.

4.1. Introduction

To maintain network connectivity, a STA may trigger a handoff procedure and reassociate with one of the available MAPs when it detects that its connection with the currently associated MAP is lost. Alternatively, instead of waiting until the current connection becomes unacceptable, STAs may frequently detect the quality of nearby MAPs and compare them with that of the associated one, so that STAs can be aware of the real time network condition and always associate with the most suitable MAP. A layer-2 handoff consists of four stages: i) triggering; ii) discovery; iii) selection; and iv) commitment [46], [48]. A STA triggers a handoff when it identifies the need to associate with a better MAP. Then it collects information about the MAPs in the vicinity through active scan or passive scan, and identifies the best MAP according to certain reassociation MAP selection criteria. Finally, if a new MAP is selected, the STA disassociates from the old MAP and reassociates with the new one.

In this chapter, we propose a Mobility-Aware Reassociation (MARA) control scheme that focuses on the selection stage, providing a solution on how to select a MAP to associate with so that network resources can be better utilized and end-to-end performance can be improved. In order to capture the network dynamics and discover better MAPs for reassociation in a timely and adaptive way, we also design a scan triggering scheme that adjusts the scan interval between two consecutive scans based on the estimated STA's moving direction as well as comparison on the MAP's backhaul cost.

A lot of research efforts on layer-2 handoff have been dedicated to reducing the interruption period caused by the handoff via shortening the AP discovery time. As for reassociation triggering mechanisms, in the current WLANs, a STA detects the loss of connection to the associated AP by indicators such as the number of lost beacons, the number of consecutive unacknowledged frames, and signal strength or quality lower than the threshold. These mechanisms result in unnecessary handoff and control message overhead under medium to high load conditions [53]. Network performance can be improved by timely reassociation with a better AP before the current connection degrades to an unusable level. In [48], STAs continuously monitor the signal strength of the APs operating on STA's current as well as overlapping channels and compare them with the associated one. However, in a real deployment, many APs operate in orthogonal channels, and this scheme may miss some good APs and result in suboptimal AP selection. In [40], STAs periodically scan each channel with a fixed scan interval to discover network dynamics. However, the scanning and reassociation processes interrupt the STA's communication and may cause packet loss. In MARA, we propose a scan interval adjustment scheme that prolongs the scan interval if no better MAPs are found and shortens the scan interval if MAPs better than the old one is found or the STA is estimated to be moving towards a MAP with better backhaul. Therefore, the total number of scans conducted will be reduced without missing opportunities to reassociate with a better MAP.

A reassociation threshold is often applied to avoid STAs from frequently changing association with certain MAPs. Reassociation with a new MAP is allowed only if the performance improvement is higher than the threshold. Instead of a fixed threshold as in [40], in MARA, the threshold is adjusted according to a STA's moving direction. When it is moving towards MAPs with smaller/larger backhaul cost, the threshold is lower/higher accordingly; as a result, the STA will associate with the better backhaul MAPs for a longer time.

4.2. MARA: Mobility-Aware Reassociation Control

We adopt the association metric proposed in Chapter 3, Link Quality aware Airtime with access Weight adjustment (LQAW), for calculating the total association cost of the MAPs. Next we introduce the reassociation procedure of MARA.

Step1: MAP information collection

STAs periodically discover MAP information in the vicinity by scanning each channel and listening to the MAP beacons that carry additional information such as access channel idleness ratio and backhaul cost. Other information about the MAPs, e.g. link rate and packet error rate, are estimated from the SNR of the received beacons. After scanning the last channel, the STA calculates and updates the total association cost of the MAPs discovered during the scan.

Step2: Moving direction estimation

At the end of a scan, a STA estimates its moving direction (*Direction*) based on the MAPs' backhaul costs and the change of distances to the MAPs as given in Algorithm 4.1. At the same time, the total association cost improvement threshold (T_{TC}) is also determined, which is to be used in Step3.

Algorithm 4.1: Moving Direction Estimation

if $\exists i : BC_i < 0.8 \cdot BC_A \wedge D_{i,t-1} - D_{i,t} > D_{th}$ then
    Direction ←*MovingToGood*
    $T_{TC} \leftarrow T_{TC\_Low}$
elseif $\exists i : 0.8 \cdot BC_A \leq BC_i \leq 1.2 \cdot BC_A \wedge D_{i,t-1} - D_{i,t} > D_{th}$ then
    Direction ←*MovingToMiddle*
    $T_{TC} \leftarrow T_{TC\_Middle}$
elseif $\exists i : BC_i > 1.2 \cdot BC_A \wedge D_{i,t-1} - D_{i,t} > D_{th}$ then
    Direction ←*MovingToBad*
    $T_{TC} \leftarrow T_{TC\_High}$
else
    Direction ←*Static*
    $T_{TC} \leftarrow T_{TC\_Middle}$

where i is a MAP in the vicinity of the STA; BC_i and BC_A are the backhaul costs of MAP i and the currently associated MAP, respectively; $D_{i,\ t\text{-}1}$ and $D_{i,t}$ are the distances to i measured in two consecutive scans; D_{th} is the distance threshold above which a STA is considered moving towards a MAP.

The first reason for setting the backhaul cost threshold 0.8 and 1.2 is to set a range of backhaul cost that is around the backhaul cost of the currently associated MAP, so that we make sure the STA is indeed moving towards a better-backhaul MAP or a bad-backhaul MAP rather than a similar-backhaul MAP. Take the network depicted in Fig. 4.1 for example. Theoretically, the backhaul cost of the Class2 MAPs (*M1*, *M2*, *M3*, and *M4*)

(1/24+1/18) is 130% higher than that of the Class1 MAPs (1/24) and 36% lower than that of the Class3 MAPs (1/24+1/18+1/18). In simulations, due to network dynamics, the measured backhaul cost of the Class2 MAPs may not be the same among themselves. By setting the (0.8, 1.2) range, we make sure the STAs estimated moving towards better-backhaul or bad-backhaul MAPs are indeed moving towards the Class1 MAPs or the Class3 MAPs rather than the Class2 MAPs.

The second reason for setting the backhaul cost threshold is to guarantee the performance improvement obtained by STA moving direction estimation. For example, when the STA is estimated moving towards a good-backhaul MAP, it will lower its reassociation threshold and decrease its scan interval to the lowest value so that it can associate with the good-backhaul MAP as early as possible. It is not necessary to conduct these actions if the backhaul of the new MAP is only marginally better than that of the current associated MAP.

The distance to a MAP can be estimated by a path loss model that properly characterizes the particular wireless environment. Alternatively, it can be estimated from the STAs' location information which can be determined by any localization methods that make use of the signal strength information of multiple MAPs obtained during one scan. We do not propose any specific localization method to use. The moving direction estimation in MARA does not require very accurate position information; only the change of location during a time interval of tens of seconds needs to be detected. In fact, the localization error does not impact much on the performance of MARA as will be shown in the simulation results.

Step3: Find MAP_{Best} and compare it with $MAP_{Associated}$

The STA searches for the MAP with the smallest total association cost (MAP_{Best}) in the set of discovered MAPs. Then it selects either MAP_{Best} or the current associated MAP (MAP_A) as a candidate for reassociation ($MAP_{Associating}$) as in (4.1) where TC is the total association cost and T_{TC} is the reassociation threshold determined in Step2. To avoid association oscillation between MAPs with similar cost, MAP_{Best} is selected only if the total association cost improvement of MAP_{Best} over MAP_A is larger than the reassociation threshold T_{TC}. When the STA is moving towards the good or bad backhaul MAPs, T_{TC} is lower or higher accordingly, so it is more likely for STAs to associate with the good-backhaul MAPs.

$$MAP_{Associating} = \begin{cases} MAP_{Best} & (TC_A - TC_{Best} > T_{TC} \cdot TC_A) \\ MAP_A & (TC_A - TC_{Best} \le T_{TC} \cdot TC_A) \end{cases} \tag{4.1}$$

Step4: Look for MAP_{BB} and determine $MAP_{ToAssociate}$

Another association candidate is the MAP with better backhaul (MAP_{BB}), i.e. the MAP with the smallest total association cost among all the MAPs whose backhaul cost is smaller than that of $MAP_{Associating}$. The final MAP selected for reassociation ($MAP_{ToAssociate}$) is determined as in (4.2). By considering MAP_{BB} as an association candidate, there are more chances for STAs to associate with the good-backhaul MAPs and the network resource can be better utilized.

$$MAP_{ToAssociate} = \begin{cases} MAP_{BB} & (TC_{BB} < 1.4 \cdot TC_{Associating}) \\ MAP_{Associating} & (TC_{BB} \ge 1.4 \cdot TC_{Associating}) \\ MAP_{Associating} & (\text{no } MAP_{BB}) \end{cases} \tag{4.2}$$

Step5: Schedule next scan

Update the scan interval and schedule next scan. Adequate number of scans is necessary for timely discovery of the network status. But too many scans will cause packet loss and disturb normal communication, and is unnecessary especially when the network dynamics are low, e.g. when STAs are static.

In MARA, the scan interval ($T_{Interval}$) is prolonged by 1.5 times if the current associated MAP is found to have the smallest total association cost, until reaching the maximum scan interval allowed ($T_{Interval\_Max}$). Otherwise, if MAPs that are better than the associated one are found or the STA is moving towards the good-backhaul MAPs, the scan interval is reduced to the minimum value ($T_{Interval\_Min}$) so that reassociation opportunities can be discovered in time.

Step6: Reassociation

Finally, if a new MAP is selected as $MAP_{ToAssociate}$, the STA disassociates with the old MAP and reassociates with the new one by exchanging corresponding management frames. Otherwise, the STA switches back to the old MAP's channel and stays associated with it.

4.3. Performance Evaluation

We have implemented the proposed reassociation scheme in network simulator ns-3. We simulate 12 MAPs in a grid or random topology and one portal at the centre of a rectangular field of 480m×140m. STAs are randomly located and moving along random directions at certain speeds until the field boundary; then they continue moving along another random direction. We use the 802.11s mesh module in ns-3 for the backhaul routing and peer management. Each STA sends UDP packets to the portal at the data generation rate of 150Kbps. The result shown is the average of 16 runs.

We compare the performance of MARA with two benchmark schemes: SNR and PF. In the SNR scheme, a STA does not conduct a scan until the SNR of the current MAP drops below the threshold, which indicates poor link quality. In our simulation the unusable link SNR is about 0.7. If the re-association threshold of SNR is set closer to 0.7, the STAs would start looking for new MAPs when its current link quality is very poor, resulting in very poor performance. We set the SNR threshold for SNR-based reassociation control scheme to be 1.05 to improve the performance of the original SNR-based reassociation scheme. On the other hand, if the threshold is larger than 1.05, there will be STAs that keep conducting scans and cannot continue with normal communication because they are located at the edge of their associated MAPs' coverage range. The PF scheme stands for periodic scan with fixed scan interval and fixed reassociation threshold. All three schemes use LQAW as the association metric. Comparing the reassociation procedure, SNR and PF only conduct Step1, Step3, and Step6 of that in MARA.

The protocol parameters are set as follows, for LQAW: $\lambda_t = 0.6$, $\omega_{Min} = 0.25$, $\omega_{Max} = 0.45$; for PF: $T_{Interval} = 10$s, $T_{TC} = 0.1$; for MARA: $D_{th} = 1$m, $T_{TC\_Low} = 0$, $T_{TC\_Middle} = 0.1$, $T_{TC\_High} = 0.6$, $T_{Interval_Min} = 10$s, $T_{Interval_Max} = 60$s.

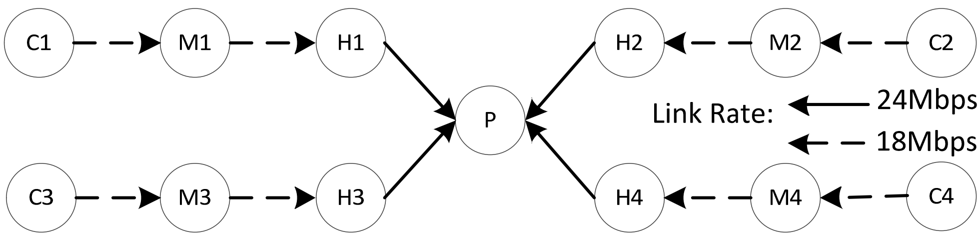

Figure 4.1: The grid MAP topology.

Fig. 4.1 shows the grid MAP topology. According to the MAPs' backhaul condition, 12 MAPs can be categorized into three classes: *H1-H4* are Class1 MAPs as they have the best backhaul condition and the highest backhaul capacity; *M1-M4* are Class2 MAPs; *C1-C4* are Class3 MAPs and their effective bandwidths are the smallest.

4.3.1. Performance of MARA

Fig. 4.2 and Fig. 4.3 depict the performances of the three schemes in the grid topology when the STA speed is 1m/s and localization error is 3m. It is clear that MARA achieves the highest aggregate throughput and the lowest average end-to-end packet delay. When the number of STAs is smaller than 30, the backhaul is not saturated and is able to handle all offered load from the STAs. When the number of STAs is larger than 30, the backhaul is saturated and becomes the bottleneck of the whole network. Fig. 4.4 shows where packets are lost when the number of STAs is 50. We can see that the majority of packet loss occurs at the backhaul. MARA achieves the lowest packet loss at both access networks and the backhaul. Next we analyse how MARA achieves that performance.

MARA achieves much less packet loss at the backhaul because STAs are associated with the good-backhaul MAPs for a longer time. It can be seen from Fig. 4.5 that with MARA, STAs have the longest association time with Class1 MAPs and the shortest association time with Class3 MAPs. MARA achieves that by reducing the reassociation threshold and shortening the scan interval when STAs are moving towards the good-backhaul MAPs and further lowering the reassociation threshold if any better-backhaul MAPs are found. As discussed previously, transmission from the good-backhaul MAPs consumes less network resource. So when more loads from STAs are transmitted by the good-backhaul MAPs, the network resource is better utilized and the backhaul network capacity is higher.

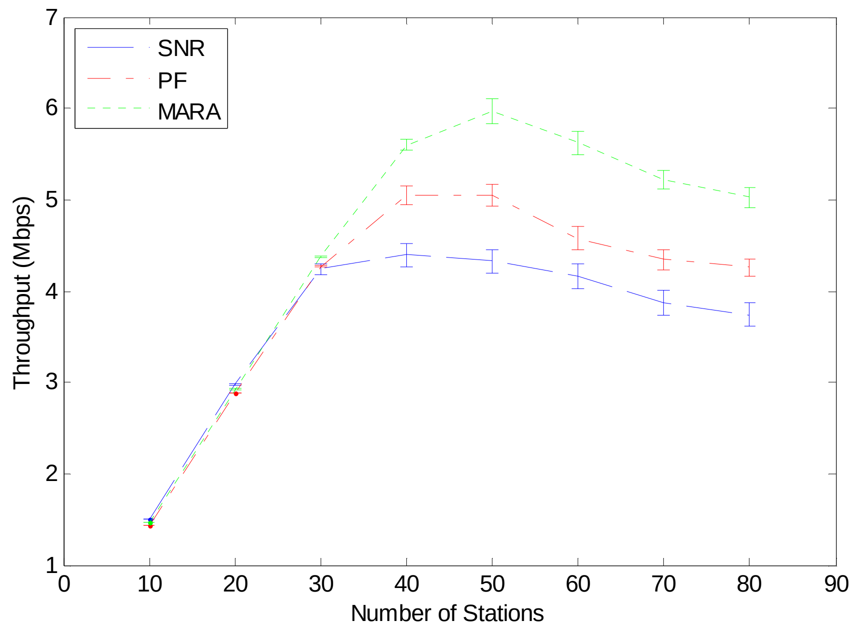

Figure 4.2: Aggregate throughput in the grid topology.

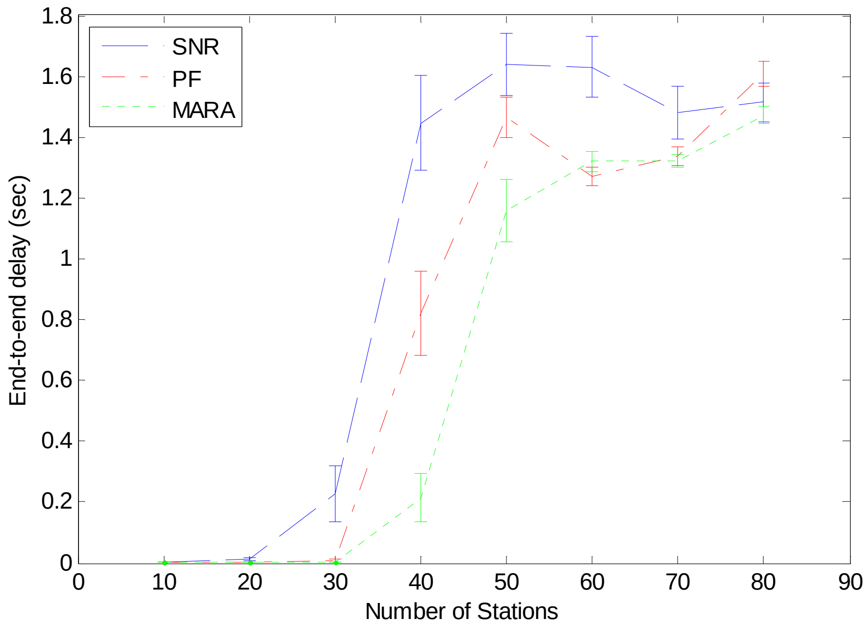

Figure 4.3: Average end-to-end packet delay in the grid topology.

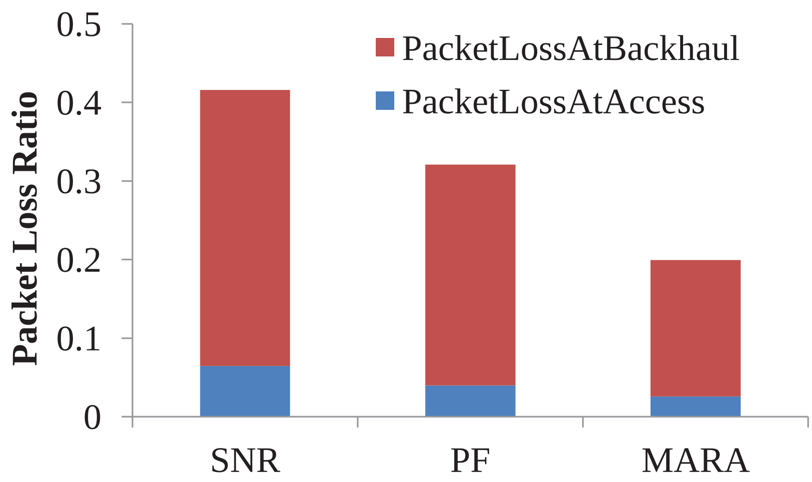

Figure 4.4: Packet loss at the access networks and at the backhaul.

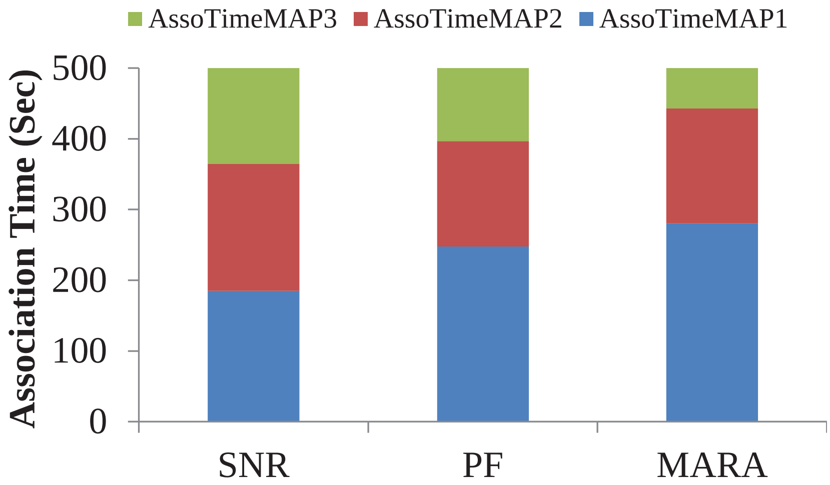

Figure 4.5: Average association time with 3 MAP classes.

We measure the interruption to communication caused by periodic scans by the packet loss at the access networks. In the simulation, each scan process lasts 400 milliseconds, and UDP packets generated during this period are dropped. In the simulations, a UDP packet will be dropped if the MAC layer is in scanning status when the packet is passed from the network layer to the MAC layer. In fact, we just make use of this number of packets dropped as a way to represent the network interruption caused by periodic scans. In the case of UDP packets being put in queues instead of being dropped, the access network packet drop for PF and MARA would be 0, and therefore we can make use of another index such as the number of scans conducted (Table 4-1) or the total time consumed by scanning to measure the interruption caused by scans. Table 4-1 lists the average number of scans conducted per STA during the simulation period of 500s. Although a very small number of scans are conducted in SNR, SNR has the largest number of packet loss at the access networks, as shown in Fig. 4.4, because of the low access network capacity and poor average link quality due to more STAs at the cell edge. For PF and MARA, the main reason for the packet loss at the access networks is the periodic scans. MARA's dynamic scan interval adjustment reduces the number of scans conducted without missing network dynamics.

Table 4-1: AVERAGE NUMBER OF SCANS CONDUCTED PER STA

Protocol	SNR	PF	MARA
No. of Scans per STA	2	49	31

4.3.2. Adaptability of MARA

We investigate the adaptability of MARA under different STA speeds and different localization errors. Fig. 4.6 shows the performance of 50 STAs under speeds from 0m/s to 8m/s, MARA achieves the highest throughput at all speeds. We simulate the STA location estimated by certain RSSI-based localization method by adding random error to STA's true location. From Table 4-2, we can see that localization error has very little impact on MARA's performance. MARA does not require very accurate location information to estimate the moving direction; only the change of distances to MAPs between two scans is needed. Even if the estimated moving direction is incorrect, reassociation decision is made mainly based on the MAP backhaul metric which is not affected by the error. Lastly, wrong direction estimation does not worsen the performance and there are so many correct estimations that the performance is still good.

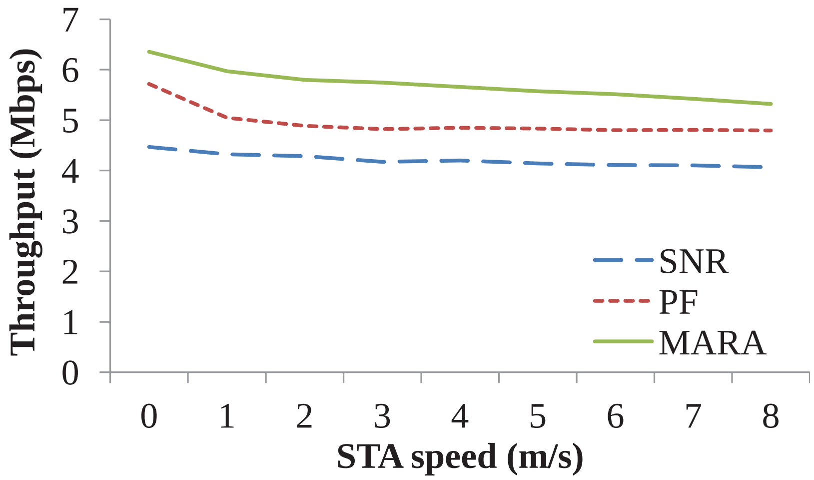

Figure 4.6: Aggregate throughput under different moving speeds.

Table 4-2: IMPACT OF THE MEAN LOCALIZATION ERROR

Mean Error (m)	1	3	6	9	12
Throughput (Mbps)	5.99	5.97	5.96	5.95	5.95

4.3.3. Random Topology

As shown in Fig. 4.7 and Fig. 4.8, again MARA achieves the highest aggregate throughput and the lowest average end-to-end packet delay in the topology of randomly placed MAPs. Compared to the grid topology, though multi-hop paths still exist in the random topology, there could be more MAPs that are one-hop away from the portal resulting in higher backhaul capacity. As the backhaul condition difference among MAPs is smaller in the random topology, the performance improvement of MARA over PF is slightly lowered compared to in the gird topology.

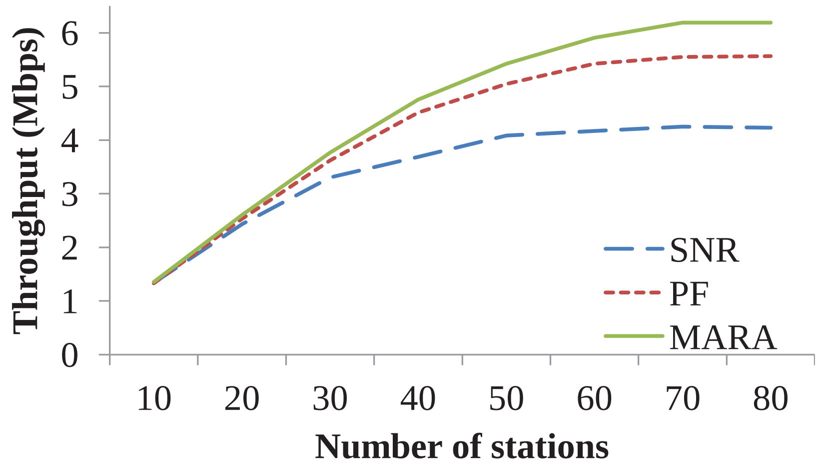

Figure 4.7: Aggregate throughput in the random topology.

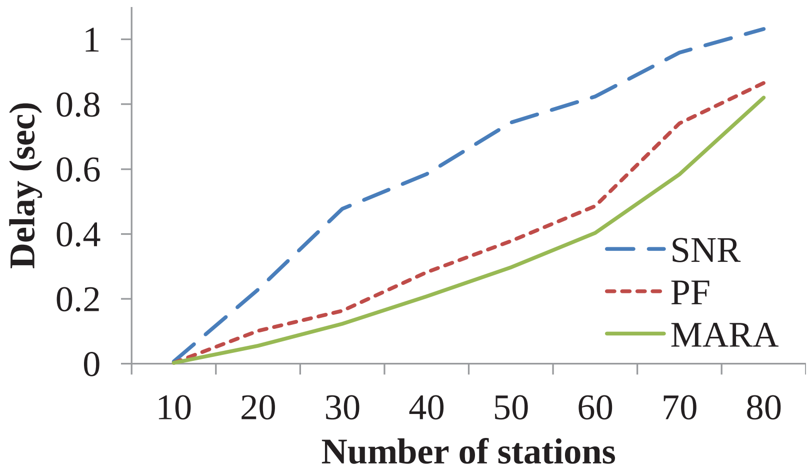

Figure 4.8: Average end-to-end packet delay in the random topology.

4.4. Conclusion

In this chapter, we have proposed MARA, a Mobility-Aware ReAssociation control scheme, which takes the wireless backhaul and stations mobility into consideration. By prolonging stations' association time with the good-backhaul MAPs, MARA improves the backhaul network resource utilization as well as the end-to-end network performance. By dynamically adjusting scan interval, MARA is able to discover network dynamics in a smart and timely way. Simulation results have demonstrated the improved performance of MARA under different network scenarios.

Chapter 5: Optimal Association in WMNs

In Chapter 3 and Chapter 4, we have proposed distributed heuristic association control schemes for static and dynamic WMNs, respectively. In this chapter, we propose and analyse centralized optimization-based association control schemes. We formulate the optimization problems of optimal joint association and bandwidth allocation in WMNs, considering max-min fairness (MM) and proportional fairness (PF) objectives. In our proposed approximation algorithms, we first relax the integral association constraint and get an optimal fractional association solution. Then we propose two rounding algorithms, Largest Fraction Rounding and Bipartite Graph Rounding, to get an integral solution, and analyse their theoretical approximation ratios. Lastly, we propose two approximation ratio improvement algorithms so that the improved approximation ratio can more accurately reflect the true performance gap between the produced solution and the optimal one. Our simulation results show that the proposed algorithms achieve performances that are close to the optimal and outperform popular heuristic algorithms. We also compare the performance of PF and MM in WMNs in terms of network throughput and fairness in user bandwidth. Finally, we compare the performances of the proposed rounding algorithms and show that the approximation ratio can be reduced to 1-2 by the proposed ratio improvement algorithms. Therefore, our proposed algorithm is able to achieve nearly optimal association control as well as bandwidth allocation considering MM or PF fairness, with small approximation ratios, in wireless mesh networks.

5.1. Introduction

The association between STAs and MAPs determines the logical network topology; therefore it has significant impact on the load distribution and the performance of the whole network such as the aggregate throughput and fairness among STAs. Association control and user bandwidth allocation are closely related to each other, and should be jointly considered for optimal network resource management, which have been demonstrated in [32]-[35]. Network throughput and user fairness usually are two conflicting objectives in bandwidth allocation algorithms [57]. There are two commonly used fairness criteria: max-min fairness (MM) [61] and proportional fairness (PF) [60]. MM tries to allocate the rate of all flows as equal as possible; PF, on the other hand, increases the network throughput by sacrificing fairness, exploiting the tradeoff between the two.

For association control in WMNs, most of the previous research works have been on metric based heuristic schemes [36]-[41]. Their association metrics consider both access and backhaul network condition, and are often a weighted sum of the two. As there are always some parameters to set, such as access weight or channel idleness ratio threshold, it is difficult for heuristic schemes to perform well in all network scenarios, which we will demonstrate in our simulation results. Therefore there is a need for centralized optimal association control schemes for WMNs, on which very few previous works exist.

We have reviewed previous works on optimization-based association control algorithms for WLANs [32]-[35] and WMNs [42], [43] in Section 2.1.2. Our proposed association control method adopts an optimization based approach just like [32]-[35], [42]. Instead of studying either max-min fairness or proportional fairness as in the previous works, we formulate optimal association problems for both fairness objectives. Unlike

[33] and [42] we provide approximation algorithms with approximation ratio analysis in addition to the optimization problem formulation. Our algorithm adopts a relaxation-rounding approximation framework similar to those in [32], [34], [35], with significant modification to take account of the wireless backhaul constraint of WMNs. In addition, we propose approximation ratio improvement algorithms which are not seen in the previous works.

In this chapter, we formulate the problem of joint association and bandwidth allocation in WMNs as an optimization problem with the objective functions considering either max-min fairness or proportional fairness. As the problem is a 0-1 integer program and NP hard, we propose approximation algorithms to get a solution that is as close to the optimal one as possible. The proposed algorithm first relaxes the integer variable constraints and gets a fractional association solution, which is then rounded to an integral solution by using one of the rounding algorithms we propose: Largest Fraction Rounding (LFR) and Bipartite Graph Rounding (BGR). We refer to the gap between the approximated solution and the optimal solution as the approximation ratio. We analyse the approximation ratio theoretically and propose two algorithms to improve the approximation ratios of LFR and BGR respectively. Our simulation results show that the proposed algorithm achieves bandwidth allocation that is very close to the optimal one and outperforms the state of the art heuristic algorithms. We also show via simulations that the approximation ratio can be reduced to 1-2 by the proposed approximation ratio improvement algorithms.

5.2. Network Model

In this chapter, we assume carefully planned channel allocation among MAP access networks so that adjacent cells do not interfere with each other. We assume the access link rates between STAs and MAPs as well as the backhaul link rates between MAPs are known. We assume the wireless multi-hop backhaul logical topology is a tree structure rooted at the portal and the routing has been done by a routing protocol such as Hybrid Wireless Mesh Protocol (HWMP), which is the default routing protocol in IEEE 802.11s [8]. In the HWMP, each MAP finds its shortest path towards the portal. Fig. 5.1 shows an example of a backhaul routing tree constructed by HWMP for 5 MAPs, where node *P* is the portal and all the links shown are equal-length and non-directional.

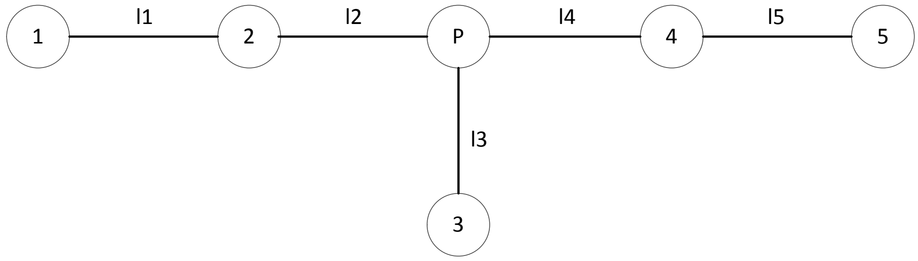

Figure 5.1: A 5-MAP backhaul routing tree.

Backhaul links that do not interfere with each other can transmit at the same time. To count the spatial reuse of the backhaul links, we make use of the concept of backhaul clique to represent the backhaul link transmission constraint. A backhaul clique is defined as a maximal set of backhaul links that are in mutual conflict with each other, i.e. at any time, only a single link within a backhaul clique is allowed to transmit. For example, in Fig. 5.1, only link l_1 and l_5 can transmit at the same time and there are 2 backhaul cliques in total, which are $clique_1=\{l_1, l_2, l_3, l_4\}$ and $clique_2=\{l_2, l_3, l_4, l_5\}$.

We briefly introduce how backhaul cliques are constructed here. We assume a fixed transmission range *TransR* and a fixed interference range *IntR*. Given the backhaul routing graph, we know all backhaul links as those shown in Fig. 5.1, i.e. $\{l_1, l_2, l_3, l_4, l_5\}$. Backhaul links are directional if we consider only upstream or downstream traffic and bi-directional if we consider both upstream and downstream traffic. We next construct a conflict graph where vertices represent backhaul links and an edge exists between two conflicting links. Two links are in conflict with each other if one's receiver is within the interference range of the other's transmitter. If the backhaul links are bi-directional, the two nodes connected by a link should be considered as both transmitter and receiver. Finally, we can find all maximal cliques within the constructed conflict graph by using algorithms such as the Bron-Kerbosch algorithm [63]. Take the network in Fig. 5.1 as an example, where the interference range is 1.2 times of the link length. Any pair of backhaul links are conflict with each other expect the pair of links (l_1, l_5). By constructing the corresponding conflict graph and applying the Bron-Kerbosch algorithm on the conflict graph, we get the set of all the backhaul cliques {$clique_1$, $clique_2$} as given above.

Next we introduce the notations used in this chapter. We use M, S, and K_B to denote the set of MAPs, the set of STAs, and the set of backhaul cliques, respectively, while using i, j, and k to denote individual MAP, STA, and backhaul clique, respectively. We denote the access link rate between MAP i and STA j by r_{ij}. We use y_{ki} to indicate whether MAP i's backhaul path passes through clique k, i.e. y_{ki} =1 if there exists a link $l \in k$ such that $l \in path(i)$, where $path(i)$ is the set of links on the routing path between i and the portal. If y_{ki} =1, we use r_{ki} to denote the effective backhaul link rate for i in k. r_{ki} is defined as in (5.1), which represents the time consumed for transmitting one bit of i's traffic in k.

$$\frac{1}{r_{ki}} = \sum_{l:l \in k \wedge l \in path(i)} \frac{1}{r_l} \tag{5.1}$$

We use x_{ij} to indicate the association between i and j. $x_{ij} \in \{0,1\}$ for integral association where each STA is allowed to associate with only one MAP. x_{ij}=1 if j is associated with i; otherwise 0. $x_{ij} \in [0,1]$ for fractional association by which the integral association constraint is relaxed such that each STA is allowed to fractionally associate with multiple MAPs. In both cases, we have $\forall j \in S : \sum_{i \in M} x_{ij} = 1$. We use b_j and B_i to denote the bandwidth allocated to j and i, where $B_i = \sum_{j \in S} x_{ij} \cdot b_j$. We use b_{ij} to denote the bandwidth allocated to j to communicate with i in a fractional association, so we have $b_j = \sum_{i \in M} b_{ij}$, $B_i = \sum_{j \in S} b_{ij}$, and $x_{ij} = b_{ij} / b_j$. We denote the set of MAPs that have fractional association with j as $M(j)$, i.e. $M(j) = \{i : x_{ij} > 0\}$, and denote the set of STAs that are fractionally associated with i as $S(i)$, i.e. $S(i) = \{j : x_{ij} > 0\}$. The final result of our algorithm is an association matrix $\{x_{ij}\}$ and a bandwidth allocation vector $\{b_j\}$, which is denoted as (X, B).

5.3. Optimal Joint Association and Bandwidth Allocation Algorithm

5.3.1. Optimization Problem Formulation

We formulate the optimal integral association problem (iAP) in WMNs as a set of optimization problems. iAP for max-min fairness is denoted as iAP-MM; iAP for proportional fairness is denoted as iAP-PF.

iAP-MM is formulated in (5.2)-(5.9). Denote the minimum STA bandwidth in a feasible rate vector as b_{min}. In the first step of iAP-MM, we maximize b_{min} and get an optimal solution $b^*_{\min}$. In the second step, the network throughput is maximized. iAP-MM is a mixed integer nonlinear program and hard to solve optimally, which can be proved by using a simple reduction from the partition problem in [64].

iAP-MM:

Step1:

Max $\quad b_{\min}$

s.t. $\quad \forall j \in S: \quad \sum_{i \in M} x_{ij} \frac{b_j}{r_{ij}} \leq 1 \qquad (5.2)$

$$\forall i \in M: \quad \sum_{j \in S} x_{ij} \frac{b_j}{r_{ij}} \leq 1 \qquad (5.3)$$

$$\forall k \in K_B: \sum_{i \in M} \frac{y_{ki}}{r_{ki}} \sum_{j \in S} x_{ij} b_j \leq 1 \qquad (5.4)$$

$$\forall j \in S: \quad \sum_{i \in M} x_{ij} = 1 \qquad (5.5)$$

$$\forall j \in S: \quad b_j \geq b_{\min} \qquad (5.6)$$

$$\forall i \in M, j \in S: \quad x_{ij} \in \{0,1\}, \quad b_{\min} \geq 0 \qquad (5.7)$$

Step2:

Max $\quad \sum_{j \in S} b_j$

s.t. $\quad$ constraints (5.2)-(5.5),and

$$\forall j \in S: \quad b_j \geq b^*_{\min} \qquad (5.8)$$

$$\forall i \in M, j \in S: \quad x_{ij} \in \{0,1\} \qquad (5.9)$$

Constraint (5.2) states that the total transmission time of one STA is less than 1. (5.3) says that the total transmission time of one MAP communicating with all of its associated STAs is less than 1. (5.4) states that the total transmission time of the backhaul links in one backhaul clique is less than 1, where the traffic load carried by the clique originates from all the STAs whose associated MAPs' backhaul paths towards the portal pass through the clique. (5.5) says that each STA is associated with one MAP only as (5.7) and (5.9) require integral association. (5.6) states that the bandwidth allocated to each STA is no less than the minimum one b_{min}.

iAP-PF is formulated in (5.10). It shares most of the constraints with iAP-MM, despite different objective functions. iAP-PF is also a mixed integer nonlinear program and hard to solve optimally, which can be proved by slightly adapting the procedure in [65].

iAP-PF:

Max $\sum_{j \in S} \log(b_j)$

s.t. constraints (5.2)-(5.5), and

$$\forall i \in M, j \in S: \quad x_{ij} \in \{0,1\}, \quad b_j \ge 0 \tag{5.10}$$

5.3.2. Introducing the Approximation Algorithm

Algorithm JABA:

1. Relax iAP to fAP.
2. Solve fAP and get an optimal fractional solution (*X'*, *B'*).
3. Round the fractional association *X'* to an integral one $\hat{X}'$ by one of the rounding algorithms.
4. Solve iAP with $X = \hat{X}'$ as input and get an integral bandwidth allocation $\hat{B}'$.
5. $(\hat{X}', \hat{B}')$ is the output.

Figure 5.2: Algorithm JABA.

The integral association problem is hard to solve due to the exponentially increasing solution space that is on the order of $2^{M \times N}$ where *M* and *N* are the number of MAPs and STAs in the network. Therefore, we propose an approximation algorithm, named Joint Association and Bandwidth Allocation (JABA), to get a working solution in polynomial time, whose approximation ratio is analysable. The algorithm is summarized in Fig. 5.2. In the first step, we relax the integral association constraint by allowing STAs to fractionally associate with multiple MAPs. The relaxed fractional association problem is referred to as fAP. fAP is either linear or convex, and therefore can be solved to the desired precision in polynomial time. In the second step, we solve fAP and get an optimal solution, denoted as (*X'*, *B'*), which is an upper bound for any integral solution due to less restriction in the optimization constraints. In the third step, we get an integral association matrix, denoted as $\hat{X}'$, by rounding the fractional solution *X'* using one of the rounding algorithms we are proposing, namely Largest Fraction Rounding (LFR) and Bipartite Graph Rounding (BGR). In the fourth step, we optimally solve iAP with $X = \hat{X}'$ as input and get an integral bandwidth allocation $\hat{B}'$. Finally $(\hat{X}', \hat{B}')$ is the output of JABA.

5.3.3. Optimization Problem Relaxation

We relax iAP by introducing a fractional bandwidth allocation matrix $\{b_{ij}\}$. fAP can be derived from iAP by replacing b_j with $\sum_{i \in M} b_{ij}$ and replacing $x_{ij} \cdot b_j$ with b_{ij}. The fractional association problem for max-min fairness (fAP-MM) is formulated in (5.11)-(5.18).

fAP-MM:

Step1:

Max $\quad b_{\min}$

s.t.
$$\forall j \in S: \quad \sum_{i \in M} \frac{b_{ij}}{r_{ij}} \le 1 \tag{5.11}$$

$$\forall i \in M: \quad \sum_{j \in S} \frac{b_{ij}}{r_{ij}} \le 1 \tag{5.12}$$

$$\forall k \in K_B: \quad \sum_{i \in M} \frac{y_{ki}}{r_{ki}} \sum_{j \in S} b_{ij} \le 1 \tag{5.13}$$

$$\forall j \in S: \quad \sum_{i \in M} b_{ij} \ge b_{\min} \tag{5.14}$$

$$\forall j \in S: \quad b_j \ge b_{\min} \tag{5.15}$$

$$\forall i \in M, j \in S: \quad b_{ij} \ge 0, \quad b_{\min} > 0 \tag{5.16}$$

Step2:

Max $\quad \sum_{j \in S} \sum_{i \in M} b_{ij}$

s.t. $\quad$ constraints (5.11)-(5.13), and

$$\forall j \in S: \quad \sum_{i \in M} b_{ij} \geq b^*_{\min} \tag{5.17}$$

$$\forall i \in M, j \in S: \quad b_{ij} \geq 0 \tag{5.18}$$

Using the same relaxation method as for max-min fairness, the fractional association problem for proportional fairness (fAP-PF) is formulated in (5.19)-(5.20).

fAP-PF:

Max $\quad \sum_{j \in S} \log(b_j)$

s.t. $\quad$ constraints (5.11)-(5.13), and

$$\forall j \in S: \quad b_j = \sum_{i \in M} b_{ij} > 0 \tag{5.19}$$

$$\forall i \in M, j \in S: \quad b_{ij} \geq 0 \tag{5.20}$$

fAP-MM is a linear program; fAP-PF is a convex program. We can solve them in polynomial time and get an optimal fractional association and bandwidth allocation solution (*X'*, *B'*).

5.3.4. Rounding Algorithms

We propose two rounding algorithms, LFR and BGR, to round the fractional association $\{x'_{ij}\}$ to binary integer so that each STA associates with only one MAP. A good rounding algorithm gives an integral solution that is as close to the optimal solution as possible, i.e. approximation ratio is as close to 1 as possible.

A. Largest Fraction Rounding

Denote the set of MAPs that have fractional association with STA j as $M(j) = \{i : b'_{ij} > 0\}$. By LFR, *j* associates with MAP i' that carries the largest portion of the bandwidth allocated to *j*, i.e. $b'_{i'j} \geq b'_{ij} \quad \forall i : i \in M(j), i \neq i'$.

B. Bipartite Graph Rounding

Algorithm BGR:

Given the optimal fractional solution of fAP, $(\{x_{ij}'\},\{b_j'\})$.

1. Calculate $B_i' = \sum_{j\in S} b_{ij}'$ for each $i \in M$.
2. Formulate a generalized assignment problem using $\{B_i'\}$ and $\{b_j'\}$.
3. Construct a bipartite graph $BG(X')$ and corresponding fractional matching weight y and utility u on the edges.
4. Find a maximum-utility integer matching $Match(y)$ that exactly matches all STA nodes in $BG(X')$ by solving a linear program named Maximum Utility Matching Problem (MUMP) (5.27)-(5.29).
5. For each edge $e_{(i,s),j} \in Match(y)$, associate STA j with MAP i, i.e. set $\hat{x}_{ij}' = 1$. The integral association matrix $\{\hat{x}_{ij}'\}$ is the output.

Figure 5.3: Algorithm BGR.

The idea of rounding fractional solution using a bipartite graph was first proposed in [66] for the generalized assignment problem in scheduling unrelated parallel machines. Our proposed BGR algorithm is summarized in Fig. 5.3. Compared to the algorithm in [66], BGR have two modifications to take into consideration the wireless backhaul constraint: the generalized assignment problem formulation and the sorting criteria in bipartite graph construction.

(a). Generalized Assignment Problem Formulation

Given the fractional solution $\{b_{ij}'\}$, we can calculate the fractional bandwidth allocation for each STA and MAP using $b_j' = \sum_{i\in M} b_{ij}'$ and $B_i' = \sum_{j\in S} b_{ij}'$. With $\{b_j'\}$ and $\{B_i'\}$ known, we reformulate the association problem as a generalized assignment problem (GAP) as in (5.21)-(5.24).

GAP:

Max $\sum_{j \in S} \sum_{i \in M} x_{ij} u_{ij}$

s.t. $\forall j \in S: \quad \sum_{i \in M} x_{ij} = 1$ (5.21)

$$\forall i \in M: \quad \sum_{j \in S} x_{ij} \frac{b_j^{'}}{r_{ij}} \le 1 \qquad (5.22)$$

$$\forall i \in M: \quad \sum_{j \in S} x_{ij} b_j^{'} \le B_i^{'} \qquad (5.23)$$

$$\forall i \in M, j \in S: \quad x_{ij} \in \{0,1\} \qquad (5.24)$$

where the utility function u_{ij} equals b_j' for max-min fairness as in (5.25) and log(b_j') for proportional fairness as in (5.26). Though the objective function of GAP is a constant as shown in (5.25) and (5.26), we need the utility function in step-4 of BGR, i.e. finding a maximum utility matching. The access network transmission time constraint in iAP is satisfied when (5.22) is satisfied. The backhaul network constraints in iAP are satisfied when (5.23) is satisfied.

$$\sum_{j \in S} \sum_{i \in M} x_{ij} u_{ij} = \sum_{j \in S} \sum_{i \in M} x_{ij} b_j^{'} = \sum_{j \in S} b_j^{'} \qquad (5.25)$$

$$\sum_{j \in S} \sum_{i \in M} x_{ij} u_{ij} = \sum_{j \in S} \sum_{i \in M} x_{ij} \log(b_j^{'}) = \sum_{j \in S} \log(b_j^{'}) \qquad (5.26)$$

(b). Bipartite Graph Construction

Next we introduce how to construct the bipartite graph $BG(X')=(S,V,E)$ where one side of the graph consists of the set of *STA nodes S*, and the other side consists of *MAP slots* $V = \{v_{i,s} : i \in M, s = 1,...,k_i\}$ where $k_i = \left\lceil \sum_{j \in S} x_{ij}^{'} \right\rceil$; there are k_i nodes $\{v_{i,s} : s = 1,...,k_i\}$ corresponding to MAP $i, i \in M$.

For each positive coordinate of $\{x_{ij}'\}$, there will be one or two corresponding edges in $BG(X')$. We define a value $y_{(i,s),j}$ for each edge $e_{(i,s),j} \in E$ in the graph as edge weight, which will have the property that $x'_{ij} = \sum_{s:e_{(i,s),j} \in E} y_{(i,s),j}$. The utility of each edge $e_{(i,s),j} \in E$ is defined to be $u_{(i,s),j} = u_{ij}$.

The edges in $BG(X')$ and the corresponding weights y are constructed in the following way.

For each MAP i , define the set of STAs that have positive fractional association with it as $S(i) = \{ j : j \in S \wedge x'_{ij} > 0 \}$. We sort the STAs in $S(i)$ in non-increasing order of a sorting criteria variable of i: $scv_i = \{ scv(i,j) : j \in S(i) \}$. scv_i is determined according to the dominating constraint for i in GAP as follows. If $r_{ij} \le B'_i$ for each STA $j \in S(i)$, we say that the dominating constraint for i is the access network constraint (5.22) and set $scv(i,j) = b'_j / r_{ij}$. On the other hand, if $r_{ij} > B'_i$ for each STA $j \in S(i)$, we say that the dominating constraint for i is the backhaul network constraint (5.23) and set $scv(i,j) = b'_j / B'_i$. Otherwise, we cannot determine the bottleneck constraint for i and set $scv(i,j) = b'_j / r_{ij} + b'_j / B'_i$.

For simplicity of notation, let for the moment $j \in [1, |S(i)|]$ be the sequence number of the STAs in the sorted set $S(i)$, i.e. assume $scv(i,1) \ge scv(i,2) \ge \ldots \ge scv(i, |S(i)|)$. The pseudo code for constructing the edges and edge weights in the bipartite graph for MAP i is given below.

Pseudo code for constructing the bipartite graph for MAP *i* :

```
if k_i = 1 then
    for j ∈ S(i)
        add e_(i,1),j to E;  y_(i,1),j ← x'_ij
    end for
else
    for s ∈ [1, k_i − 1]
        find min. j_s : Σ_{j=1}^{j_s} x'_ij ≥ s
        for j ∈ [j_{s−1} + 1, j_s − 1]
            add e_(i,s),j to E;  y_(i,s),j ← x'_ij
        end for
        add e_(i,s),j_s to E;  y_(i,s),j_s ← s − Σ_{j=1}^{j_s − 1} x'_ij
        if Σ_{j=1}^{j_s} x'_ij > s then
            add e_(i,s+1),j to E; y_(i,s+1),j_s ← Σ_{j=1}^{j_s} x'_ij − s
        end if
    end for
    for j ∈ (j_{k_i − 1}, |S_i|]
        add e_(i,k_i),j to E;  y_(i,k_i),j ← x'_ij
    end for
end if
```

If $k_i = 1$, there is only one node $v_{i,1} \in V$ corresponding to i. For each $j \in S(i)$, add edge $e_{(i,1),j}$ to E and set $y_{(i,1),j} = x'_{ij}$. Otherwise, for each $s = 1,2,...,k_i - 1$, find the minimum index j_s such that $\sum_{j=1}^{j_s} x'_{ij} \geq s$. Define $j_0 = 0$. For $j = j_{s-1} + 1,..., j_s - 1$ add edges $e_{(i,s),j}$ to E and set $y_{(i,s),j} = x'_{ij}$. For $j = j_s$, add edges $e_{(i,s),j}$ to E and set $y_{(i,s),j_s} = s - \sum_{j=1}^{j_s - 1} x'_{ij}$. If $\sum_{j=1}^{j_s} x'_{ij} > s$, add edges $e_{(i,s+1),j}$ to E and set $y_{(i,s+1),j_s} = \sum_{j=1}^{j_s} x'_{ij} - s$. Finally, for each $j > j_{k_i - 1}$ add an edge $e_{(i,k_i),j}$ to E and set $y_{(i,k_i),j} = x'_{ij}$. By now, we have constructed, for MAP i, the edges between MAP slots $\{v_{i,s} : s = 1,\ldots,k_i\}$ and STA nodes $\{j : j \in S(i)\}$ as well as the corresponding edge weights. After repeating this procedure for all MAPs in *M*, we have got the final bipartite graph *BG*(*X'*).

(c).Maximum Utility Matching

With *BG*(*X'*), next we find an integral matching $Match(y) \subseteq BG(X')$ that exactly matches all STA nodes by solving a linear program: maximum utility matching problem (MUMP) that is given in (5.27)-(5.29) [67].

MUMP:

Max $\quad \sum_{j \in S} \sum_{(i,s):e_{(i,s),j} \in E} u_{(i,s),j} y_{(i,s),j}$

s.t. $\quad \forall j \in S: \quad \sum_{(i,s):e_{(i,s),j} \in E} y_{(i,s),j} = 1 \qquad (5.27)$

$\forall v_{i,s} \in V: \quad \sum_{j:e_{(i,s),j} \in E} y_{(i,s),j} \le 1 \qquad (5.28)$

$\forall e_{(i,s),j} \in E: \quad y_{(i,s),j} \ge 0 \qquad (5.29)$

where (5.27) says that, for each STA node *j*, there is exactly one edge of *Match*(*y*) incident to *j*; (5.28) says that, for each MAP slot node $v_{i,s}$, there is at most one edge of *Match*(*y*) incident to $v_{i,s}$.

By Theorem 11.1 in [67], the linear program MUMP has the property that each extreme point is integer. Therefore we can find an optimal integral solution $\{\hat{y}_{(i,s),j}\}$ in polynomial time. Finally, for each edge $e_{(i,s),j} \in M(y)$, i.e. $\hat{y}_{(i,s),j} = 1$, by associating STA *j* with MAP *i,* i.e. setting $\hat{x}'_{ij} = 1$, we get an integral association matrix $\{\hat{x}'_{ij}\}$ as the output of BGR.

5.3.5. Integral Bandwidth Allocation

In the final step of JABA, with the integral association matrix $\{\hat{x}_{ij}^{'}\}$ that is obtained from either the LFR or BGR rounding algorithm, as input to iAP, we can optimally solve iAP and get an integral rate vector $\{\hat{b}_j^{'}\}$. Finally $(\hat{X}', \hat{B}')$ is the integral association and bandwidth allocation solution of JABA.

JABA is a centralized optimization-based algorithm. The centralized algorithms generally outperform distributed algorithms as the central controller is aware of the whole network condition and optimization algorithms can be implemented. In the centralized algorithms, it is assumed that the central controller is aware of the entire network topology as well as the achievable link rates between each pair of MAPs and STAs. The network topology and achievable link rates are assumed to be stable. It is also assumed that these information can be sent to the central controller from the MAPs and STAs efficiently and reliably.

In practical implementation, the scalability could be an issue because the central controller needs to know the entire network condition. Another issue would be the algorithm triggering mechanism. The centralized algorithm should be triggered if the network condition has adequately changed, such as joining/leaving of MAPs/STAs and change of the backhaul routing (including broken or blocked paths). The triggering mechanism could be periodic time based or based on real time measurement of the network condition. Finally single point failure could be another issue with centralized system. Unlike distributed algorithms, if the central controller collapsed, the whole network cannot function, and therefore a backup/recovery mechanism is needed.

For centralized algorithms, we would expect more overhead than in the distributed algorithms as the MAPs and STAs need to report their link rates and association status to the central controller and the central controller needs to distribute its control messages to the MAPs. There will be overhead due to control message exchange. Depending on how fast the network condition changes, the amount of the overhead would be different. If the network is stable, the amount of control messages would be small. For example, each MAP may update the central controller with its current association information once every 10 seconds.

We conducted simulations in Matlab where no MAC protocol was simulated. Given the STA link rates, the bandwidth allocation is done through transmission time allocation within unit time. A centralized MAC protocol that is capable of allocating link transmission time/opportunities, such as 802.11 PCF, is assumed to be available.

5.4. Approximation Ratio Analysis and Improvement

In this section, we do theoretical analysis on the approximation ratio of JABA- LFR and JABA-BGR. We then propose an approximation ratio improvement algorithm for each of them.

5.4.1. Approximation Ratio Analysis

A. Analysis of JABA-LFR

Theorem 5.1: Consider an optimal integral association solution $(\hat{X}^*, \hat{B}^*)$ of iAP and an integral solution $(\hat{X}', \hat{B}')$ produced by the proposed JABA-LFR algorithm. It holds that $f_{AP}(\hat{X}', \hat{B}') \geq f_{AP}(\hat{X}^*, \{\frac{\hat{b}_j^*}{\alpha_{LFR}}\})$, where $f_{AP}(\,)$ is the objective function value of iAP and fAP;

α_{LFR} is the approximation ratio of JABA-LFR algorithm and equals $\max\{|M(j)| : j \in S\}$, where $|M(j)|$ is the number of MAPs with which STA j has fractional association in the fractional solution (*X'*, *B'*) of fAP.

Proof: Consider a STA j that is associated with MAP i' in the integral solution produced, i.e. $\hat{x}'_{i'j} = 1$. Consider another integral bandwidth allocation vector B'' where the bandwidth of j, b''_j, is equal to the fractional bandwidth received from $i', b'_{i'j}$, in the fractional solution, i.e. $b''_j = b'_{i'j}$. As (*X'*, *B'*) is a feasible solution to fAP and $b'_j = \sum_{i \in M(j)} b'_{ij}$, it is clear that $(\hat{X}', B'')$ is a feasible solution to iAP. By LFR, $b'_{i'j}$ is the largest among all fractional bandwidth allocations of j, so we have $b''_j = b'_{i'j} \geq b'_j / |M(j)|$. Therefore, $(\hat{X}', \{b'_j / |M(j)|\})$ is also a feasible solution to iAP. As $\hat{B}'$ is the optimal bandwidth allocation when the association matrix is $\hat{X}'$, we have

$$f_{AP}(\hat{X}', \hat{B}') \geq f_{AP}(\hat{X}', \{\frac{b'_j}{|M(j)|}\}). \tag{5.30}$$

$f_{AP}(X, B)$ is the objective function value of iAP and fAP; and it is a function of B when (X, B) is feasible. We have shown that $(\hat{X}', \{b'_j / |M(j)|\})$ is feasible to iAP and it is clear that $(X', \{b'_j / |M(j)|\})$ is feasible to fAP. Therefore, we have

$$f_{AP}(\hat{X}', \{\frac{b'_j}{|M(j)|}\}) = f_{AP}(X', \{\frac{b'_j}{|M(j)|}\}) \tag{5.31}$$

Due to the relaxed constraint on X, the fractional solution (*X'*, *B'*) achieves better objective function value than that of any optimal integral solution, i.e. $f_{AP}(X', B') \geq f_{AP}(\hat{X}^*, \hat{B}^*)$. Therefore, we have

$$f_{AP}(X^{'},\{\frac{b_j^{'}}{|M(j)|}\}) \geq f_{AP}(\hat{X}^{*},\{\frac{\hat{b}_j^{*}}{|M(j)|}\}) \qquad (5.32)$$

Combining (5.30), (5.31), and (5.32) we have

$$f_{AP}(\hat{X}^{'},\hat{B}^{'}) \geq f_{AP}(\hat{X}^{'},\{\frac{b_j^{'}}{|M(j)|}\}) = f_{AP}(X^{'},\{\frac{b_j^{'}}{|M(j)|}\}) \geq f_{AP}(\hat{X}^{*},\{\frac{\hat{b}_j^{*}}{|M(j)|}\})$$

So the performance of the integral solution given by JABA-FLR is at least as good as the optimal integral bandwidth allocation divided by $\max\{|M(j)| : j \in S\}$. This finishes the proof. □

B. Analysis of JABA-BGR

Lemma 5.1: Consider an integral solution $(\hat{X}^{'},\hat{B}^{'})$ that is the result of applying BGR on the fractional solution (*X'*, *B'*) of a fAP and the corresponding constructed GAP. It holds that the integral association matrix $\hat{X}^{'}$ is feasible if the associated STAs of a MAP *i* are allocated with bandwidth that equals their fractional solution divided by an approximation ratio, i.e. $(\hat{X}^{'},\{\frac{b_j^{'}}{AppRatio(i)} \mid i : \hat{x}_{ij}^{'} = 1\})$ is a feasible solution of iAP, where *AppRatio*(*i*) is the approximation ratio of *i* determined by the dominating constraint for *i* in GAP and is defined in (5.33)-(5.35). The dominating constraint is the access constraint in (5.33) and the backhaul constraint in (5.34). In (5.35) *i* has no dominating constraint.

$$AppRatio(i) = 1 + \max\{b_j^{'}/r_{ij} : j \in S(i)\} \qquad (5.33)$$

$$AppRatio(i) = 1 + \max\{b_j^{'}/B_i^{'} : j \in S(i)\} \qquad (5.34)$$

$$AppRatio(i) = 2 + \max\{b_j^{'}/r_{ij} + b_j^{'}/B_i^{'} : j \in S(i)\} \qquad (5.35)$$

Proof: by a simple reduction from the proof of Theorem 11.2 in [67], we can get the following property of the constructed bipartite graph. For each MAP $i \in M$:

$$\sum_{j\in S}\hat{x}'_{ij}scv(i,j) \le \max\{scv(i,j): j\in S_i\} + \sum_{j\in S}x'_{ij}scv(i,j) \tag{5.36}$$

When the dominating constraint for *i* in GAP is the access constraint (5.22), we have $scv(i,j) = b'_j / r_{ij}$ and $r_{ij} \le B'_i$ for each STA $j \in S(i)$. Equation (5.36) becomes

$$\begin{aligned}\sum_{j\in S}\hat{x}'_{ij}\, b'_j / r_{ij} &\le \max\{b'_j / r_{ij} : j \in S(i)\} + \sum_{j\in S}x'_{ij}\, b'_j / r_{ij} \\ &\le \max\{b'_j / r_{ij} : j \in S(i)\} + 1 \\ &= AppRatio(i)\end{aligned},$$

where the second inequality is due to that (*X'*, *B'*) is feasible to fAP and the equality is by (5.33). Therefore, we have

$$\sum_{j\in S}\hat{x}'_{ij}\frac{b'_j / AppRatio(i)}{r_{ij}} \le 1. \tag{5.37}$$

As $r_{ij} \le B'_i$ for each STA $j \in S(i)$, we have

$$\sum_{j\in S}\hat{x}'_{ij}\frac{b'_j}{AppRatio(i)} \le B'_i \tag{5.38}$$

Eq. (5.37) shows that $(\hat{X}', \{b'_j / AppRatio(i)\})$ satisfies the access constraint (5.3) in iAP. In fAP, the backhaul constraint is satisfied when the MAPs are allocated bandwidth $\{B'_i\}$. Eq. (5.38) shows that $(\hat{X}', \{b'_j / AppRatio(i)\})$ allocates bandwidth to each MAP no more than its bandwidth in $\{B'_i\}$, therefore the backhaul constraint (5.4) in iAP is satisfied. As $\hat{X}'$ is the result of an integer complete matching for STAs, each STA is associated with one MAP only and the integrity constraint (5.5) in iAP is satisfied. For an integral association, the STA transmission time constraint (5.2) is satisfied when (5.3) is satisfied. Therefore, $(\hat{X}', \{b'_j / AppRatio(i)\})$, where $AppRatio(i)$ is defined in (5.33), satisfies all of the constraints in iAP and is a feasible solution to iAP.

When the dominating constraint for i in GAP is the backhaul constraint (5.23), we have $scv(i,j)=b_j^{'}/B_i^{'}$ and $r_{ij}>B_i^{'}$ for each STA $j\in S(i)$; when i has no dominating constraint in GAP, we have $scv(i,j)=b_j^{'}/r_{ij}+b_j^{'}/B_i^{'}$. Using a similar procedure as for the first case, we can prove that $(\hat{X}^{'},\{b_j^{'}/AppRatio(i)\})$ is a feasible solution to iAP, where $AppRatio(i)$ is as defined in (5.34) and (5.35), respectively. Thus, we have finished the proof. □

Theorem 5.2: Consider an optimal integral association solution $(\hat{X}^{*},\hat{B}^{*})$ of iAP and an integral solution $(\hat{X}^{'},\hat{B}^{'})$ produced by JABA-BGR algorithm. It holds that $f_{AP}(\hat{X}^{'},\hat{B}^{'})\geq f_{AP}(\hat{X}^{*},\{\hat{b}_j^{*}/\alpha_{BGR}\})$ where α_{BGR} is the approximation ratio of JABA-BGR algorithm and equals $\max\{AppRatio(i):i\in M\}$.

Proof: By Lemma 5.1, we know $(\hat{X}^{'},\{b_j^{'}/\alpha_{BGR}\})$ is feasible to iAP, where α_{BGR} is as defined in the theorem. By replacing $|M(j)|$ in (5.30), (5.31) and (5.32) with α_{BGR} , we get the equation below and finish the proof.

$$f_{AP}(\hat{X}^{'},\hat{B}^{'})\geq f_{AP}(\hat{X}^{'},\{\frac{b_j^{'}}{\alpha_{BGR}}\})=f_{AP}(X^{'},\{\frac{b_j^{'}}{\alpha_{BGR}}\})\geq f_{AP}(\hat{X}^{*},\{\frac{\hat{b}_j^{*}}{\alpha_{BGR}}\}) \qquad □$$

5.4.2. Approximation Ratio Improvement Algorithms

The approximation ratio α_{LFR} and α_{BGR} given by the above analysis is loose. The gap between the optimal integral solution and the one generated by JABA is much smaller in fact. For example, consider a network scenario with one STA and m MAPs where the access link rates between the STA and the MAPs are equal, denoted as r_a, and much smaller than the MAP's backhaul link rate. In the fractional solution (X', B') of fAP, the STA would have equal fractional associations with all MAPs, and the fractional bandwidth allocation to the STA and MAPs would be $b_j^{'} = r_a$ and $B_i^{'} = r_a / m$. So we have the approximation ratio $\alpha_{LFR} = m$ and $\alpha_{BGR} = 1 + m$. However, the integral bandwidth of the STA $\hat{b}_j^{'}$ produced by JABA is the same as the optimal one, which equals r_a, and the true approximation ratio is 1.

To better understand the true gap between the approximated solution and the optimal one, we propose two approximation ratio improvement (ARI) algorithms for LFR and BGR respectively. The basic idea is to reduce α_{LFR} or α_{BGR} by gradually removing fractional associations from the chosen MAP i^* or STA j^* while keeping the objective function value non-decreasing. We divide the fractional association matrix $\{x_{ij}\}$ into two sets, *xRemoved* $\{x_{ij} : x_{ij} = 0\}$ and *xRemain* $\{x_{ij} : x_{ij} > 0\}$. In each iteration, a fAP with *xRemain* as unknown variables is solved; if one fractional association $x_{i^* j^*}$ is selected to be removed from *xRemain to xRemoved*, the available bandwidth is redistributed among the rest of *xRemain.* The details of the proposed ARI algorithms are shown in Fig. 5.4 and Fig. 5.5. In the previous example, after applying the ARI algorithms, the STA will have fractional association with only one of the MAPs and the approximation ratio becomes $\alpha_{LFR} = 1$ and $\alpha_{BGR} = 2$, which are the best results we can get for LFR and BGR.

To analyse the computational complexity of the approximation ratio improvement algorithms (ARIAs) in the worst case, consider a WMN consisting of *n* STAs and *m* MAPs, where all access link rates between the STAs and the MAPs are equal and all backhaul link rates between the MAPs and the portal are equal. As the STAs are facing the identical network condition, the fractional associations in *xRemain* for each STA are equal. Therefore, in the initial fractional association solution that is the input to ARIAs, there are in total $m \times n$ fractional associations (each STA having *m* identical associations). In each iteration of ARIAs, one fractional association is removed and one linear program or convex program needs to be solved. In the output of ARIAs, there remain n associations in total (each STA having 1). Therefore, the total number of iterations carried out is $(m-1)\times n$. As linear program and convex program can be solved in polynomial time, ARIA for both LFR and BGR are polynomial time algorithms.

ARI algorithm for LFR:

Input: fractional solution (X', B')

$f_{optimal} \leftarrow f_{AP}(X^{'}, B^{'})$

$xRemain \leftarrow \{x_{ij} : x_{ij} > 0, x_{ij} \in X^{'}\}$

$(X_R, B_R) \leftarrow (X^{'}, B^{'})$

$Terminate \leftarrow$ **false**

while $Terminate =$ **false do**

Based on (X_R, B_R), find $M(j)$ and b_j for each STA j

Sort STAs in non-increasing order of $|M(j)|$; sort STAs with the same $|M(j)|$ in non-decreasing order of b_j

Denote the first STA in the sorted sequence of STAs as $j*$

$(i^*, X^*, B^*) \leftarrow$ FindMAPToRemove($j*$)

if $i^* = 0$ **then**

$Terminate \leftarrow$ **true**

else

$xRemain \leftarrow xRemain - x_{i^* j^*}$

$(X_R, B_R) \leftarrow (X^*, B^*)$

end if

end while

return (X_R, B_R)

Function $(i^*, X^*, B^*) =$ FindMAPToRemove($j*$)

Sort the MAPs in $M(j^*)$ in non-decreasing order of b_{ij^*}

$n \leftarrow 1$ {let $i(n)$ represent the nth MAP in the sorted $M(j^*)$ }

while $n \leq |M(j^*)|$ **do**

$(X^{"}, B^{"}) \leftarrow$ fAP($xRemain - x_{i(n) j^*}$)

$f^{"} \leftarrow f_{AP}(X^{"}, B^{"})$

if $f^{"} = f_{optimal}$ **then**

return $(i(n), X^{"}, B^{"})$

else

$n \leftarrow n + 1$

end if

end while

return (0,0,0)

Figure 5.4: Approximation ratio improvement algorithm for LFR.

ARI algorithm for BGR:

Input: fractional solution (*X'*, *B'*)

$f_{optimal} \leftarrow f_{AP}(X^{'}, B^{'})$

$xRemain \leftarrow \{x_{ij} : x_{ij} > 0, x_{ij} \in X^{'}\}$

$(X_R, B_R) \leftarrow (X^{'}, B^{'})$

$Terminate \leftarrow$ **false**

while $Terminate =$ **false do**

  Based on (X_R, B_R), find *AppRatio*(*i*) for each MAP *i*

  Sort MAPs in non-increasing order of *AppRatio*(*i*)

  Denote the first MAP in the sorted sequence of MAPs as *i**

  $(j^*, X^*, B^*) \leftarrow$ FindSTAToRemove(*i**)

  if $j^* = 0$ **then**

    $Terminate \leftarrow$ **true**

  else

    $xRemain \leftarrow xRemain - x_{i^* j^*}$

    $(X_R, B_R) \leftarrow (X^*, B^*)$

  end if

end while

return (X_R, B_R)

Function $(j^*, X^*, B^*) =$ FindSTAToRemove(*i**)

Denote the set of STAs $\{j : x_{i^* j} > 0, scv(i^*, j) = AppRatio(i^*)\}$ as $S_{\max}(i^*)$

Sort the STAs in $S_{\max}(i^*)$ in non-decreasing order of b_j

$n \leftarrow 1$ {let *j*(*n*) represent the *n*th STA in the sorted $S_{\max}(i^*)$ }

while $n \le |S_{\max}(i^*)|$ **do**

  $(X^{''}, B^{''}) \leftarrow$ fAP$(xRemain - x_{i^* j(n)})$

  $f^{''} \leftarrow f_{AP}(X^{''}, B^{''})$

  if $f^{''} = f_{optimal}$ **then**

    return $(j(n), X^{''}, B^{''})$

  else

    $n \leftarrow n + 1$

  end if

end while

return (0,0,0)

Figure 5.5: Approximation ratio improvement algorithm for BGR.

5.5. Performance Evaluation

5.5.1. Simulation Setting

We present simulation results for a WMN that consists of 20 MAPs, 1 portal, and 150 STAs. The MAPs are uniformly placed at random in a rectangular field of 300m$\times$ 200m, where the portal is located at the centre of the lower left quarter field. We investigate two user distributions: uniform topology where the STAs are uniformly distributed in the covered area at random; hotspot topology where the STAs are distributed in a circle shape hotspot of radius 60m located at the centre of the field. We have also conducted simulations on other configurations, such as grid MAP topology and different number of STAs; their results are qualitatively similar to those of the presented.

We assume a transmission range of 100m and an interference range of 120m. A backhaul routing tree rooted at the portal is constructed using the 802.11s HWMP routing protocol. The backhaul cliques are found using the Bron-Kerbosch algorithm. We adopt the log-distance path loss model,

$$P_l(d) = P_{Tx} - P_{Rx} = P_l(d_0) + n10\log_{10}(d/d_0),$$

where $P_l(d)$ is the path loss in dB for path length d; P_{Tx} and P_{Rx} are the transmitting power and the received power in dBm; n is the path loss exponent; $P_l(d_0)$ is the reference loss at the reference distance d_0. In our simulation, d_0 = 100m, $P_l(d_0)$= 83, n = 2.2 and P_{Tx} = 17dBm.

We assume perfect frequency allocation among the access networks such that we do not count the interference from other cells. Assuming a receiver noise N_0 of -80 dBm, we can get the Signal-to-Noise Ratio (SNR) at the receiver by $SNR=P_{Rx}-N_0$. The link rate is determined by the SNR at the receiver. In our simulations, the access links operate on the 802.11n standard with one spatial stream on 20MHz channels. The access link rate model is shown in Table 5-1, where the minimum SNR value for the corresponding link rate is taken from [68] and the required SNR equals the minimum SNR plus a 9dB fade margin. As MAPs are more powerful than STAs, we consider two types of link rates for backhaul links: one is equal to the access link rates; the other is quadruple of the access link rates. We refer to the two configurations as *LinkRateRatio*=1 and *LinkRateRatio*=4. The second can be achieved by applying 4 spatial streams on 20MHz channels or 2 spatial streams on 40MHz channels.

Table 5-1: LINK RATE MODEL FOR 802.11N WITH ONE SPATIAL STREAM ON 20MHZ CHANNELS

Rate(Mbps)	6	12	18	24	36	48	54	60
Minimum SNR(dB)	5	7	9	13	17	20	22	23
Required SNR(dB)	14	16	18	22	26	29	31	32
Maximum Path Length (m)	100	81	66	43	28	21	17	15

We measure the performance of different algorithms in terms of aggregated network throughput, individual user bandwidth, and Jain's fairness index [12]

$$F = \left(\sum_{j\in S} b_j\right)^2 \Big/ \left(|S| \cdot \sum_{j\in S} b_j^2\right) \tag{5.39}$$

which is between 0 and 1. F equals 1 when all STAs have equal rate and decreases as the rate vector deviates from the ideal equal-rate vector.

5.5.2. Performance of Association Algorithms and Fairness Objectives

We compare the performances of the following association protocols:

- SS: Strongest Signal is the default association metric in 802.11 standards which says a STA associates with the MAP from which the received signal strength is the highest.
- CL: Cross Layer association metric based heuristics proposed for association control in WMNs [37], [38], [41]. According to CL, a STA associates with the MAP with which total association cost is the smallest. The total association cost is a weighted sum of the access cost (*AC*) and the backhaul cost (*BC*) as in(5.40), which reflects the estimated amount of channel time consumed by a successful end-to-end packet transmission. In our simulation, the weight ω_A =0.3.

$$TC_{i,j} = \omega_A \cdot AC_{i,j} + (1-\omega_A) \cdot BC_i \qquad (5.40)$$

- FRAC: Fractional association solution that is obtained by solving fAP problems. FRAC allows a STA to associate with multiple MAPs, and its bandwidth allocation vector is an upper bound of any integral solution.
- JABA: our proposed approximation algorithm.

We also compare the performances of two fairness objectives in the context of WMNs:

- PF: proportional fairness.
- MM: max-min fairness.

Fig. 5.6 depicts per-STA bandwidth performance of the association algorithms under different network settings of *STA topology* and *LinkRateRatio*. The results presented are averaged over 50 runs. In each run, the STA location is different and we sort the STAs in non-decreasing order of their allocated bandwidth. So the bandwidth of a STA indexed x in the figure indicates the average bandwidth of the x-th lowest bandwidth in each run.

We also give some numerical results of the aggregate throughput and Jain's fairness index in Table 5-2 where *LinkRateRatio*=4.

Comparing the performances of SS, CL and JABA, we can see that, for both MM and PF, the performance of SS is significantly poorer than the other two. The reason is that, unlike CL and JABA, SS only considers the access network condition, resulting in a lot of STAs associated with MAPs with poor backhaul condition and underutilizing backhaul network resource.

Comparing CL and JABA, the performance is as expected in that JABA outperforms CL since CL is a heuristic scheme without any optimization attempt. In Fig. 5.6 (a) and (b), where *LinkRateRatio*=1, CL follows JABA closely which indicates CL is a good heuristic considering its much simpler implementation. However, when the backhaul link rate is four times of the access link rate as in Fig. 5.6 (c) and (d), the performance gap between CL and JABA is significantly larger. That is due to the fundamental limitation of heuristic association schemes: it is difficult for CL to adapt to network dynamics. The access weight $\omega_A = 0.3$ is a good setting for CL when *LinkRateRatio*=1, but it is no longer good when *LinkRateRatio* is increased. In the second case, the backhaul cost is lower and contributes less to the total association cost. As a result, more STAs are associated with MAPs with poor backhaul condition, and the same as in the SS case, the backhaul capacity is lowered.

Comparing JABA and FRAC, we can see that in Fig. 5.6 (a) (b) and (c), for both PF and MM, JABA and FRAC have almost coinciding performances, which is the optimal performance one can achieve. The results indicate that the true approximation ratio in the simulated network is very close to 1. As for the hotspot topology in Fig. 5.6 (d), JABA has again nearly optimal performance for PF, but the gap between JABA and FRAC is wider for MM. The reason is that most of the STAs are associated with the hotspot MAPs, making the access network of hotspot MAPs very congested. Max-min fairness tries to allocate equal bandwidth to all STAs no matter what their link rate is. The STAs at the cell edge have very low link rate and their transmission consumes too much access network resource, which further lowers the access network capacity of hotspot MAPs [4]. As a result, the bottleneck of the hotspot STAs is at the congested access networks and their bandwidth is slightly lower than that in the corresponding fractional solution, as seen on the left and middle of Fig. 5.6 (d). For non-hotspot STAs, their bandwidth is determined by the backhaul capacity available to their associated MAPs. The lower the hotspot MAPs' access network capacities are, the less backhaul resource they consume, and the more bandwidth is for non-hotspot STAs. That is why we see the few STAs on the right of Fig. 5.6 (d) have bandwidth much larger than the corresponding fractional one.

PF is known to be able to achieve higher aggregate throughput than MM by sacrificing certain degree of user fairness. As shown in Table 5-2, for JABA algorithm, PF achieves 27% more aggregate throughput than MM in the uniform topology and the improvement is 5% in the hotspot topology. Depending on how to perceive fairness, we can measure fairness performance in two ways: (1) Jain's fairness index considering the bandwidth of all 150 STAs; (2) Jain's fairness index considering the bandwidth of the STAs indexed from 1 to 140. In the second measurement, we exclude a small number of STAs whose bandwidth is much larger than that of the majority. When Jain's index takes into account all the STAs' bandwidth, JABA-PF achieves better fairness than JABA-MM in both uniform (0.83 vs. 0.73) and hotspot (0.94 vs. 0.91) scenarios. When Jain's index excludes the highest 7% bandwidth (10 STAs), JABA-MM achieves better fairness than JABA-PF in both uniform (1 vs. 0.84) and hotspot (1 vs. 0.96) scenarios. In summary, considering the aggregate throughput, JABA-PF is better than JABA-MM; considering the fairness in throughput, either JABA-PF or JABA-MM can be the winner depending on how we perceive fairness.

To test the scalability of JABA, we have conducted simulations of a larger scale topology where 80 MAPs and 500 STAs are randomly placed in a rectangular field of 600m$\times$500m, and *LinkRateRatio*=16. Fig. 5.7 (a) and (b) depicts the average per-STA bandwidth performance for MM and PF fairness respectively. We can see that the performance improvement of JABA is consistent with that in Fig. 5.6. Fig. 5.7 (c) and (d) depicts the per-STA bandwidth standard deviation (S.D.) results for MM and PF fairness respectively. Compared to SS and CL, the S.D. of FRAC and JABA is slightly higher for the low-bandwidth STAs, and significantly lower for the high-bandwidth STAs. So considering all STAs, the overall performance of JABA is more stable than that of SS and CL.

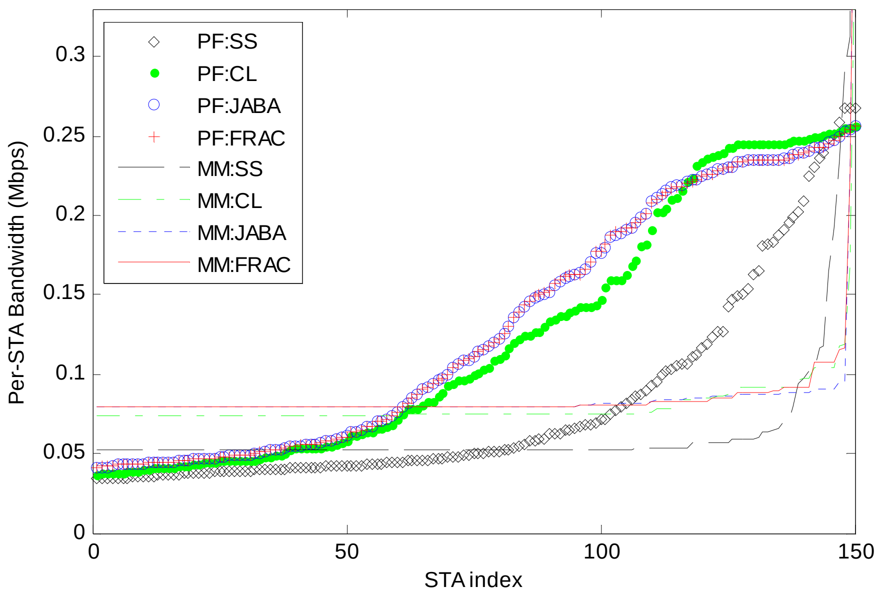

(a) Uniform topology, *LinkRateRatio*=1

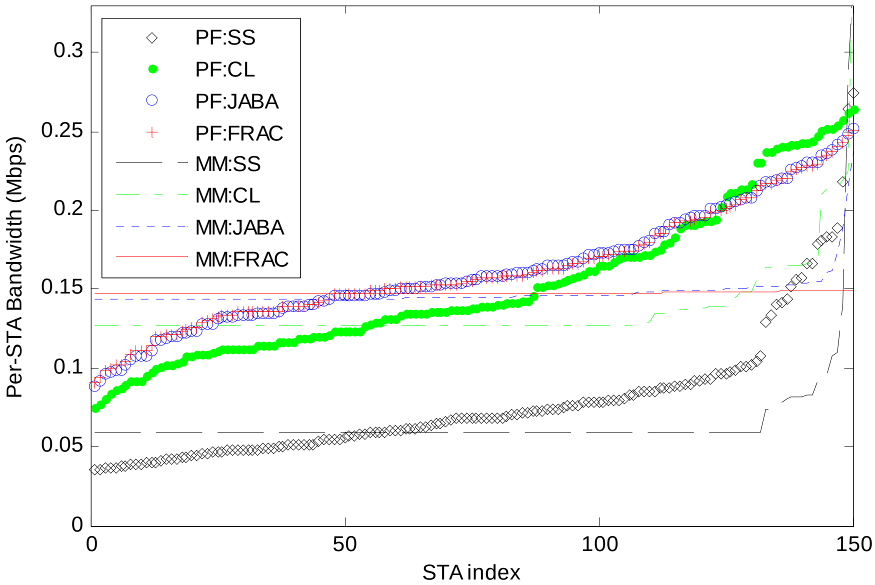

(b) Hotspot topology, *LinkRateRatio*=1

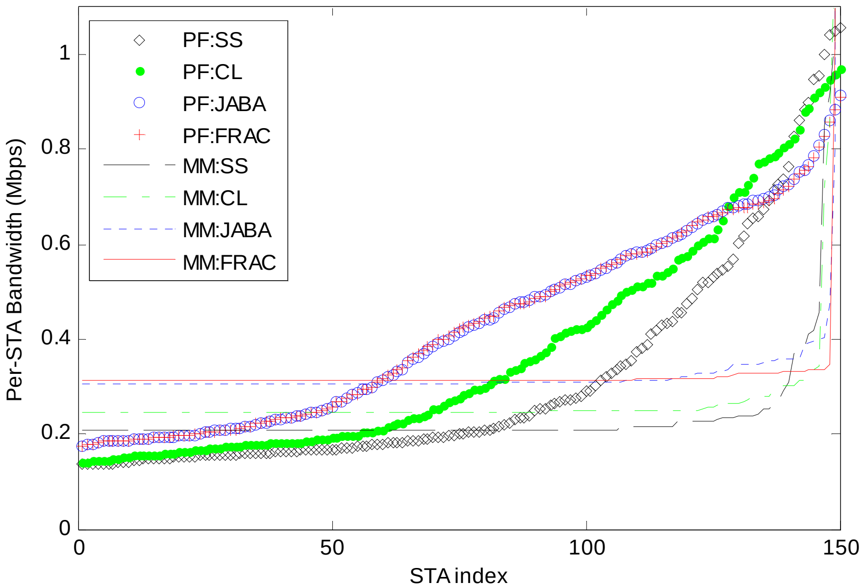

(c) Uniform topology, *LinkRateRatio*=4

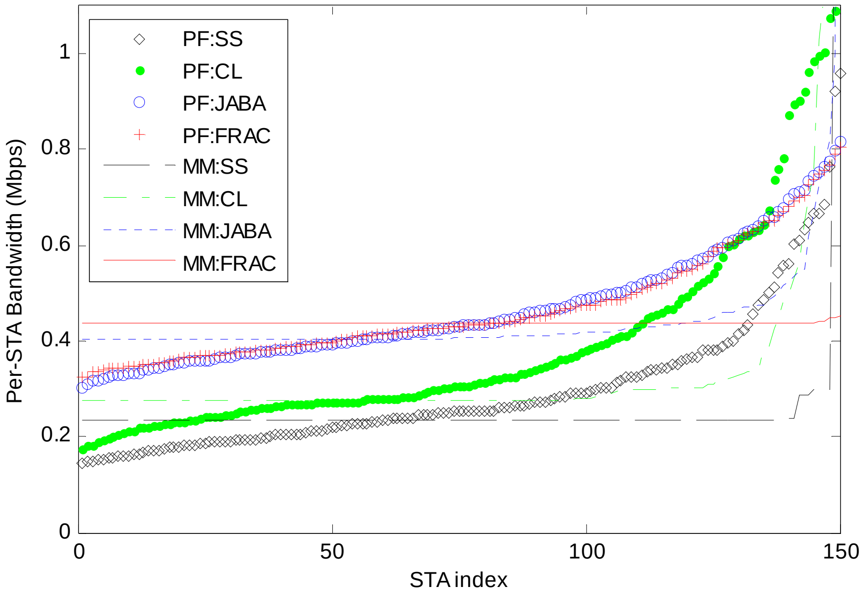

(d) Hotspot topology, *LinkRateRatio*=4

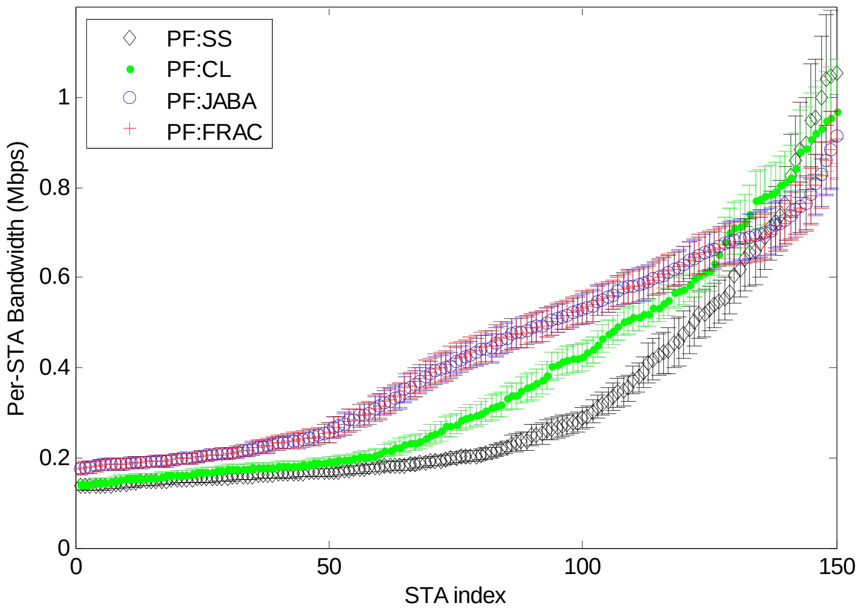

(e) Uniform topology, *LinkRateRatio*=4, 95% confidence interval, PF

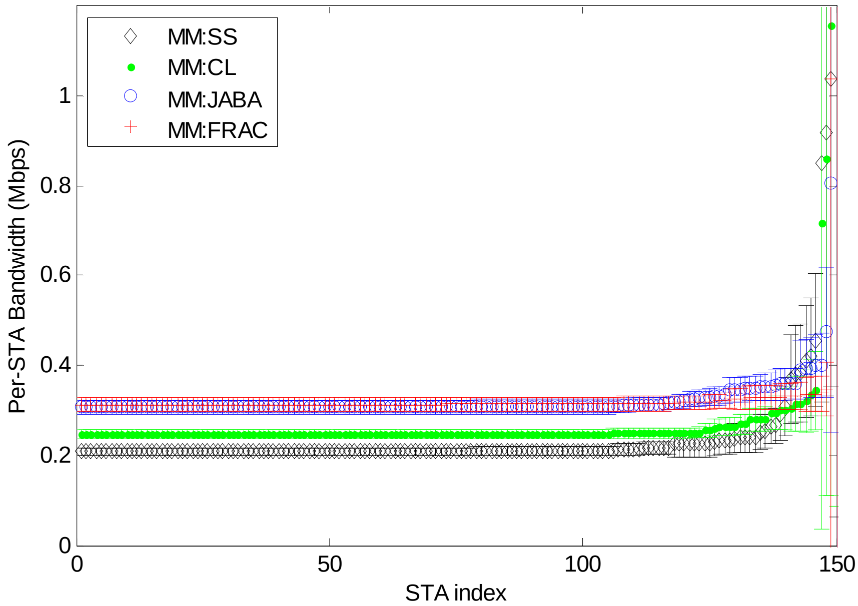

(f) Uniform topology, *LinkRateRatio*=4, 95% confidence interval, MM

Figure 5.6: Per-STA bandwidth performance of the association protocols.

Table 5-2: AGGREGATE THROUGHPUT AND JAIN'S FAIRNESS INDEX RESULTS

		Uniform				Hotspot			
		SS	CL	JABA	FRAC	SS	CL	JABA	FRAC
PF	Throughput	47.4162	56.0307	63.6921	63.7492	42.829	58.4748	68.5416	68.5593
	F for all STAs	0.6538	0.7281	0.8252	0.8261	0.8271	0.7828	0.9388	0.9438
	F for 140 STAs	0.7227	0.7563	0.8392	0.84	0.9129	0.8621	0.9567	0.9611
MM	Throughput	37.5071	41.1223	50.1366	49.7494	36.821	57.576	65.316	64.2497
	F for all STAs	0.5736	0.8393	0.7273	0.8152	0.9604	0.2386	0.9096	1
	F for 140 STAs	0.9956	0.9988	0.9997	1	1	0.9908	0.9968	1

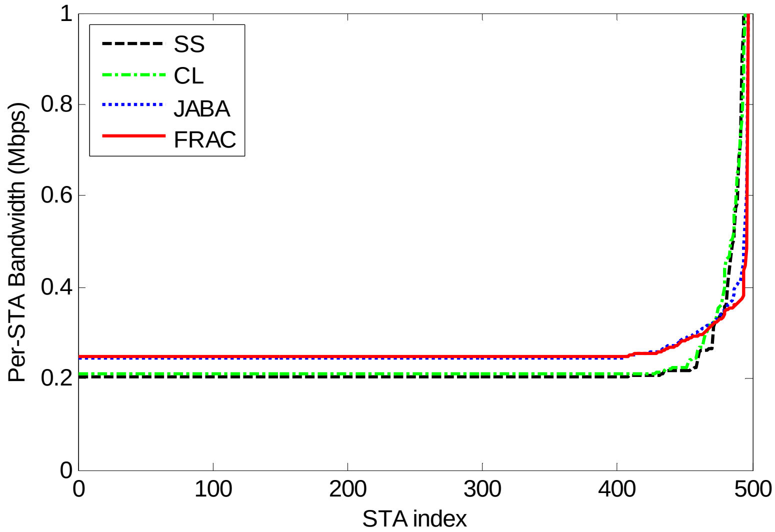

(a) Average per-STA bandwidth, MM

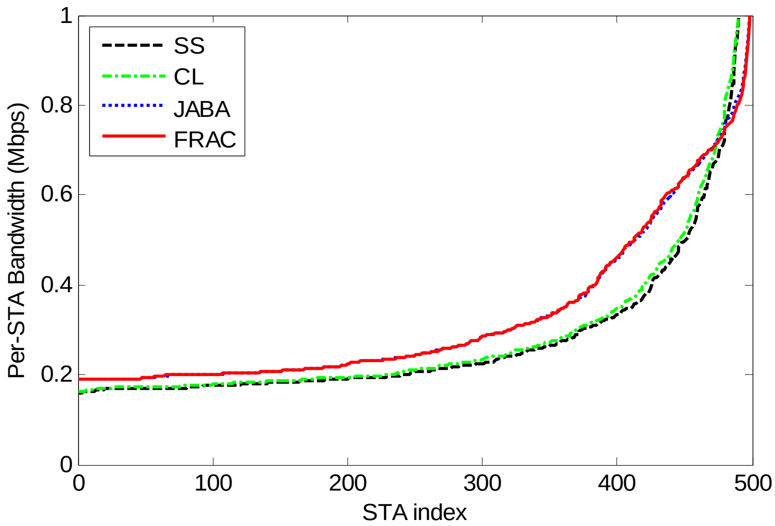

(b) Average per-STA bandwidth, PF

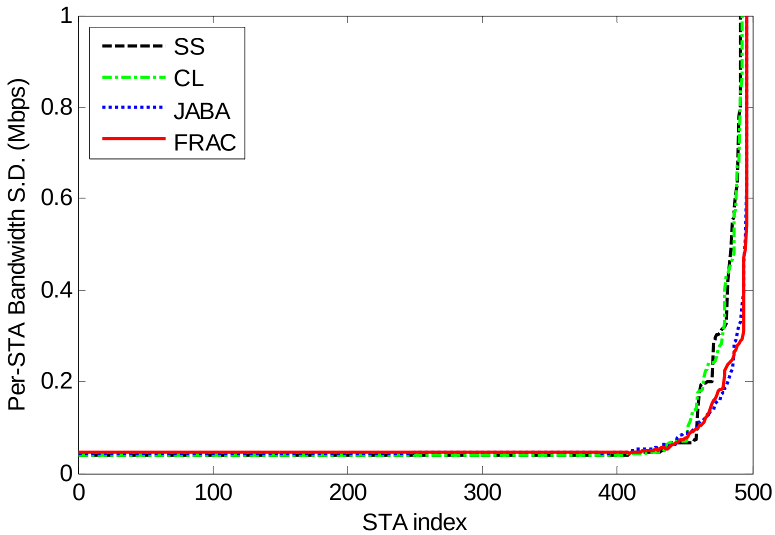

(c) Per-STA bandwidth standard deviation, MM

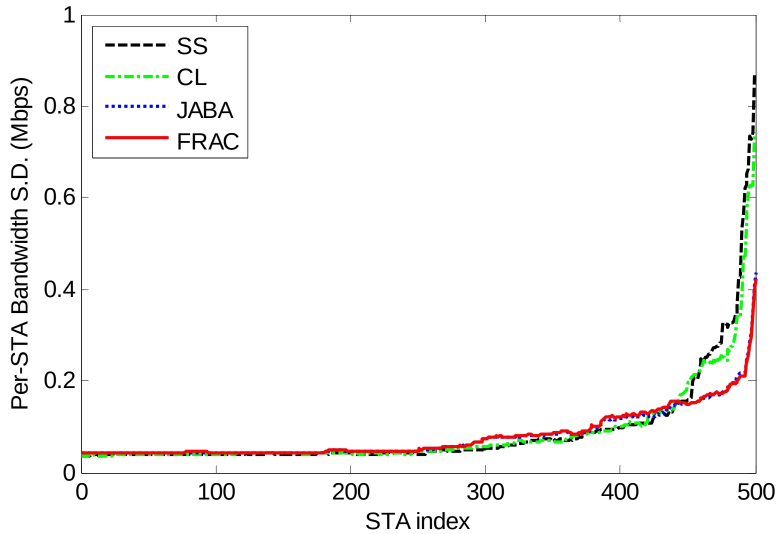

(d) Per-STA bandwidth standard deviation, PF

Figure 5.7: Per-STA bandwidth performance for large networks.

5.5.3. Comparison of the Rounding Algorithms

We compare the performance of rounding algorithms BGR and LFR and examine the performance of the corresponding approximation ratio improvement (ARI) algorithms BGR-ARI and LFR-ARI. Fig. 5.8 depicts per-STA bandwidth performance of the rounding algorithms. Table 5-3 gives the approximation ratio (A.R.) results in terms of A.R. mean and variance based on the results of 20 runs.

In Fig. 5.8 (a) and (b), we can see that BGR with and without ARI have consistent performance, for both PF and MM and both uniform and hotspot topologies, which is almost the same as that of the upper bound performance of FRAC.

In Fig. 5.8 (c) and (d), LFR-ARI performance is quite close to that of FRAC. In Fig. 5.8 (d), we can see that LFR-ARI significantly improves the performance of LFR. The reason is that using LFR, a lot of STAs are associated with hotspot MAPs, lowering the hotspot MAP capacity. Using LFR-ARI, the STAs fractionally associated with the hotspot MAPs are gradually removed from the hotspot MAPs, resulting in less congested hotspots and improved throughput performance. Fig. 5.9 depicts the standard deviation of the per-STA bandwidth presented in Fig. 5.8 (d). We can see that, compared to LFR, the standard deviation (S.D.) curve of LFR-ARI is closer to that of FRAC and the overall performance of LFR-ARI is more stable.

A.R. represents the largest possible gap between the approximated solution and the optimal solution. The closer to 1 the A.R. value is, the more confident in the produced solution we are. From Table 5-3 we can see that BGR-ARI achieves A.R. close to 2 and LFR-ARI achieves A.R. between 1 and 2; both are much smaller than that of corresponding non-ARI algorithms. Comparing the A.R. values of the two rounding methods, without ARI algorithms, BGR significantly outperforms LFR; on the other hand, with ARI algorithms, LFR-ARI achieves even better performance than BGR-ARI. Note that the theoretical A.R. presented here is not necessarily the true gap between the approximated solution and the optimal solution. As seen in Fig. 5.6 and Fig. 5.7, JABA and FRAC have almost similar performances, which is the optimal performance one can achieve. The results in Fig. 5.6 and Fig. 5.7 indicate that the true approximation ratio in the simulated network is almost 1, although the theoretical A.R. is around 2.

In summary, if we consider bandwidth performance only, BGR without ARI is a suitable choice. If we want the best approximation ratio only, LFR with ARI is the best algorithm. Otherwise, if we want a balance between the two performances, BGR with ARI is recommended.

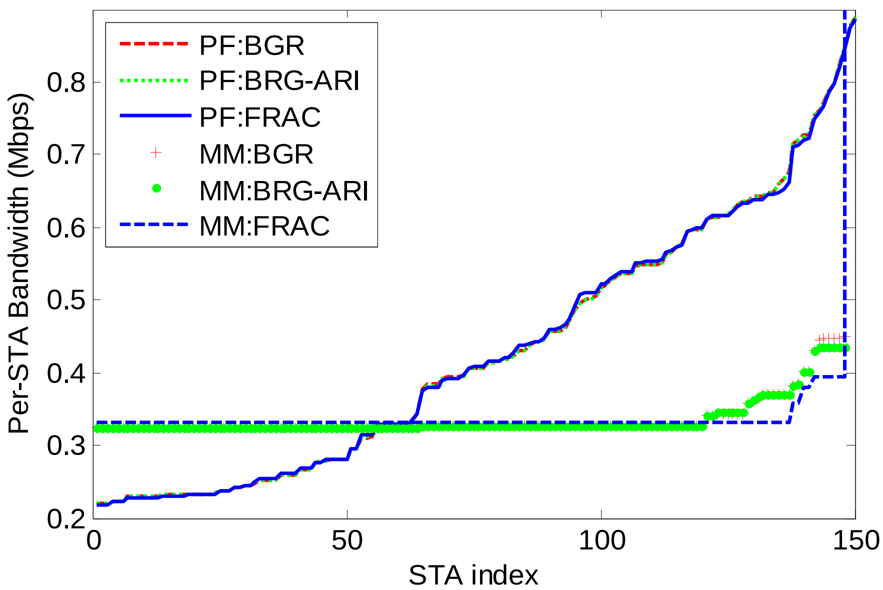

(a) Uniform topology, BGR

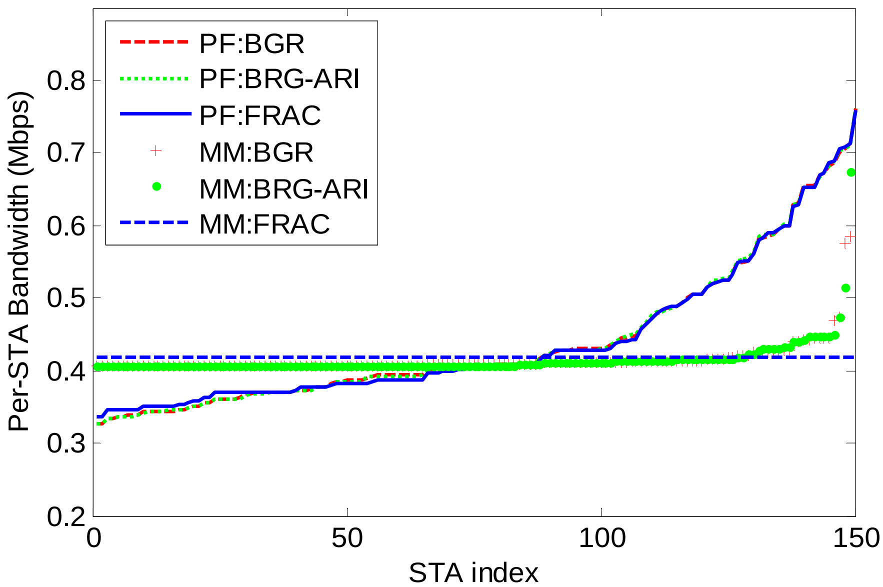

(b) Hotspot topology, BGR

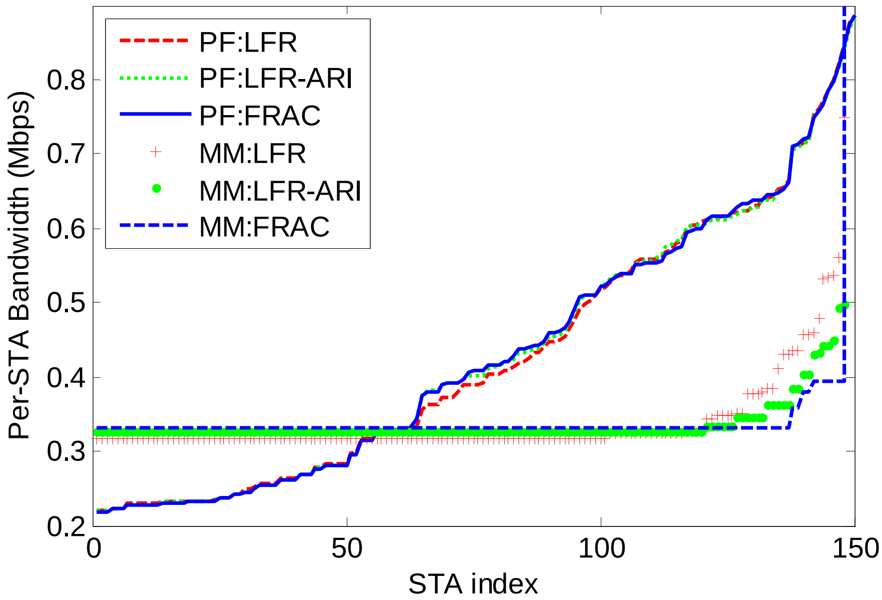

(c) Uniform topology, LFR

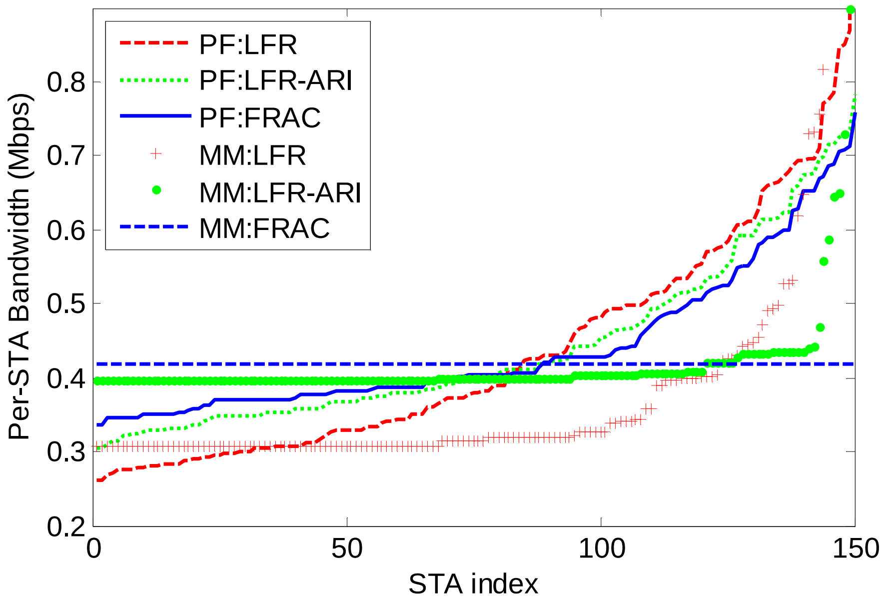

(d) Hotspot topology, LFR

Figure 5.8: Performance of the rounding algorithms.

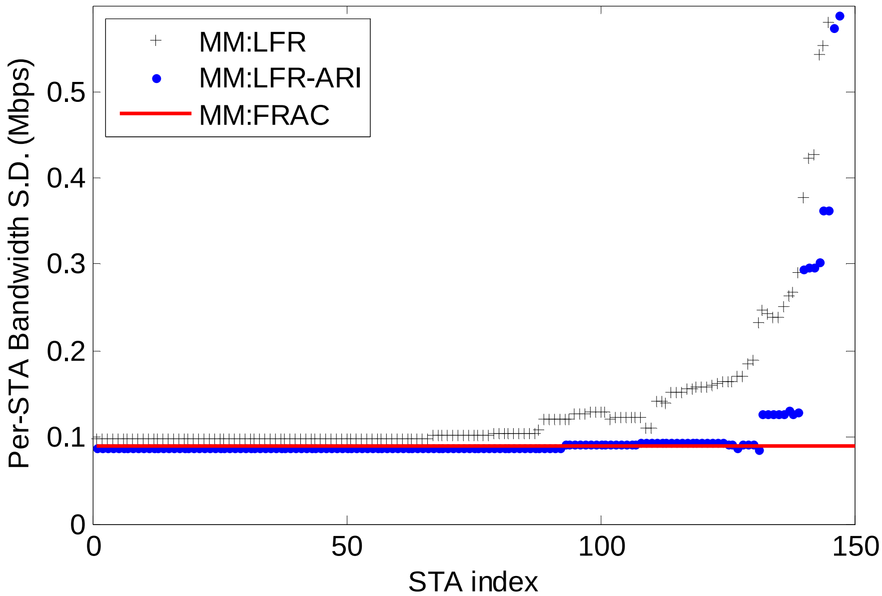

(a) MM

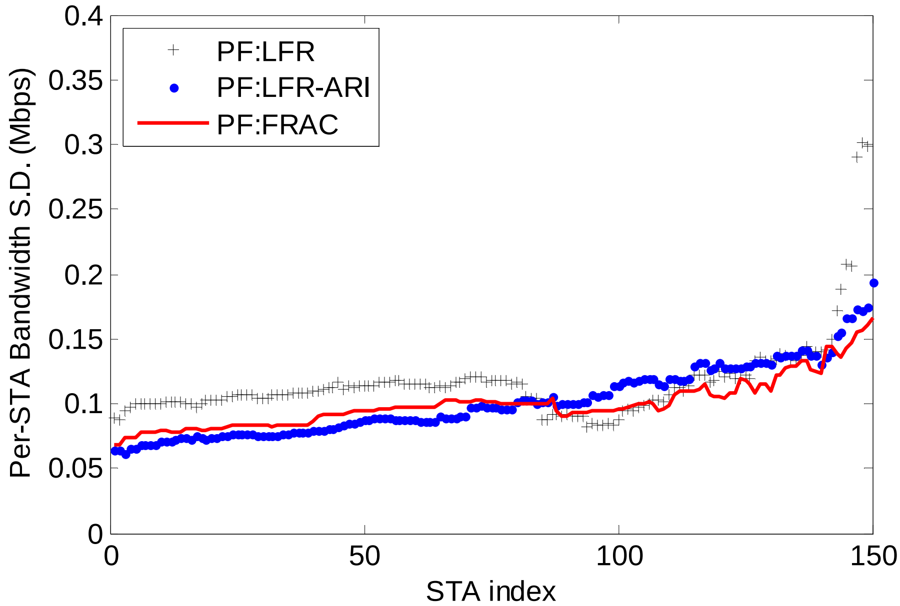

(b) PF

Figure 5.9: Per-STA bandwidth standard deviation, hotspot topology, LFR

Table 5-3: APPROXIMATION RATIO RESULTS

		Uniform				Hotspot			
		BGR	LFR	BGR-ARI	LFR-ARI	BGR	LFR	BGR-ARI	LFR-ARI
PF	A.R. Mean	2.87	8.5	2.252	1.857	4.595	6.643	2.122	2
	A.R. Var.	3.333	1.654	0.18	0.132	7.508	9.016	0.003	0
MM	A.R. Mean	2.424	8.214	2.332	1.143	4.843	6.5	2.105	1.214
	A.R. Var.	0.537	2.489	0.554	0.132	11.024	9.808	0.001	0.181

5.6. Conclusion

In this chapter, we have formulated and proposed approximation algorithms for the problem of optimal joint association and bandwidth allocation in wireless mesh networks considering max-min fairness (MM) and proportional fairness (PF) objectives. In the proposed approximation algorithms, named JABA, we first relax the integral association constraint and get an optimal fractional association solution. Then we propose two rounding algorithms, LFR and BGR, to get an integral association solution. We have analysed the approximation ratios of the proposed rounding algorithms, which reflect the gap between the produced solution and the optimal one. To let the theoretical approximation ratio more closely reflect the true performance gap, we propose two approximation ratio improvement algorithms. We demonstrate via simulations that the proposed JABA algorithm achieves nearly optimal performance and outperforms popular heuristic algorithms. We have seen that PF outperforms MM in network throughput and either one can achieve better user fairness depending on how fairness is defined. Finally, we have shown that BGR achieves nearly optimal bandwidth allocation performance and the approximation ratio improvement algorithm for LFR can improve the approximation ratio to 1-2.

Chapter 6: Utility Fairness via Association Control in WMNs

6.1. Introduction

In Chapter 5, we have studied the optimal association control achieving MM and PF user bandwidth allocation. In previous works on optimization-based association control [32]-[35], [42], their objective functions also consider either MM or PF fairness. It has been shown that PF is able to increase the network throughput by trading off certain degree of fairness in user bandwidth. With PF, the degree of the tradeoff, i.e. the preference of the fairness over throughput, is fixed. However, depending on the application scenarios and user portfolios, network operators may have various requirements on the network performance in terms of aggregate throughput and user fairness, i.e. sometimes more fairness is preferred while in some situations throughput is the main concern.

In this chapter, we study the problem of utility fair bandwidth allocation via association control in WMNs. Utility fairness is more general than other commonly used fairness objectives in resource management such as MM and PF. It is more flexible in controlling the tradeoff between resource utilization efficiency and user fairness. We formulate and approximately solve an optimization problem that achieves a utility fairness objective. In addition, we introduce control mechanisms to restrict the range of the allowed user bandwidth to make the tradeoff more controllable and at the same time prevent extreme unfairness. We demonstrate through simulations how to control the tradeoff between efficiency and fairness to achieve the desired performance by adjusting the corresponding control parameters. We also demonstrate which part of the STAs' bandwidth is compromised for higher efficiency by showing the relationship between STAs' allocated bandwidth and their associated MAP's backhaul condition.

6.2. Utility Fair Bandwidth Allocation and Association Control

We first introduce the utility function that composes the objective function of utility fairness. Then we present the optimization problem formulation for integral association and bandwidth allocation. Lastly we present the approximation algorithm.

6.2.1. Utility Fairness

Utility fairness is less egalitarian than max-min fairness and more flexible than proportional fairness in balancing efficiency and fairness. The utility of a user's allocated bandwidth is a convenient way to represent the user's satisfaction and can be calculated by a concave function *U*() that is called utility function. The utility function used in our algorithm is (6.1) that was first proposed in [69].

$$U_\alpha(b_j) = \begin{cases} \log b_j, & \text{if } \alpha = 1 \\ (1-\alpha)^{-1} b_j^{\,1-\alpha}, & \text{if } \alpha \neq 1 \end{cases} \tag{6.1}$$

α is the parameter that represents the priority of fairness and can be used to control the tradeoff between efficacy and fairness. When $\alpha=0$, the objective is to maximize network throughput, with no consideration to fairness. When $\alpha=1$, proportional fairness is the objective. As α increases, fairness becomes more and more important and finally absolute fairness dominates when α approaches infinity.

6.2.2. Problem Formulation

By adopting the same network model and conventions as those in Chapter 5, the problem of optimal integral Association and Bandwidth Allocation (iABA) for utility fairness is formulated in (6.2)-(6.9). iABA consists of 2 steps. Denote the minimum STA bandwidth in a feasible rate vector as b_{min}. In the first step, we maximize b_{min} and get an optimal solution $b_{\min}^*$ that is the largest possible b_{min} in any feasible bandwidth allocation. In the second step, we maximize the total network utility. Besides the fairness control parameter α, we introduce two bandwidth boundary constraint parameters in (6.8), B_{lower} and B_{upper}, which are used to control the lower bound and upper bound of the STA bandwidth, so that we can make sure no STA starves and no STA gains extremely larger bandwidth than the others.

iABA:

Step1:

Max $\quad b_{\min}$

s.t.
$$\forall j \in S: \quad \sum_{i \in M} x_{ij} \frac{b_j}{r_{ij}} \le 1 \tag{6.2}$$

$$\forall i \in M: \quad \sum_{j \in S} x_{ij} \frac{b_j}{r_{ij}} \le 1 \tag{6.3}$$

$$\forall k \in K_B: \quad \sum_{i \in M} \frac{y_{ki}}{r_{ki}} \sum_{j \in S} x_{ij} b_j \le 1 \tag{6.4}$$

$$\forall j \in S: \quad \sum_{i \in M} x_{ij} = 1 \tag{6.5}$$

$$\forall j \in S: \quad b_j \ge b_{\min} \tag{6.6}$$

$$\forall i \in M, j \in S: \quad x_{ij} \in \{0,1\}, \ \ b_{\min} \ge 0 \tag{6.7}$$

Step2:

Max $\quad \sum_{j \in S} U_\alpha(b_j)$

s.t. $\quad$ constraints (6.2)-(6.5) and

$$\forall j \in S: \quad B_{lower} \cdot b_{\min}^* \leq b_j \leq B_{upper} \cdot b_{\min}^* \qquad (6.8)$$

$$\forall i \in M, j \in S: \quad x_{ij} \in \{0,1\} \qquad (6.9)$$

6.2.3. Approximation Algorithm

As the problem iABA is a mixed integer nonlinear program, we propose a relaxation-rounding approximation algorithm, named approximated Association and Bandwidth Allocation (aABA), to get a working solution in polynomial time.

In the first step of aABA, we relax the integral association constraint by allowing STAs to fractionally associate with multiple MAPs. The relaxed fractional association problem is convex and named fractional Association and Bandwidth Allocation (fABA). By introducing the fractional bandwidth allocation matrix $\{b_{ij}\}$, fABA can be derived from iABA by replacing b_j with $\sum_{i \in M} b_{ij}$ and replacing $x_{ij} \cdot b_j$ with b_{ij}.

In the second step, we solve fABA and get an optimal fractional solution, denoted as (X', B'), which is an upper bound for any integral solution due to less restriction in the optimization constraints.

In the third step, the fractional association X' is rounded to an integral one, denoted as $\hat{X}'$, via randomization rounding. Denote the set of MAPs that have fractional association with STA j in X' as $M(j)$. By randomization rounding, STA j randomly selects one of the MAPs in $M(j)$ to associate with. The approximation ratio of randomization rounding is hard to analyse theoretically, although the final integral solution won't have much difference, which can be seen in Fig. 6.1 that aABA and FRAC have almost similar performance. In fact, we can adopt either LFR or BGR from Chapter 5 as the rounding algorithm in Chapter 6 too, and their theoretical approximation ratios are analysable.

In the fourth step, we optimally solve iABA with $X = \hat{X}'$ as input and get an integral bandwidth allocation vector $\{\hat{b}_j'\}$. Finally $(\hat{X}', \hat{B}')$ is the output of aABA.

6.3. Performance Evaluation

We present simulation results for a WMN that consists of 20 MAPs, 1 portal, and 100 STAs. The MAPs are uniformly placed at random in a rectangular field of 300m×200m, where the portal is located at the centre of the lower-left quarter field. We investigate two user distributions: uniform topology where the STAs are uniformly distributed in the coverage area at random; hotspot topology where the STAs are distributed in a circle shape hotspot of radius 60m located at the centre of the field. We have also conducted simulation on other configurations, such as grid MAP topology and different number of STAs; their results are qualitatively similar to those presented. We adopt the same transmission and link rate model as that used in Chapter 5. The backhaul *LinkRateRatio* equals 4.

We measure the fairness of a bandwidth allocation $\{b_j\}$ using Jain's fairness index F (5.39). We measure the resource efficiency of $\{b_j\}$ using the efficiency index

$$E = \sum_{j \in S} b_j \Big/ \sum_{j \in S} b_j^{\alpha=0} \qquad (6.10)$$

where $\{b_j^{\alpha=0}\}$ is the rate vector when $\alpha = 0$, i.e. when network throughput is maximized. The efficiency index is between 0 and 1.

6.3.1 Comparison of the Association Algorithms

We compare the performance of aABA against the benchmark schemes SS, CL, and FRAC, which have been introduced in Chapter 5, in the context of utility fairness. Fig. 6.1 depicts the per-STA bandwidth performance of the association algorithms where the fairness control parameter α is set to be 1 and 10 to simulate PF and MM fairness respectively.

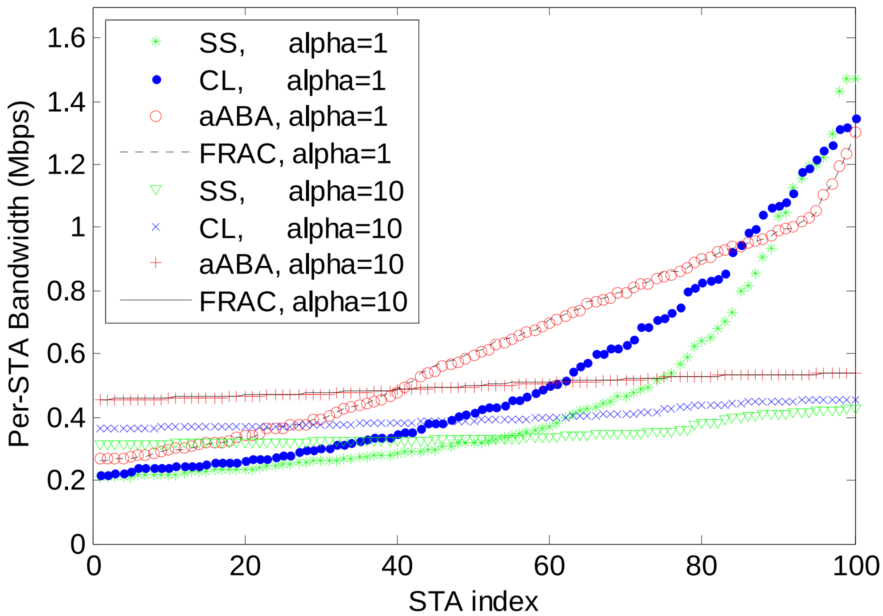

(a) Uniform topology

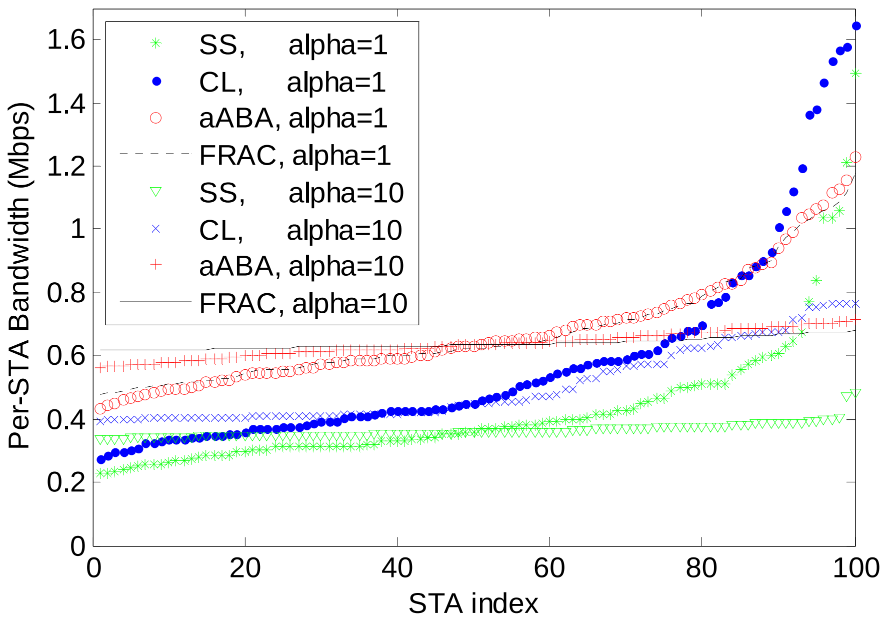

(b) Hotspot topology

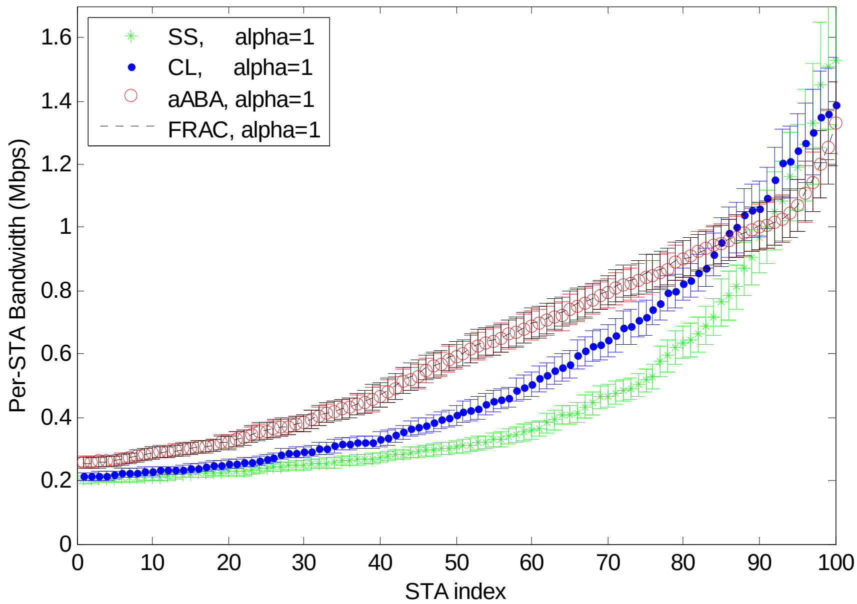

(c) Uniform topology, 95% confidence interval, alpha=1

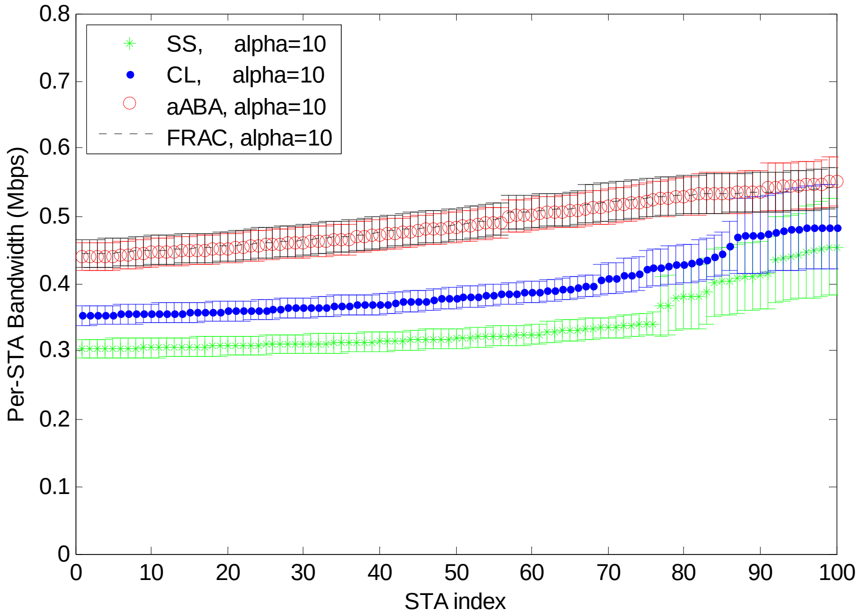

(d) Uniform topology, 95% confidence interval, alpha=1

Figure 6.1: Per-STA bandwidth performance of the association protocols.

In Fig. 6.1, the performance of SS is always the worst regardless of the topology and α value, because SS only considers the access network condition, resulting in lots of STAs associated with the poor-backhaul MAPs and underutilizing backhaul network resource. CL achieves better performance than SS because it considers both access and backhaul network condition. CL has no optimization attempt and it has no consideration of utility fairness objective when making association decision. Therefore, it is as expected that CL performance is significantly poorer than that of FRAC and aABA. Our proposed aABA algorithm achieves nearly optimal performance, which can be seen from the almost coinciding lines of aABA and FRAC.

6.3.2. Tradeoff between Efficiency and Fairness

We show the tradeoff between resource efficiency and user fairness by tuning the fairness control parameters. The results shown below are for uniform topology; the hotspot topology has similar results.

Fig. 6.2 depicts the efficiency index and fairness index for rate vectors obtained under different α values and different rate boundary constraints (B_{lower}, B_{upper}). When α is small, high network throughput is achieved by sacrificing fairness. As α increases, fairness index increases approaching 1 and efficiency index decreases approaching a steady state value. In other words, as α increases, user fairness becomes dominant in the utility function and the two indexes approach the value that would be obtained if max-min fairness is the objective.

We can also see in Fig. 6.2 that the changing rates of the two indexes are very high when α is small, i.e. the majority of the tradeoff is done within a small range of α value. When there are no boundary constraints and α is small, the fairness is very poor; in addition, it is difficult to get a desired level of fairness, as a small change in α would cause a large change in the performance. Therefore we introduce the boundary constraints (B_{lower}, B_{upper}) that prevent extreme unfairness and make the tradeoff smoother and more controllable.

Fig. 6.3 depicts the per-STA bandwidth allocation results. It is clear that as α decreases, STAs on the right, whose bandwidth are larger than the average, are getting more and more bandwidth while STAs on the left are getting less and less, i.e. it is getting more and more unfair. When there are no boundary constraints and α is small, we can see in Fig. 6.3 (a) that some STAs receive extremely low bandwidth while a few STAs receive excessively high bandwidth. With the boundary constraints introduced, in Fig. 6.3 (b), no STA is starved and we can more effectively control the bandwidth allocation.

Next we are interested in finding which part of STAs is sacrificed for higher efficiency. Fig. 6.4 shows the relationship between a STA's allocated bandwidth and the backhaul cost (*BC*) of its associated MAP. The *BC* of MAP *i* is calculated by $BC_i = \sum_{l \in path(i)} 1/r_l$. A lower *BC* indicates higher backhaul link rates or shorter backhaul path, and better backhaul condition. As discussed before, transmission from these MAPs consumes less network resource, therefore improves resource efficiency. In Fig. 6.4, it is as expected that STAs with higher bandwidth are those associated with lower backhaul cost MAPs.

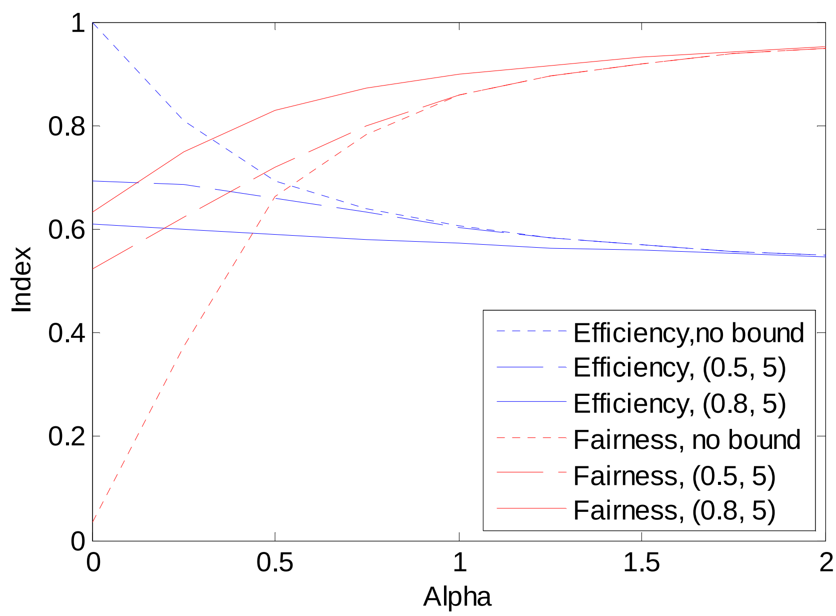

Figure 6.2: Efficiency index and fairness index.

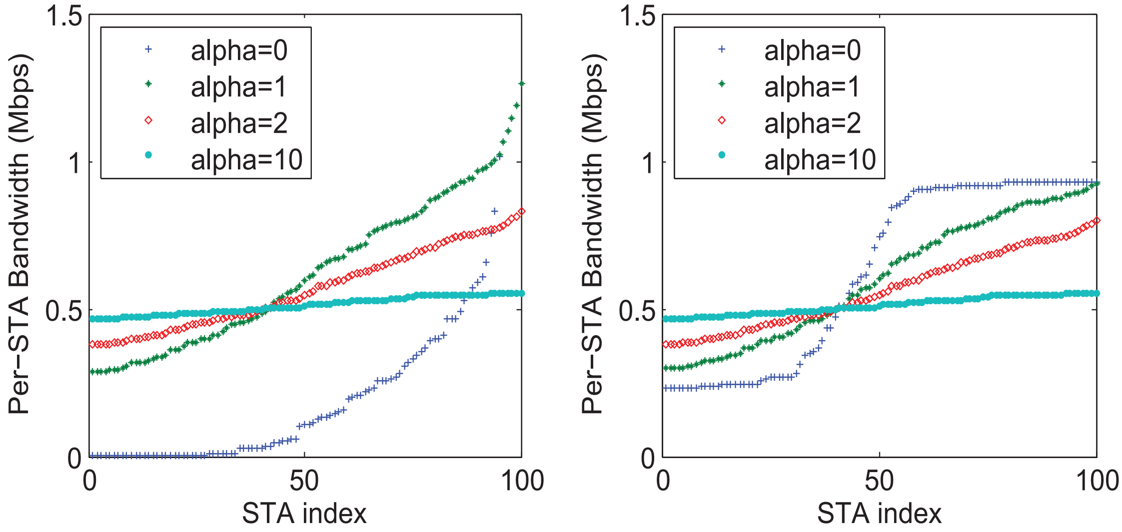

(a) with no boundary (b) with boundary (0.5,2)

Figure 6.3: Per-STA bandwidth performance for varying α value.

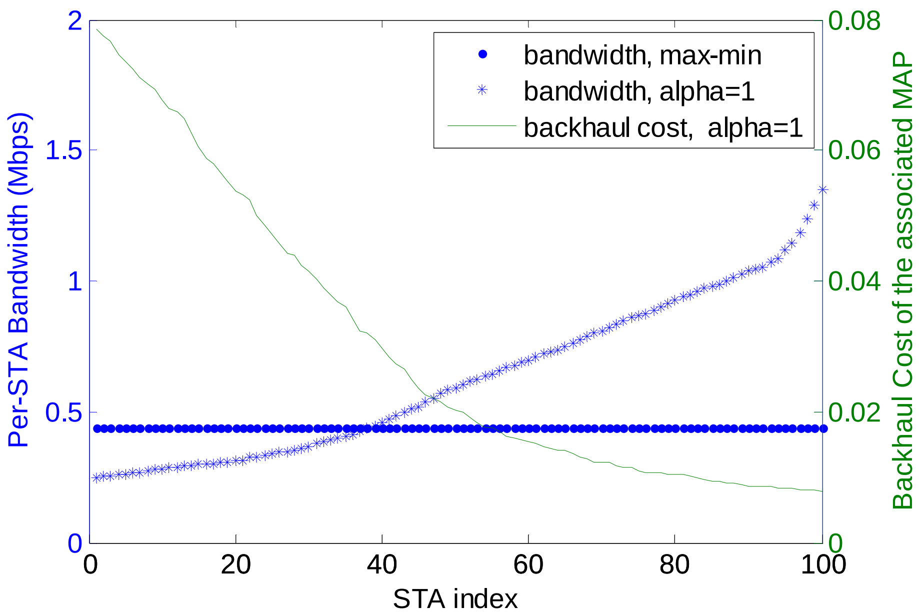

Figure 6.4: STA bandwidth and MAP backhaul cost.

6.4. Conclusion

Utility fairness is less egalitarian than max-min fairness and more flexible than proportional fairness in balancing efficiency and fairness. In this chapter, we have studied the problem of utility fair bandwidth allocation via association control in wireless mesh networks. We have formulated and approximately solved an optimization problem considering utility fairness objective. We have shown in our simulations how to control the tradeoff between resource efficiency and user fairness to achieve the desired performance by tuning the control parameters including the proposed bandwidth boundary constraints.

Chapter 7: A Network Resource Management Framework for WMNs

In this chapter, by taking the features of WMNs and the inter-cell interference into consideration, we propose a network resource management framework for WMNs that improves the network performance by jointly managing MAP channel assignment, MAP-STA association, and user bandwidth allocation. The proposed framework is composed of three components: a utility-fair bandwidth allocation algorithm, a channel assignment algorithm that effectively increases the network capacity by reducing the interference at the good-backhaul MAPs, and an optimization-based association control algorithm. In addition, to model the concurrent transmission constraints in WMNs, we propose an efficient local-clique-based network modeling method whose performance is almost identical to that of the exponential-time optimal algorithms. We demonstrate the superior performance of the proposed algorithms over the other state-of-the-art schemes through simulations with various network topologies and conditions.

7.1. Introduction

Almost all of the existing studies on association control [28]-[43], no matter it is for WLANs or WMNs, and no matter it is distributed algorithm or centralized algorithm, assume carefully planned network deployment such that there is no interference between adjacent cells. However, that is rarely the case in reality. In this chapter, we take the interference among co-channel MAP cells into consideration. We propose a centralized optimization-based association control scheme as one component of the proposed resource management framework, based on a realistic WMN network model that considers both access and backhaul network transmission constraints.

As more and more APs are deployed to support the fast growing Wi-Fi enabled mobile devices, the inter-cell interference becomes more and more inevitable. In the 2.4 GHz frequency band of the IEEE 802.11 standards, there are only 3 or 4 non-overlapping 20MHz-wide channels and the number is 12 or 13 for the 5 GHz frequency band [70]. If the new standard such as 802.11ac that supports channel bandwidth up to 160MHz is considered, the number of non-overlapping channels is even smaller. Many channel assignment schemes have been proposed for WLANs in the literature [70]. The objective of these schemes is usually minimize the total interference experienced by either APs or STAs. However, in WMNs, as discussed above, it is preferred that the good-backhaul MAPs carry more traffic. As a result, it makes sense to reduce the interference at these MAPs with priority so that they can accommodate more STAs. In this chapter, we propose a channel assignment scheme as another component of the proposed resource management framework, which iteratively improves the channel assignment using a metric of total weighted interference where the weight of a MAP is its traffic load.

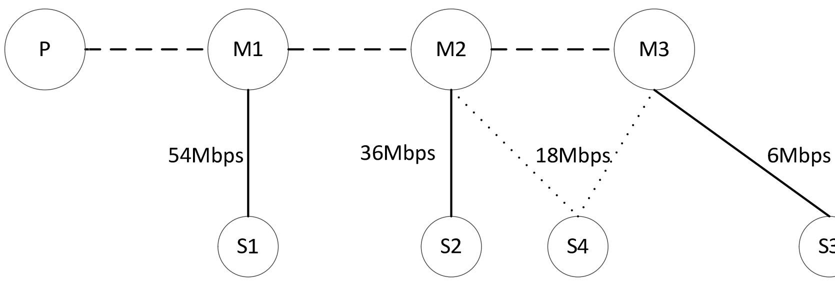

Figure 7.1: An association control and channel assignment example.

We take the network in Fig. 7.1 as an example to illustrate the importance of joint association control (AC) and channel assignment (CA). There are 3 MAPs, 4 STAs and 1 portal in Fig. 7.1 and the access link rates are labelled next to the links. STA S_1, S_2, and S_3

are associated with MAP M_1, M_2, and M_3 respectively. STA S_4 needs to associate with either M_2 or M_3. Suppose the backhaul links do not interfere with the access links and have enough bandwidth to support all the traffic of the STAs. Suppose there are totally 2 non-overlapping channels $\{ch_1$ and $ch_2\}$ to be assigned to the MAPs, and at any time, only one of the MAPs assigned with the same channel can transmit or receive. Suppose the STAs on the same channel get equal transmission time. To see how AC makes difference, we first consider a CA in which M_1, M_2, and M_3 are assigned with ch_1, ch_2, and ch_1 respectively. If S_4 is associated with M_2, the aggregate throughput would be 57Mbps (54/2+36/2+18/2+6/2). On the other hand, if S_4 is associated with M_3, the aggregate throughput would be 62Mbps (54/3+36+18/3+6/3). Next we illustrate how CA makes a difference by changing the channel of M_3 from ch_1 to ch_2. Now the aggregate throughput is further increased to 73Mbps (54+32/3+18/3+6/3). Later we will show how our proposed CA algorithm gets the second CA from the first one.

A survey of channel assignment schemes for WLANs is given in [70]. Least Congested Channel Search (LCCS) [71] is a widely used channel selection method in current WLANs, in which each AP autonomously searches every channel and switches to operate on the channel with the fewest number of STAs or the least amount of traffic. In [16], each AP locally measures the interference power experienced on every channel and switches to operate on a random channel according to a switching probability that is computed based on an annealed Gibbs sampler technique; the global interference is minimized when the algorithm converges. Graph colouring is another classic approach for channel assignment, i.e. treat the APs as vertices of a graph and assign colours (channels) to the vertices such that the number of colours used is minimal or the number of same coloured interfering (connected) nodes is minimal. Optimal colouring is NP-hard. In [72], a heuristic vertex colouring algorithm using the "degree of saturation" (so called

"DSATUR") is introduced, where a vertex with the largest number of differently coloured neighbours is chosen to be coloured in each iteration. If there are more than one vertices of the highest saturation degree, the selection is made in the order of decreasing number of the uncoloured neighbours. Unlike the above AP-centric approaches, [73] is a client-driven approach for channel management. With a model that classifies various interference scenarios, the algorithm repeatedly assigns a channel to each AP such that the number of the conflict-free clients is maximized until that number cannot be improved any more. Instead of using the objectives such as the interference at the AP, the number of coloured APs, and the number of conflicting clients as above that implicitly translate to clients' throughput, our channel assignment algorithm repeatedly invokes an optimal bandwidth allocation procedure to iteratively improve the utility objective function value which explicitly counts the bandwidth of each client. In addition, in the process of finding the best channel for each MAP, we make use of a metric of total-weighted-interference that takes into consideration the load carried by the MAP; through that, the interference at the good-backhaul MAPs can be reduced and the network capacity of the entire WMN can be improved.

The last essential component of our resource management framework is a utility maximization based STA bandwidth allocation algorithm. In the previous example, we only compare the aggregate throughput without considering user fairness. Network aggregate throughput and user fairness in bandwidth are usually two conflicting objectives in bandwidth allocation algorithms. For example, in the example network in Fig. 7.1, we can get the maximum aggregate throughput of 90 Mbps by allowing only S_1 and S_2 to transmit and starving S_3 and S_4, which is obviously very unfair to S_3 and S_4. The IEEE 802.11 MAC protocols implicitly enforce max-min throughput fairness among users in the long term, i.e. each user gets equal transmission opportunity and achieves equal throughput [4]. Researchers have proposed other definitions of fairness such as proportional fair [62] and time-based fairness [60] to make better use of the network resource. Instead of targeting at any single type of fairness as above, our bandwidth allocation algorithm achieves utility-based fairness which is flexible in adjusting the trade-off between resource utilization efficiency and user fairness, which makes it a desirable feature of balanced network operation.

7.2. Network Model

We adopt a protocol-based transmission model to simulate the transmission constraints in a CSMA/CA-alike MAC protocol, where each node has a fixed transmission range and a fixed interference range. To take account of both upstream and downstream traffic, we consider two links conflicting with each other if either end of one link is in the interference range of either end of the other link. Then we can construct a conflict graph for the backhaul links and conflict graphs for the access links on different channels.

We make use of the concept of "clique of links" to model the concurrent transmission constraint of links. A clique is a set of links that are in mutual conflict with each other, i.e. at any time, only a single link within a clique is allowed to transmit. With the constructed conflict graphs, we can find all maximal cliques using algorithms such as Bron-Kerbosch algorithm [63]. However, finding all the maximal cliques over the entire network is NP-hard [63] and not scalable for large networks with thousands of links. Therefore we propose two clique modeling methods, for the backhaul network and the access networks respectively, which approximate the optimal maximal cliques by finding local-maximal cliques. We will see in the simulation results in section 7.4 that the performance of the proposed methods is almost identical to that of the exponential-time optimal algorithm.

Backhaul-link Cliques

Given the set of the backhaul links L_B and the backhaul conflict graph (*BCG*), we can find *a set of backhaul-link cliques* by finding a set of local-maximal backhaul-cliques for each link $l \in L_B$. We first find the set of links that are in conflict with link *l*:

$$L_{cfl}(l) = \{l' : l' \in L_B \wedge BCG(l, l') = 1\} ,$$

where *BCG*(*l*, *l'*)=1 means link *l* and *l'* are in conflict with each other. Then we can find all the local-maximal cliques among the links in $L_{cfl}(l)$ using the Bron-Kerbosch algorithm:

$$K_{cfl}(l) = \{k = \{l'\} : \forall l_1^{'}, l_2^{'} \in k : l_1^{'}, l_2^{'} \in L_{cfl}(l) \wedge l_1^{'} \neq l_2^{'} \wedge BCG(l_1^{'}, l_2^{'}) = 1\} .$$

Including the link *l* itself, we get the set of local-maximal cliques at *l*:

$$k(l) = \{\{l \bigcup k\} : k \in K_{cfl}(l)\} .$$

After combining and simplifying the local-maximal cliques of all the backhaul links, we finally get the set of backhaul-link cliques:

$$K_B = \{k(l) : l \in L_B\} .$$

Access-link Cliques

Given the set of MAPs *M*, the set of STAs *S*, the transmission range *TransR*, the interference range *IntR*, and the locations of the MAPs and STAs, we can find *a set of access-link cliques* by finding a set of local-maximal MAP cliques among the interfering MAPs of each MAP $i \in M$. We first find the set of MAPs that are within the interference range of *i*:

$$M_{IR}(i) = \{i' : i' \in M \wedge dis(i', i) < IntR\} ,$$

the set of STAs that are within the interference range of *i*:

$$S_{IR}(i) = \{j : j \in S \wedge dis(j,i) < IntR\},$$

and the set of STAs that are within the transmission range of i:

$$S_{TR}(i) = \{j : j \in S \wedge dis(j,i) < TransR\},$$

where $dis(\ ,\ )$ is the distance between the two nodes. Given a channel assignment $C=\{c_i\}$, where c_i is the channel assigned to MAP $i \in M$, we can find two sets of interfering MAPs of i. One is the set of MAPs that are within the interference range of i:

$$M_{itf,1}(i) = \{i' : i' \in M \wedge c_{i'} = c_i \wedge i' \in M_{IR}(i)\};$$

the other is the set of MAPs that are outside the interference range of i, but have access links interfering with i:

$$M_{itf,2}(i) = \{i' : i' \in M \setminus M_{IR}(i) \wedge c_{i'} = c_i \wedge (\exists j : j \in S_{TR}(i') \wedge j \in S_{IR}(i))\}.$$

Combining the two, we get

$$M_{itf}(i) = M_{itf,1}(i) \bigcup M_{itf,2}(i).$$

Applying the Bron-Kerbosch algorithm among the MAPs in $M_{itf}(i)$, we can find all the local-maximal MAP cliques of i:

$$Q_{itf}(i) = \{q = \{i'\} : \forall i_1', i_2' \in q : i_1', i_2' \in M_{itf}(i) \wedge i_1' \neq i_2' \wedge i_1' \in M_{IR}(i_2') \wedge i_2' \in M_{IR}(i_1')\}.$$

For each MAP clique $q \in Q_{itf}(i)$, we get an access-link clique:

$$k(i,q) = \{l_{ij} : j \in S\} \bigcup \{l_{i'j} : i' \in q \bigcap M_{itf,1}(i), j \in S\} \bigcup \{l_{i'j} : i' \in q \bigcap M_{itf,2}(i), j \in S_{IR}(i)\},$$

where l_{ij} is the access link between MAP i and STA j. The set of local access-link cliques at i is

$$k(i) = \{k(i,q) : q \in Q_{itf}(i)\}.$$

After combining and simplifying the local access-link cliques of all the MAPs, we finally get the set of access-link cliques

$$K_A = \{k(i) : i \in M\}.$$

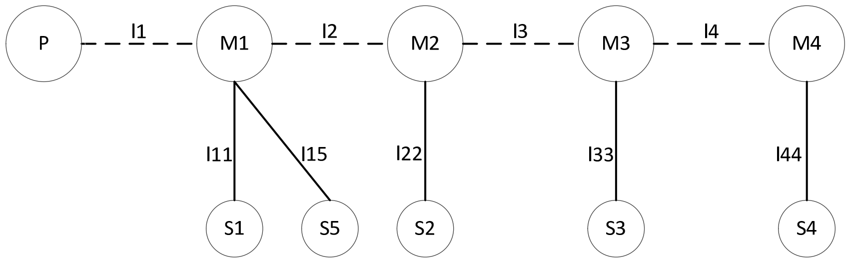

Figure 7.2: A clique modeling example.

We take the network in Fig. 7.2 as an example to illustrate how our clique modeling method works. The set of backhaul links is $\{l_1, l_2, l_3, l_4\}$. The interference range of MAPs is longer than one-hop distance and shorter than two-hop distance. The optimal set of all maximal backhaul-link cliques is $MC_B = \{\{l_1, l_2, l_3\}, \{l_2, l_3, l_4\}\}$. In our modeling framework, taking link l_2 for example, we have $L_{cfl}(l_2) = \{l_1, l_3, l_4\}$, $K_{cfl}(l_2) = \{\{l_1, l_3\}, \{l_3, l_4\}\}$, $k(l_2) = \{\{l_1, l_2, l_3\}, \{l_2, l_3, l_4\}\}$. Combining $k(l_2)$ with the local-maximal cliques at l_1, l_3, and l_4, we get K_B that is the same as the optimal MC_B.

The set of access links in Fig. 7.2 is $\{l_{11}, l_{15}, l_{22}, l_{33}, l_{44}\}$. MAP M_1, M_2, and M_3 operate on ch_1, while M_4 operates on ch_2. STA S_5 is in the interference range of M_3, while S_1 is not. The optimal set of all maximal access-link cliques is $MC_A = \{\{l_{11}, l_{15}, l_{22}\}, \{l_{15}, l_{22}, l_{33}\}, \{l_{44}\}\}$. In our modeling framework, taking MAP M_3 for example, we have $M_{itf,1}(M_3) = \{M_2\}$, $M_{itf,2}(M_3) = \{M_1\}$, $Q_{itf}(M_3) = \{\{M_1, M_2\}\}$, $k(M_3) = \{l_{15}, l_{22}, l_{33}\}$. Combining $k(M_3)$ with the local cliques at M_1, M_2, and M_4, we get K_A that is the same as the optimal MC_A.

Table 7-1: NOTATIONS

Symbol	Semantics
M	The set of all MAPs $\{i\}$.
S	The set of all STAs $\{j\}$.
CH	The set of all non-overlapping channels $\{ch_1, ch_2, \ldots, ch_{N\text{-}CH}\}$.
X	A STA-MAP association matrix $\{x_{ij}\}$.
B	A STA bandwidth allocation vector $\{b_i\}$.
C	A channel assignment vector $\{c_i\}$.
K_B	The set of all backhaul-link cliques.
y_{ki}	Indicating whether backhaul clique k is on MAP i's backhaul path.
r_{ki}	The effective backhaul link rate of MAP i in backhaul clique k.
r_{ij}	The access link rate between MAP i and STA j.
b_{ij}	The bandwidth allocated to STA j to communicate with MAP i.
$M_{itf}(i)$	The set of MAPs that have access links interfering with MAP i on the same channel.
$Q_{itf}(i)$	The set of maximal MAP cliques among the MAPs in $M_{itf}(i)$.

Table 7-1 summarizes some of the notations used in this chapter. The outcome of our resource management framework is a channel assignment vector $\{c_i\}$, an association matrix $\{x_{ij}\}$, and a bandwidth allocation vector $\{b_j\}$, which is denoted as (C, X, B).

7.3. A Network Resource Management Framework for WMNs

Our resource management framework consists of three components: bandwidth allocation (BA), channel assignment (CA), and association control (AC). First, we formulate the optimal utility fair bandwidth allocation problems. Then we introduce a joint channel assignment and bandwidth allocation algorithm. Finally, we present an optimization-based association control scheme as well as the complete resource management framework.

7.3.1. Utility-based Bandwidth Allocation

The objective of our bandwidth allocation algorithm is to maximize the sum of the utility of user bandwidth. The utility function we use is given in (7.1) that has been introduced in Chapter 6.

$$U_\alpha(b_j) = \begin{cases} \log b_j, & \text{if } \alpha = 1 \\ (1-\alpha)^{-1} b_j^{1-\alpha}, & \text{if } \alpha \neq 1 \end{cases} \tag{7.1}$$

Our bandwidth allocation algorithm is named Utility-based Bandwidth allocation (UBa) and given in Fig. 7.3. Given the network topology and a channel assignment C, we can construct the set of backhaul-link cliques, K_B, and the set of local maximal cliques of the interfering MAPs, $Q_{itf}(i)$, for each MAP i. If we are given an integral association matrix X, we formulate an optimization problem named Integral Problem (IntP) as in (7.2) -(7.6), where each STA is allowed to associate with one MAP only. By solving IntP, we get an integral bandwidth allocation vector $\{b_j\}$. On the other hand, if the integral association is unknown, we formulate another optimization problem named Fractional Problem (FracP) as in (7.7)-(7.11), where each STA is allowed to fractionally associate with multiple MAPs. By solving FracP, we get a fractional bandwidth allocation matrix $\{b_{ij}\}$.

Algorithm UBa:

Given: the network topology, the backhaul routing tree, the backhaul link set L_B
Input: (C, X)

1. Construct a backhaul link conflict graph *BCG*
2. Find $L_{cfl}(l)$ and $K_{cfl}(l)$ for each link $l \in L_B$
3. Find K_B, $\{y_{ki}\}$, $\{r_{ki}\}$
4. **for** each MAP $i \in M$ **do**
   a. Find $M_{IR}(i)$, $S_{IR}(i)$, $S_{TR}(i)$
   b. Find $M_{itf,1}(i)$, $M_{itf,2}(i)$, and $M_{itf}(i)$
   c. Construct a conflict graph for MAPs in $M_{itf}(i)$
   d. Find $Q_{itf}(i)$

   end for
5. **if** X=0 **then**
   Formulate and solve the problem FracP
   return the fractional BA solution $\{b_{ij}\}$

   else
   Formulate and solve the problem IntP
   return the integral BA solution $\{b_j\}$

end if

Figure 7.3: Algorithm UBa

IntP:

Max $\quad \sum_{j \in S} U_\alpha(b_j)$

s.t.

$$\forall j \in S: \quad \sum_{i \in M} x_{ij} = 1 \tag{7.2}$$

$$\forall j \in S: \quad \sum_{i \in M} x_{ij} \frac{b_j}{r_{ij}} \le 1 \tag{7.3}$$

$$\forall k \in K_B: \sum_{i \in M} \frac{y_{ki}}{r_{ki}} \sum_{j \in S} x_{ij} b_j \le 1 \tag{7.4}$$

$$\forall q \in Q_{itf}(i), i \in M:$$

$$\sum_{j \in S} x_{ij} \frac{b_j}{r_{ij}} + \sum_{i':i' \in q \wedge i' \in M_{IR}(i)} \sum_{j \in S} x_{i'j} \frac{b_j}{r_{i'j}} + \sum_{i':i' \in q \wedge i' \notin M_{IR}(i)} \sum_{j \in S_{IR}(i)} x_{i'j} \frac{b_j}{r_{i'j}} \le 1 \tag{7.5}$$

$$\forall i \in M, j \in S: \quad x_{ij} \in \{0,1\}, \quad b_j \ge 0 \tag{7.6}$$

FracP:

Max $\quad \sum_{j \in S} U_\alpha(b_j)$

s.t. $$\forall j \in S: \quad b_j = \sum_{i \in M} b_{ij} \tag{7.7}$$

$$\forall j \in S: \quad \sum_{i \in M} \frac{b_{ij}}{r_{ij}} \le 1 \tag{7.8}$$

$$\forall k \in K_B: \sum_{i \in M} \frac{y_{ki}}{r_{ki}} \sum_{j \in S} b_{ij} \le 1 \tag{7.9}$$

$$\forall q \in Q_{itf}(i), i \in M: \sum_{j \in S} \frac{b_{ij}}{r_{ij}} + \sum_{i': i' \in q \wedge i' \in M_{IR}(i)} \sum_{j \in S} \frac{b_{i'j}}{r_{i'j}} + \sum_{i': i' \in q \wedge i' \notin M_{IR}(i)} \sum_{j \in S_{IR}(i)} \frac{b_{i'j}}{r_{i'j}} \le 1 \tag{7.10}$$

$$\forall i \in M, j \in S: \quad b_{ij} \ge 0 \tag{7.11}$$

Constraint (7.2) states that each STA is associated with one MAP only. (7.3) states that the total transmission time of one STA is less than the unit time 1. (7.4) states that the total transmission time of the backhaul links in one backhaul clique is less than 1, where the traffic load carried by the clique originates from all the STAs whose associated MAP backhaul paths towards the portal pass through the clique. (7.5) states that the total transmission time of the access links belonging to one access clique is less than 1, where the access clique consists of the links of a MAP *i* and the links that interfere with *i* and belonging to a set of MAPs that mutually conflict with each other. By introducing the fractional bandwidth allocation matrix $\{b_{ij}\}$, FracP is derived from IntP by replacing b_j with $\sum_{i \in M} b_{ij}$ and replacing $x_{ij} \cdot b_j$ with b_{ij}.

7.3.2. Joint Channel Assignment and Bandwidth Allocation

We propose a channel assignment scheme, named Joint Channel assignment and Bandwidth allocation (JCaBa), which iteratively improves channel assignment and network performance by invoking the bandwidth allocation algorithm UBa and makes use of an interference metric that measures the interference experienced by a MAP as well as the interference caused by the MAP to the others. Algorithm JCaBa is given in Fig. 7.4.

Algorithm JCaBa:

C^* ← random CA
B^* ← UBa(C^*,0)
$Load_{self}^*$ ← CalculateLs(B^*) {sort $Load_{self}^*$ in non-increasing order}
n ← 1 {let $i(n)$ represent the nth MAP in the sorted vector $Load_{self}^*$}
$M_{allocated}$ ← ∅
$change$ ← 0
while $n \le |M|$ **do**
    if $i(n) \notin M_{allocated}$ **then**
        c_0 is the current channel of $i(n)$ in C^*
        for $c \in CH \setminus c_0$ **do**
            change the channel of $i(n)$ to c, denote the new CA as C_c
            $load_c$ ← CalculateWI(C_c, B^*, $i(n)$)
        end for
        $load_{\min} \leftarrow \min\{load_c : c \in CH \setminus c_0\}$, denote the corresponding CA as C'
        B' ← UBa(C',0)
        $Load_{self}'$ ← CalculateLs(B')
        if $f_{utility}(B') > f_{utility}(B^*)$ **then**
            {assign $i(n)$ with the new channel}
            $C^* \leftarrow C'$; $B^* \leftarrow B'$; $Load_{self}^* \leftarrow Load_{self}'$; $n \leftarrow 1$; $change \leftarrow 1$
        else
            $n \leftarrow n+1$ {keep the channel of $i(n)$ unchanged}
        end if
        Add $i(n)$ to $M_{allocated}$
    else
        $n \leftarrow n+1$ {the channel of $i(n)$ has been assigned already}
    end if
    if $n = |M|+1$ and $change = 1$ **then**
        $n \leftarrow 1$; $change \leftarrow 0$; $M_{allocated} \leftarrow \emptyset$
    end if
end while
return C^* and $f_{utility}(B^*)$

Figure 7.4: Algorithm JCaBa.

Given a CA C, we can get an optimal fractional BA matrix $B = \{b_{ij}\}$ by applying algorithm UBa with input (C,0). Denote the utility objective function value of B as $f_{utility}(B)$. For each MAP $i \in M$, denote the total traffic to be carried by i for its associated STAs as $load_{self}(i)$, i.e. self-load of i:

$$load_{self}(i) = \sum_{j \in S} b_{ij} \,. \tag{7.12}$$

For each MAP $i' \in M_{itf}(i)$, i.e. i' is one of the interfering MAPs of i, denote the traffic that is carried by i' and interferes with i as $load_{itf}(i,i')$, i.e. interference-load to i from i':

$$load_{itf}(i,i') = \begin{cases} \sum_{j \in S} b_{i'j}, & \text{if } i' \in M_{itf,1}(i) \\ \sum_{j \in S_{IR}(i)} b_{i'j}, & \text{if } i' \in M_{itf,2}(i) \end{cases} \tag{7.13}$$

Denote the total self-load of i and its interfering MAPs in $M_{ift}(i)$ as $load_{t\text{-}self}(i)$:

$$load_{t-self}(i) = load_{self}(i) + \sum_{i' \in M_{itf}(i)} load_{self}(i') \tag{7.14}$$

We define a metric of total weighted interference for i, denoted as $load_{t\text{-}w\text{-}itf}(i)$. The metric is formulated in (7.15) and consists of two parts. The first part is the total interference experienced by i, weighted by $load_{self}(i)$ / $load_{t\text{-}self}(i)$. The second part is the total interference to MAPs in $M_{itf}(i)$ caused by i, weighted by $load_{self}(i')$ / $load_{t\text{-}self}(i)$ for each $i' \in M_{itf}(i)$. By weighting a MAP with its self-load divided by the total load, the interference experienced by the heavy-self-load MAPs contributes more to the total interference. As introduced previously, in WMNs, it is preferred that the good-backhaul MAPs carries more traffic load. Therefore, by reducing the total-weighted-interference metric defined in (7.15), we reduce the interference experienced by the good-backhaul MAPs and increase the network capacity.

$$load_{t-w-itf}(i) = \frac{load_{self}(i)}{load_{t-self}(i)} \cdot \sum_{i' \in M_{itf}(i)} load_{itf}(i,i') + \sum_{i' \in M_{itf}(i)} \frac{load_{self}(i')}{load_{t-self}(i)} \cdot load_{itf}(i',i) \tag{7.15}$$

In Fig. 7.4, the function CalculateLs(B) calculates the self-load vector $Load_{self}$ $=\{load_{self}(i)\}$ using (7.12). The function CalculateWI(C, B, i) calculates the total-weighted-interference $load_{t\text{-}w\text{-}itf}(i)$ for MAP i using (7.15), when the CA is C and the BA is B. We sort MAPs in decreasing order of their self-load so that the MAPs carrying heavier load are assigned channels first. In one round of the while-loop, the sorted MAPs, one by one from the beginning, decide to stay in the current channel or switch to a new channel. In order to make that decision, a MAP first searches for the channel with the least total-weighted-interference; denote the corresponding CA and BA as C' and B' respectively, while the current CA and BA are C^* and B^*. If the objective function value of the new BA, $f_{utility}(B')$, is larger than that of B^*, the MAP switches to the new channel; otherwise, it stays with the current channel. The algorithm terminates if no MAP switches channel in the last round of the while-loop. In our simulations, the algorithm always terminates within a few rounds of the while-loop.

Revisit the network in Fig. 7.1. Suppose we are given a CA $C_0 = \{ch_1, ch_2, ch_1\}$ that is produced by a vertex colouring algorithm. We demonstrate how the JCaBa algorithm improves C_0 and find a better CA. With C_0, the best aggregate throughput is 62 Mbps that is obtained when S_4 associates with M_3, and the corresponding self-load vector is {18, 36, 8}. In the first round of the while-loop: M_2 exams CA $\{ch_1, ch_1, ch_1\}$, for which the aggregate throughput is 28.5 Mbps, and decides to stay with ch_2; then M_1 exams CA $\{ch_2, ch_2, ch_1\}$, for which the best aggregate throughput is 57 Mbps, and decides to stay with ch_1; finally, M_3 exams CA $\{ch_1, ch_2, ch_2\}$, for which the aggregate throughput is 74 Mbps, and decides to switch to ch_2. In the second round of the while-loop, as no MAP can find a better CA, the algorithm terminates and returns CA $\{ch_1, ch_2, ch_2\}$.

7.3.3. The Resource Management Framework

Algorithm JCBA:

1. CA: Apply the JCaBa algorithm a few times and select the best CA *C'*.
2. AC: Generate an integral association $\hat{X}'$ by applying the oAC algorithm:
    1) Get a fractional BA *B'* by the algorithm UBa(*C'*, 0).
    2) Generate a fractional association *X'* from *B'*.
    3) Round *X'* to $\hat{X}'$ by the randomization rounding.
3. BA: Get an integral BA $\hat{B}'$ using the algorithm UBa(C', $\hat{X}'$).

$(C', \hat{X}', \hat{B}')$ is the output.

Figure 7.5: Algorithm JCBA.

Our resource management framework jointly considers CA, BA, and AC, so we name it Joint Channel assignment, Bandwidth allocation and Association control algorithm (JCBA), which is given in Fig. 7.5. It has been shown in [74] that CA should be conducted prior to AC for better network performance. It makes sense as CA determines the interference between cells in large scale and should be performed less frequently compared to AC. Therefore, the first step of JCBA is to determine a proper CA by applying the JCaBa algorithm a few times with different initial random CAs. The reason to do that is JCaBa locally searches for better channels and rarely generates a global optimal CA in a single run. The CA that achieves the largest objective function value is selected and denoted as *C'*.

The second step of JCBA is to generate an integral association, denoted as $\hat{X}'$, by applying an association control algorithm, named optimization-based Association Control (oAC). The first step of oAC is to find a fractional BA, *B'*, by applying the UBa algorithm with (*C'*, 0) as input. Then we convert *B'* to a fractional association matrix *X'* according to the equation

$$x'_{ij} = b'_{ij} / \sum_{i \in M} b'_{ij} \ .$$

In the third step of oAC, *X’* is rounded to the integral solution $\hat{X}'$, via randomization rounding. Denote the set of MAPs that have fractional association with STA *j* in *X’* as *M*(*j*), i.e. $M(j) = \{i : b'_{ij} > 0\}$. By the randomization rounding, *j* randomly selects one of the MAPs in *M*(*j*) to associate with.

In the final step of JCBA, we get an integral BA, denoted as $\hat{B}'$, by applying the UBa algorithm with $(C', \hat{X}')$ as input. Finally, $(C', \hat{X}', \hat{B}')$ is the output of the JCBA algorithm.

7.4. Performance Evaluation

We present simulation results for a WMN that consists of 20 MAPs, 100 STAs, and 1 portal. The MAPs are randomly placed in a square field of size 250m $\times$ 250m. The portal is located at the centre of the lower-left quarter field. We simulate two user topologies: uniform topology where the STAs are randomly placed in the field; hotspot topology where the STAs are distributed in two randomly located hotspots of radius 50m each. We provide two network topology examples in Fig. 7.6, one for uniform topology and the other for hotspot topology. In Fig. 7.6, we use diamond, bigger circles, and smaller circles to represent the portal, the MAPs, and the STAs, respectively; the backhaul links are displayed in red lines.

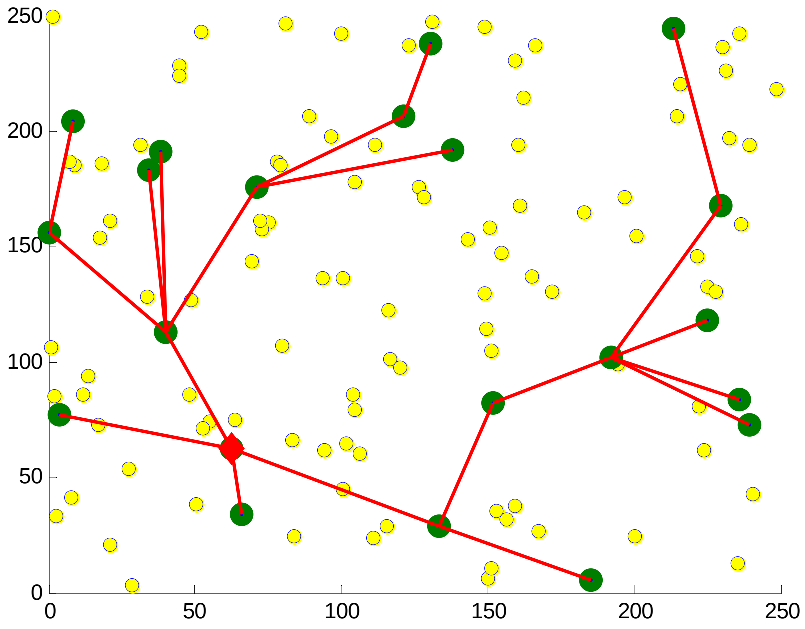

(a) Uniform topology

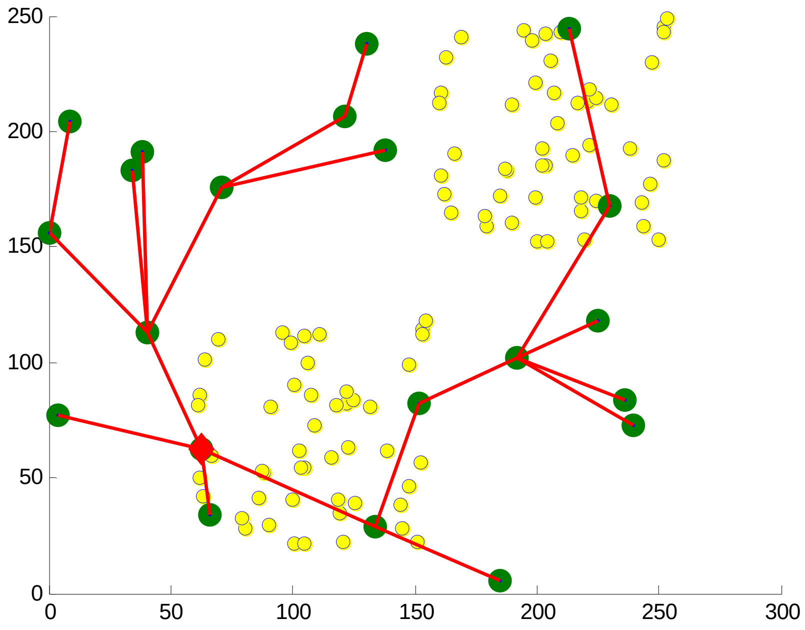

(b) Hotspot topology

Figure 7.6: Network topology examples.

We assume a transmitter power of 17dBm and a receiver noise power of -80dBm. We adopt a log-distance path loss model, $P_l(d)$=92+4*10log$_{10}$(d/100), where $P_l(d)$ is the path loss in dB for a path of length d m. Considering a normal Clear Channel Access

(CCA) threshold of -76dBm [7], our protocol-based network model simulates a MAC protocol similar to the CSMA/CA with a transmission range of 100m and an interference range of 150m. In our simulation, the access networks operate on 4 non-overlapping 20MHz channels in the 2.4GHz frequency band, while the backhaul network operates on a single 160MHz channel in the 5GHz frequency band. The backhaul routing tree rooted at the portal is constructed using the 802.11s HWMP routing protocol. We model the transmission constraints at the backhaul and the access networks using the local-clique-based modeling methods introduced in section 7.2.

Using the transmission model above, an access link rate model is constructed and given in Table 7-2, where the required minimum Signal-to-Noise Ratio (SNR) is taken from [68]. As the wireless backhaul carries the aggregate traffic of the entire network and the MAPs are more powerful than the STAs, in our simulation, the backhaul link rates are 16 times of the access link rates, which can be achieved by applying two spatial streams on the 160MHz backhaul channel. We have done simulations with other configurations, such as different MAP/portal topologies, different number of STAs, and different backhaul/access link rate ratios; their results are qualitatively similar to those we are presenting.

Table 7-2: LINK RATE MODEL FOR ACCESS LINKS

Rate(Mbps)	6	12	18	24	36	48	54	60
Min. SNR (dB)	5	7	9	13	17	20	22	23
Max. Path Length (m)	100	89	79	63	50	42	38	35

We measure the performance of different algorithms in terms of aggregate network throughput, per-user bandwidth, and Jain's fairness index [12].

7.4.1. Performance of the Local-clique-based Modeling Method

A backhaul clique modeling method finds the set of backhaul-link cliques, K_B, which is required for formulating the backhaul transmission constraint (7.4) and (7.9) in the bandwidth allocation algorithm UBa. We compare the performance of the following backhaul clique modeling methods:

- local-BC: our backhaul-link local-clique-based modeling method that constructs K_B by finding the set of conflicting links, $L_{cfl}(l)$, and the set of local maximal cliques of the conflicting links, $K_{cfl}(l)$, for each link $l \in L_B$.
- o-BMC: optimal clique modeling method that finds all backhaul maximal cliques in the network by an exponential-time algorithm such as the Bron-Kerbosch algorithm.
- a-BC: a maximal clique approximation method used in [42] that approximates a backhaul maximal clique by the set of conflicting links of a backhaul link, i.e. $K_B = \{\{L_{cfl}(l) \bigcup l\} : l \in L_B\}$.

An access clique modeling method finds a set of access-link cliques for each channel, which is required for formulating the access network transmission constraints in UBa. We compare the performance of the following access clique (transmission constraint) modeling methods:

- local-AC: our MAP local-clique-based modeling method that constructs the access transmission constraints (7.5) and (7.10) by finding the set of interfering MAPs, $M_{itf}(i)$, and the set of local maximal cliques of the interfering MAPs, $Q_{itf}(i)$, for each MAP $i \in M$.

- o-AMC: optimal clique modeling method that finds all the access maximal cliques in the network by an exponential-time algorithm such as the Bron-Kerbosch algorithm. Accordingly, constraints (7.5) and (7.10) are replaced by (7.16) and (7.17) respectively, where $K_A(c)$ is the set of all access cliques on channel c.
- a-AC: an access clique approximation method that approximates an access clique by the links of the MAPs interfering with a MAP, i.e.

$$K_A = \{\{\{l_{ij}\} \cup \{l_{i'j} : i' \in M_{IR}(i) \wedge c_{i'} = c_i\}\} : i \in M\} .$$

  Accordingly, constraints (7.5) and (7.10) are replaced by (7.18) and (7.19) respectively.

$$\forall k \in K_A(c), c \in CH: \quad \sum_{l_{ij} \in k} x_{ij} \frac{b_j}{r_{ij}} \le 1 \tag{7.16}$$

$$\forall k \in K_A(c), c \in CH: \quad \sum_{l_{ij} \in k} \frac{b_{ij}}{r_{ij}} \le 1 \tag{7.17}$$

$$\forall i \in M: \quad \sum_{j \in S} x_{ij} \frac{b_j}{r_{ij}} + \sum_{i': i' \in M_{IR}(i) \wedge c_{i'} = c_i} \sum_{j \in S} x_{i'j} \frac{b_j}{r_{i'j}} \le 1 \tag{7.18}$$

$$\forall i \in M: \quad \sum_{j \in S} \frac{b_{ij}}{r_{ij}} + \sum_{i': i' \in M_{IR}(i) \wedge c_{i'} = c_i} \sum_{j \in S} \frac{b_{i'j}}{r_{i'j}} \le 1 \tag{7.19}$$

Fig. 7.7 depicts the bandwidth allocation results of the UBa algorithm with different transmission constraints that are obtained from the clique modeling methods. The results presented are averaged over 50 runs. In each run, the STA location is different and we sort the STAs in non-decreasing order of their allocated bandwidth. So the bandwidth of a STA indexed x in the figure indicates the average bandwidth of the x-th lowest bandwidth in each run. We compare the backhaul (access) clique modeling methods, while using o-AMC (o-BMC) to model the access (backhaul) cliques. The α parameter in the UBa algorithm equals 5.

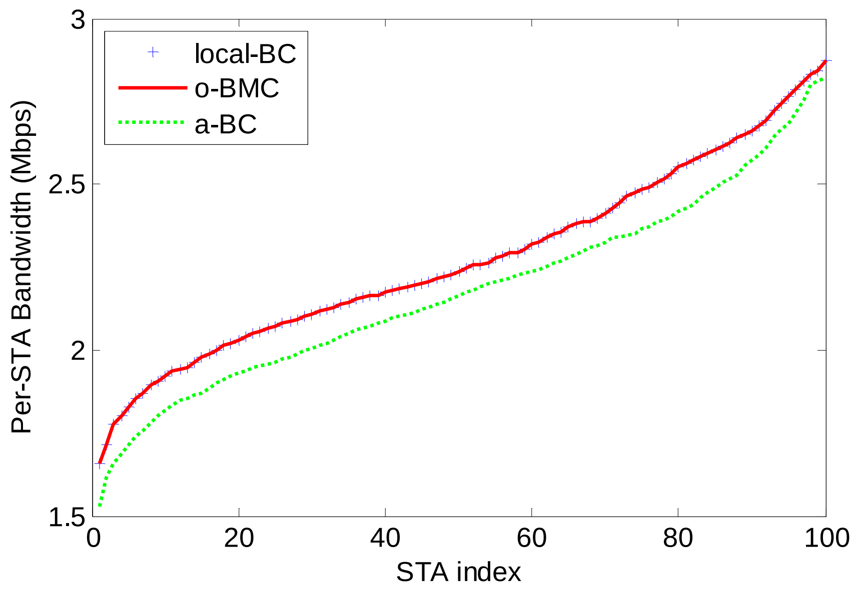

(a) Backhaul clique

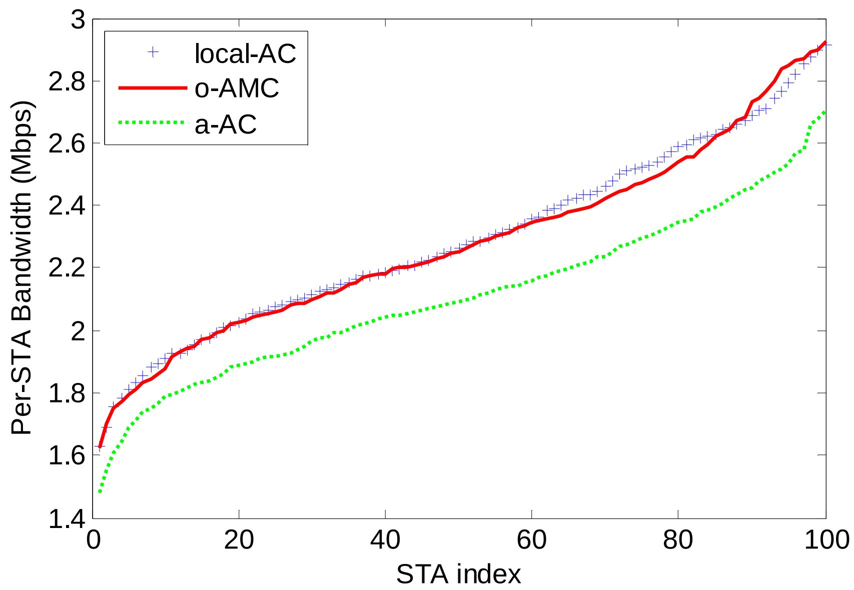

(b) Access clique

Figure 7.7: Performance of the clique modeling methods

In Fig. 7.7 (a), local-BC and o-BMC have identical result, which means local-BC is able to find all the backhaul maximal cliques in the simulated networks. In contrast, the results of a-BC clearly deviate from the optimal. That is because in a-BC, links that are in conflict with the same link but do not interfere with each other are prohibited from concurrent transmission, while they are able to do so actually.

In Fig. 7.7 (b), the curve of local-AC almost coincides with that of o-AMC. The reason for the small difference is that local-AC is based on the local maximal cliques of the interfering MAPs rather than the maximal clique of the access links. As a result, local-AC may miss some links that should have been included in the clique, resulting in a loosened access network transmission constraint. The results of a-AC seriously deviate from the optimal one. a-AC prohibits MAPs that interfere with one common MAP but do not interfere with each other from concurrent transmission, even though that will not cause any collision.

The optimal methods, o-BMC and o-AMC, search for maximal cliques over the entire network using exponential-time algorithm; therefore, they are very time consuming for large networks. Our local-clique-based approximation methods, local-BC and local-AC, on the other hand, locally search for maximal cliques where the number of variables is much smaller; therefore, they are more efficient than the exponential-time methods. In addition, as seen in Fig. 7.7, our methods achieve almost optimal performance. Therefore, we can say that the local-clique-based modeling methods are efficient and effective.

7.4.2. Performance of JCBA

In the JCBA algorithm, the channel assignment is done by the JCaBa algorithm and the association control is done by the oAC algorithm. We compare the bandwidth allocation results of the algorithms in JCBA against other state-of-the-art CA and AC schemes.

We compare the following CA schemes:

- VC: vertex coloring algorithm DSATUR [72] that is introduced in section 7.1.

- JCaBa: joint channel assignment and bandwidth allocation algorithm that is used in the first step of JCBA.

We compare the following AC schemes:

- SS: strongest signal, i.e. a STA associates with the MAP from which the received signal strength is the highest.
- CL: cross layer association metric based AC [38]. The total association cost is a weighted sum of the access cost and the backhaul cost, which reflects the estimated amount of channel time consumed by a successful end-to-end packet transmission.
- oAC: optimization-based association control algorithm that is used in the second step of JCBA.

Table 7-3: AGGREGATE THROUGHPUT AND FAIRNESS INDEX OF THE CA-AC SCHEMES

		VC-SS	VC-CL	VC-oAC	JCaBa-oAC
Uniform	Throughput	195.7083	203.4558	229.4323	238.4053
	Fairness	0.9693	0.9581	0.9835	0.984
Hotspot	Throughput	190.0122	196.0362	209.3868	224.3168
	Fairness	0.8157	0.8113	0.9864	0.9827

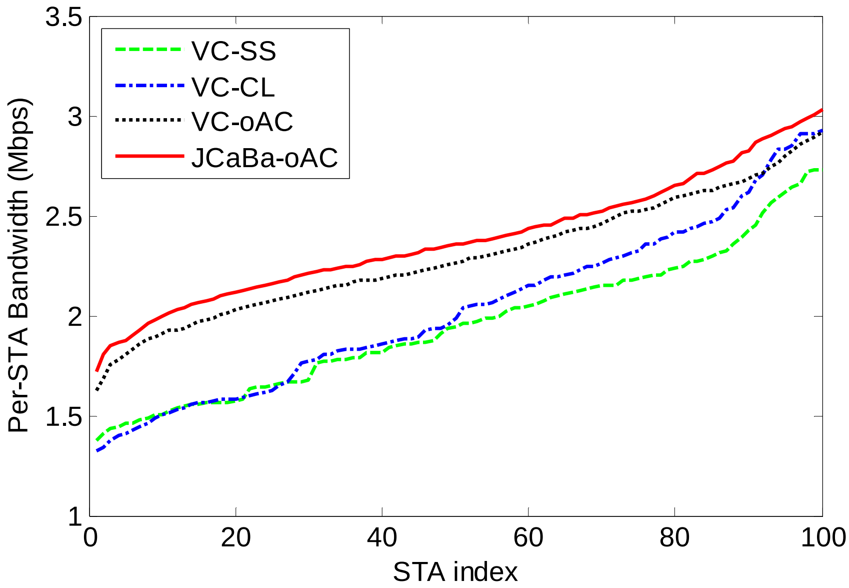

(a) Uniform topology

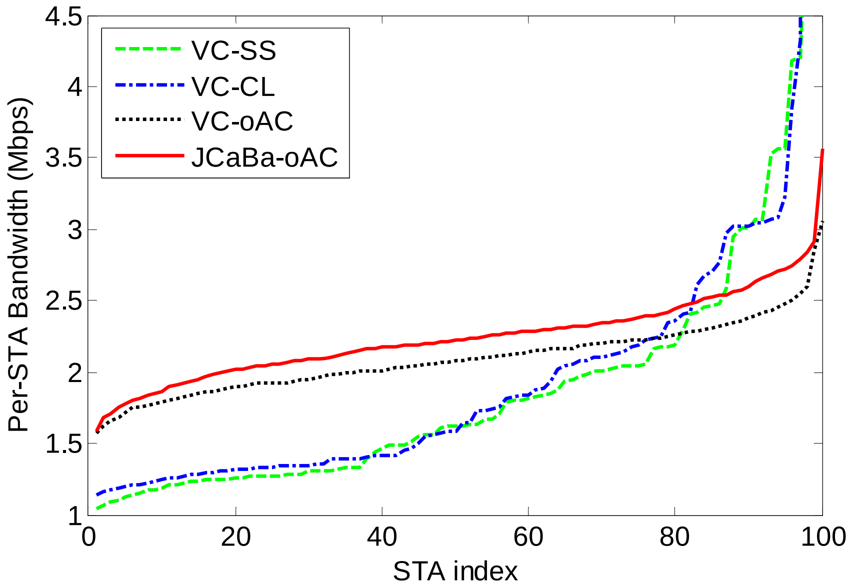

(b) Hotspot topology

Figure 7.8: Performance of the CA-AC schemes.

Table 7-4: PERFORMANCE OF THE CA SCHEMES

		3-CH	4-CH	5-CH	6-CH
Throughput	VC	214.2037	229.4323	239.766	249.7643
	JCaBa	221.8147	238.4053	249.12	258.5956
Fairness	VC	0.984	0.9835	0.9832	0.9795
	JCaBa	0.9824	0.984	0.9831	0.9791

Fig. 7.8 depicts the per-STA bandwidth performance of four combinations of CA-AC schemes under uniform user topology and hotspot user topology; Table 7-3 gives the corresponding numerical results of the aggregate throughput and Jain's fairness index. Under the same channel assignment done by the VC algorithm, we compare the performances of the AC schemes. The performance of CL is slightly better than that of SS, because CL considers not only the access network condition but also the backhaul condition. As a result, CL has more STAs associated with the good-backhaul MAPs and makes better use of the network resource. However, due to the nature of the heuristic algorithms, CL has no optimization attempt and it has no consideration in the utility objective when making association decision. Therefore, it is as expected in that CL performance is significantly poorer than that of oAC in terms of both throughput and fairness. Under the hotspot topology, the bandwidth allocation in SS and CL is very unfair because too many STAs associate with the hotspot MAPs and the STAs associated with the non-hotspot MAPs are allocated with excessive bandwidth. In contrast, oAC is able to achieve very fair user bandwidth allocation no matter what the user topology is.

Using oAC as the AC algorithm, we compare the performances of the CA schemes. In Fig. 7.8 and Table 7-3, it is clear that JCaBa is able to improve the user bandwidth as well as the aggregate throughput without sacrificing the user fairness. As it is NP-hard to find the optimal channel assignment for comparison, we measure the performance improvement of JCaBa over VC by varying the number of non-overlapping channels available in the access networks, and the results are given in Table 7-4. It is interesting to notice that, when the number of channels is 4 or 5, with nearly unchanged fairness index, the throughput increment of JCaBa over VC almost equals the throughput increment that would be gained by adding one more channel to VC, i.e. JCaBa-4CH : VC-5CH = 238.4 : 239.7 and JCaBa-5CH : VC-6CH = 249.1 : 249.7. In other words, the channel utilization efficiency of JCaBa is about 20%-25% higher than that of VC. The objective of VC is to minimize the total interference experienced by the MAPs, which equally weights each MAP. In contrast, in JCaBa, the interference experienced by the good-backhaul MAPs contributes more to the total interference, and it is minimized with priority. As JCaBa increases the capacity of the good-backhaul MAPs, more STAs can associate with these MAPs, which further improves the network resource utilization efficiency.

The JCaBa results presented are the best of 10 runs of the JCaBa algorithm with different random initial channel assignments. In each run, 3.97 while-loops are conducted in average, with a standard deviation of 1.22. In each while-loop, $|M|$, which is 20 in our simulation, the FracP convex problems are solved. So the JCaBa algorithm terminates within a few rounds of convex problem solving.

Comparing the CA and AC schemes in Fig. 7.8, it is noticed that the performance improvement of oAC over SS/CL is much more obvious than that of JCaBa over VC. In other words, the performance improvement of JCBA algorithm is mostly contributed by the oAC algorithm in the AC step.

JCBA is a centralized optimization based resource management framework. It should be triggered when the network condition has significantly changed, e.g. mass joining/leaving of MAPs/STAs, and blocked/broken backhaul paths. The triggering mechanism could be periodic-time-based or based on real time network condition measurement. Excessive triggering would cause unnecessary interruption to the normal communication and should be avoided. On the other hand, inadequate triggering may miss network dynamics and result in inferior performance. In JCBA framework, oAC should be triggered more frequently than JCaBa for three reasons. Firstly, a channel switch at a MAP incurs channel switching at all of its associated STAs, while an association change requires action at one STA only, i.e. invoking JCaBa interrupts more users. Secondly, oAC is more effective in improving user bandwidth as seen in Fig. 7.8. Thirdly, oAC is more time efficient as only one convex problem needs to be solved.

Besides the simulation results for networks of 20 MAPs and 100 STAs presented above, we also conduct simulation for networks of higher node density, where 40 MAPs and 200 STAs are randomly located in a square field of the same size as above. The numerical results are given in Table 7-5. Compared to the results in the low density networks, in the high density networks, the performance of all the CA-AC schemes is better, and the advantage of JCBA over the other schemes is more obvious. That can be explained from two aspects. Firstly, although the higher node density introduces more inter-cell interference, the average link rate of the access links and the backhaul links are higher due to the shorter inter-node distance. What is more important is that with more MAPs available in the vicinity, a STA has more opportunities to associate with a good-backhaul MAP, which can be better utilized by oAC to find a better association. Therefore, the advantage of oAC over SS/CL is more obvious in the high density networks. However, the performance improvement of JCaBa over VC is not as significant as before, which can also be explained from two aspects. Firstly, due to the high node density, the interference at the good-backhaul MAPs cannot be eliminated or significantly reduced no matter how effective a CA scheme is. Secondly, by oAC, a lot of STAs are already associated with the good-backhaul MAPs, so even though JCaBa can reduce the interference at the good-backhaul MAPs, there would not be many more STAs switching to associate with these MAPs.

Table 7-5: PERFORMANCE FOR THE NETWORKS OF HIGHER NODE DENSITY

		VC-SS	VC-CL	VC-oAC	JCaBa-oAC
Uniform	Throughput	225.0974	244.648	288.4014	295.6415
	Fairness	0.9837	0.9818	0.9882	0.9851
Hotspot	Throughput	232.8061	239.213	270.2059	282.0215
	Fairness	0.9238	0.8379	0.9928	0.9913

Finally, we take a look at the performance of UBa, which is the utility fair bandwidth allocation algorithm in the JCBA algorithm. Fig. 7.9 (a) depicts the aggregate throughput and Jain's fairness index result when the fairness control parameter α varies from 0.5 to 4. It is clear that as α increases, the aggregate throughput deceases and the fairness index increases. Fig. 7.9 (b) depicts the per-STA bandwidth results. It is obvious that with a larger α, the line is flatter, which indicates a fairer bandwidth allocation. With a smaller α, the line is steeper and the area below the line is larger, which indicates a less fair bandwidth allocation and higher aggregate throughput.

Note that the fairness index here reflects the fairness in user bandwidth. There are also other definitions of fairness, such as the fairness in user transmission time. A proper α value should be determined by the network designer/operator, so that the desired fairness can be enforced. As α becomes larger and larger, we get better and better fairness in user bandwidth at the expense of lower and lower network resource utilization efficiency. It is interesting to notice that in Fig. 7.9 (b), as α increases, the bandwidth of the low-bandwidth STAs on the left, which is about 60% of the entire STAs, slightly decreases, while the bandwidth of the high-bandwidth STAs on the right, which is the rest 40% of STAs, dramatically increases. So it might be a good idea to select a smaller α. Anyway, UBa is a powerful tool for bandwidth allocation that is flexible in adjusting the trade-off between resource efficiency and user fairness.

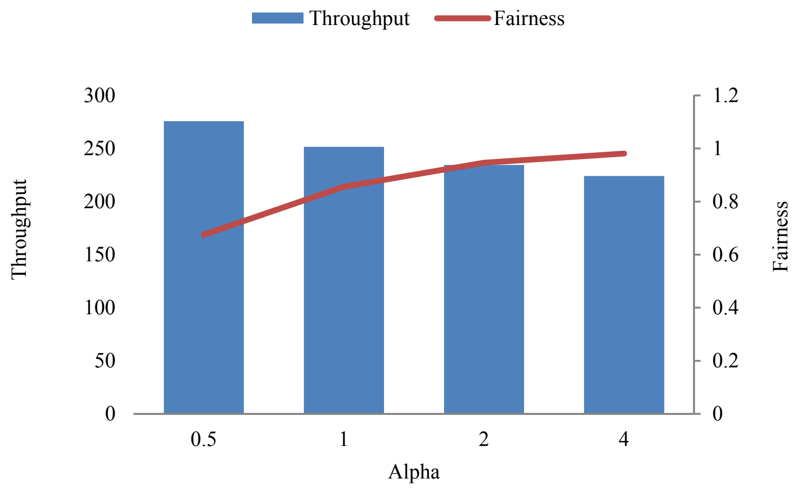

(a) Aggregate throughput and fairness index

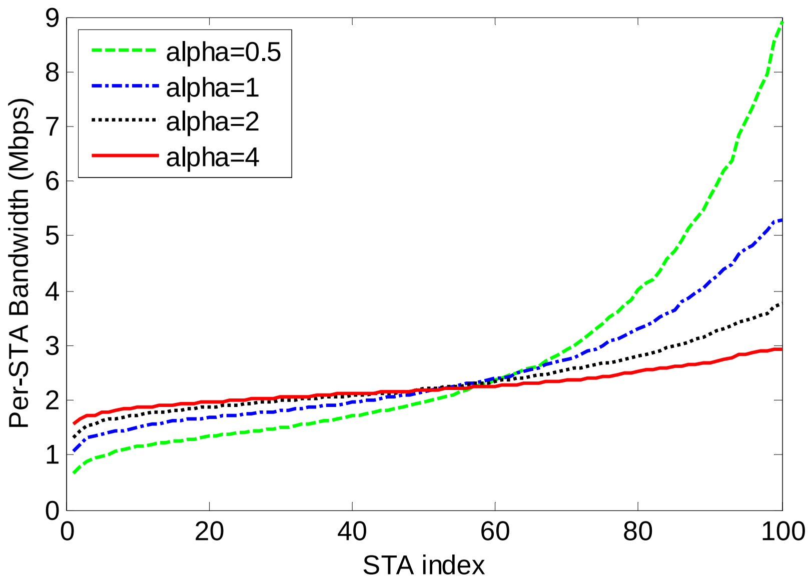

(b) Per-STA bandwidth

Figure 7.9: Performance of UBa with different α value.

7.5. Conclusion

In this chapter, we have proposed a network resource management framework, named JCBA, for WMNs, which jointly considers channel assignment, association control, and bandwidth allocation. JCBA framework is composed of three components: a utility-based bandwidth allocation algorithm, named UBa, which is flexible in adjusting the trade-off between resource utilization efficiency and user fairness in bandwidth; a channel assignment algorithm, named JCaBa, which effectively increases the network capacity by reducing the interference at the good-backhaul MAPs; an optimization-based association control algorithm, named oAC, which finds approximately optimal association solutions such that the network capacity can be further improved by letting more STAs associate with the good-backhaul MAPs. In addition, we have proposed a local-clique-based network modeling method, to model the concurrent transmission constraints in WMNs, whose performance is almost identical to that of the exponential-time optimal algorithms. We have demonstrated the superior performance of the proposed algorithms over the other state-of-the-art schemes through simulations with various network topologies and conditions.

Chapter 8: Conclusion and Future Works

8.1. Conclusion

In this thesis, we have investigated association control mechanisms for wireless mesh networks from various aspects. We have proposed several new association control schemes for WMNs, which take into consideration the capacity-limited wireless multi-hop backhaul of WMNs and improve the network performance in terms of aggregate throughput, end-to-end packet delay, resource utilization efficiency, user fairness, etc. We have proposed practical heuristic association and re-association control schemes for static and dynamic WMNs. We have formulated the optimal association problems, for which we have proposed approximation algorithms and conducted theoretical analysis. As association control, MAP channel assignment, and STA bandwidth allocation are closely related to each other, we have proposed a resource management framework that jointly considers the three subjects and further improves the network performance. We have demonstrated the superior performance of the proposed schemes against the state-of-the-art schemes via simulations on ns-3 simulator as well as our customized simulator.

In Chapter 3, we proposed a cross-layer heuristic association scheme that is able to effectively allocate more STAs to the good-backhaul MAPs and at the same time avoid over-congestion at these MAPs.

In Chapter 4, we proposed a mobility-aware re-association control scheme that is able to prolong mobile STAs' association time with the good-backhaul MAPs and discover network dynamics in a smart and timely way without interrupting normal communication too much.

In Chapter 5, we formulated the problem of optimal joint association and bandwidth allocation in WMNs, considering max-min fairness and proportional fairness objectives. We proposed two approximation algorithms for the optimization problems and analysed the theoretical approximation ratios as well as the corresponding ratio improvement algorithms.

In Chapter 6, we formulated an optimal joint association and bandwidth allocation problem that achieves a utility fairness objective in WMNs. We demonstrated how to control the trade-off between resource efficiency and user fairness to achieve the desired performance by tuning the proposed control parameters.

In Chapter 7, we proposed a network resource management framework that is composed of three components: a utility-fairness-based bandwidth allocation algorithm, a channel assignment algorithm, and an optimization based association control algorithm. In addition, we proposed an efficient local-clique based network modeling method whose performance is almost identical to that of the exponential-time optimal algorithms.

8.2. Future Works

We may find applications of the algorithms, methodologies, and network models of our association control schemes proposed for infrastructure WMNs in other network scenarios, such as cluster formation in wireless sensor networks or vehicular networks, gateway association in ad hoc or mesh networks, congestion relief at hot-spot cells in WLANs or cellular networks, user association/re-association in relay networks, user association in hybrid mesh networks where inter-STA communication is possible, etc.

In our heuristic association control schemes proposed in Chapter 3 and Chapter 4, we adopted the 802.11 DCF as the MAC protocol of the wireless backhaul. It has been shown in [6] that such random access protocol, when applied in the wireless multi-hop backhaul network, results in serious unfairness problem, i.e. the MAPs that are hops away from the portal achieve extremely low throughput. Therefore, it may be better for the wireless backhaul in WMNs to adopt deterministic access control protocols such as TDMA. We can propose a joint association control and backhaul transmission scheduling scheme. In such a scheme, more backhaul transmission time slots can be allocated to the MAPs with more associated STAs and STAs can make better association decision as the MAPs' backhaul capacity are deterministic.

Jointly consider association control and backhaul routing. Congestion may occur at the access networks or the wireless backhaul. Association control can relief the access network congestion by controlling load distribution among neighbouring MAPs, but cannot help much with the backhaul congestion. In case of congestion at certain backhaul path, re-routing may be necessary to improve the backhaul capacity. However, changes in backhaul routing may trigger re-association. Therefore, association and routing should be jointly considered to maximize the end-to-end performance.

To further improve the reassociation performance, we can propose a novel access network beaconing scheme such that at the beginning of a Beacon Transmission Window (BTW), all STAs and MAP access interfaces switch to a common beaconing channel and the MAPs send beacons in their allocated Beacon Transmission Slot (BTS). At the end of a BTW, all nodes switch back to their originally associated channels. A STA can switch to the neighbouring channels to measure the interference when its associated channel is busy. With such a synchronized beaconing scheme, seamless handoff and real time network condition discovery are possible as STAs do not need to scan all the channels and wait for beacons for at least 5ms at each channel. In addition, beacon collision can be eliminated.

Besides channel assignment and association control, another powerful resource management tool is power control. There could be two types of power control for MAPs. One is the data packet power control that can reduce the inter-cell interference and increase the aggregate throughput, but it requires cooperation at the MAC protocol to avoid serious hidden node problem. The other is the beacon frame power control that enlarges or shrinks a MAP's cell by accordingly adjusting the beacon transmission power. The second one is preferred as it requires no additional modifications at the STAs or the protocols. Since we prefer more STAs to associate with the good-backhaul MAPs, it can be foreseen that the MAPs near to the portal would have larger cell range and higher beacon power. An algorithm needs to be derived for the optimal beacon transmission power control.

Compare the performance of distributed schemes and centralized schemes. For WMNs, the access network association control and the backhaul transmission control must be jointly considered. Based on different degree of centralization across layers, we can have 3 types of WMNs: 1) fully distributed network where STAs make their own association decisions based on local measurement and backhaul transmission is coordinated by distributed contention-based schemes; 2) half distributed network where the association decision is made locally by STAs while the backhaul transmission is coordinated by a central controller; 3) fully centralized network where association and transmission are optimized and fully centrally controlled. The first type of network is good at scalability and easy implementation, but suffers from poor performance, low capacity, and unfairness, due to the backhaul contention. The third type of network is optimal but may not be scalable since the entire network condition must be known. The second type of network is promising. With certain degree of backhaul capacity stability, STAs may locally make association decisions that are closer to the optimal. Besides pure heuristic metric-based association schemes, other distributed schemes need to be studied. For example we can apply the annealed Gibbs sampler technique to achieve optimal performance through distributed association control. However, this technique requires STAs keep changing their associations with certain probability until reaching convergence; we need to study the convergence speed and the impact on performance caused by the disrupted communication in the process of convergence.

Bibliography

[1] I. F. Akyildiz, X. Wang, and W. Wang, "Wireless mesh networks: a survey," *Computer Networks*, vol. 47, no. 4, pp. 445-487, 2005.

[2] I. F. Akyildiz, and X. Wang, "A survey on wireless mesh networks," *IEEE Communications Magazine* ,vol. 43, no. 9, pp. 23-30, 2005.

[3] P. Pathak and R. Dutta. "A Survey of Network Design Problems and Joint Design Approaches in Wireless Mesh Networks," *IEEE Commn. Surv. & Tuto.*, vol.13, no. 3, pp. 396-428, 2011.

[4] M. Heusse, F. Rousseau, G. Berger-Sabbatel, and A. Duda, "Performance anomaly of 802.11b," in *Proc. IEEE INFOCOM*, Apr. 2003, pp. 836-843.

[5] A. Kumar, E. Altman, D. Miorandi, and M. Goyal, "New insights from a fixed point analysis of single cell IEEE 802.11 WLANs," in *Proc. IEEE INFOCOM*, Mar. 2005. pp. 1550-1561.

[6] V. Gambiroza, B. Sadeghi and E. W. Knightly, "End-to-end performance and fairness in multihop wireless backhaul networks," in *Proc. ACM MobiCom*, Sep. 2004, pp. 287-301.

[7] 802.11-2012: IEEE Standard for Information technology - Telecommunications and information exchange between systems - Local and metropolitan area networks - Specific requirements - Part 11: Wireless LAN Medium Access Control (MAC) and Physical Layer (PHY) Specifications.

[8] 802.11s: IEEE Standard for Information Technology - Telecommunications and information exchange between systems - Local and metropolitan area networks -

Specific requirements - Part 11: Wireless LAN Medium Access Control (MAC) and Physical Layer (PHY) specifications Amendment: Mesh Networking.

[9] R. C. Carrano, L. C. S. Magalhães, D. C. Saade, and C. V. Albuquerque, "IEEE 802.11 s multihop MAC: A tutorial," *IEEE Commn. Surv. & Tuto.*, vol. 13, no. 1, pp. 52-67, 2011.

[10] G. R. Hiertz, D. Denteneer, S. Max, R. Taori, J. Cardona, L. Berlemann, and B. Walke, "IEEE 802.11 s: the WLAN mesh standard," *IEEE Wireless Communications*, vol. 17, no. 1, pp. 104-111, 2010.

[11] The ns-3 network simulator. [Online]. Available: http://www.nsnam.org/

[12] R. Jain, D. Chiu, and W. Hawe, "A quantitative measure of fairness and discrimination for resource allocation in shared computer systems", DEC Report, DEC-TR-301, Sep. 1984.

[13] H. Velayos, V. Aleo, and G. Karlsson, "Load balancing in overlapping wireless LAN cells," in *Proc. IEEE ICC*, Jun. 2004, pp. 3833-3836.

[14] A. J. Nicholson, Y. Chawathe, and M. Y. Chen, "Improved Access Point Selection," in *Proc. ACM MobiSys*, June 2006, pp. 233-245.

[15] A.P. Jardosh, K. Mittal, K. N. Ramachandran, E. M. Belding, and K. C. Almeroth, "IQU: practical queue based user association management for WLANs," in *Proc. 12th ACM MobiCom*, Sep. 2006, pp 158-169.

[16] B. Kauffmann, F. Baccelli, A. Chaintreau, V. Mhatre, K. Papagiannaki, and C. Diot, "Measurement-based self organization of interfering 802.11 wireless access networks," in *Proc. IEEE INFOCOM*, May 2007, pp.1451-1459.

[17] L. H. Yen, T. T. Yeh and K. H. Chi, "Load balancing in IEEE 802.11 networks," *IEEE Internet Computing*, vol. 13, no. 1, pp. 56-64, 2009.

[18] F. Xu, C. C. Tan, Q. Li, G. Yan, and J. Wu, "Designing a practical access point association protocol," in *Proc. IEEE INFOCOM*, Mar. 2010, pp. 1-9.

[19] S. Vasudevan, K. Papagiannaki, C. Diot, J. Kurose, and D. Towsley, "Facilitating access point selection in IEEE 802.11 wireless networks," in *Proc. ACM SIGCOMM conference on Internet Measurement*, Oct. 2005, pp. 293-298.

[20] T. Korakis, O. Ercetin, S. Krishnamurthy, L. Tassiulas, and S. Tripathi, "Link Quality based Association Mechanism in IEEE 802.11h compliant Wireless LANs," in *Workshop on Resource Allocation in Wireless Networks* (*RAWNET*), April 2005.

[21] M. Abusubaih, J. Gross, S. Wiethoelter, and A. Wolisz, "On access point selection in IEEE 802.11 wireless local area networks," in *Proc. 31st IEEE LCN*, Nov. 2006, pp. 879-886.

[22] H. Lee, S. Kim, O. Lee, S. Choi, and S.-J. Lee. "Available bandwidth-based association in IEEE 802.11 wireless LANs," in *Proc. 11th ACM MSWiM*, Oct. 2008, pp. 132-139.

[23] S. Keranidis, T. Korakis, I. Koutsopoulos, and L. Tassiulas, "Contention and traffic load-aware association in IEEE 802.11 WLANs: algorithms and implementation," in *Proc. IEEE WiOpt*, May 2011, pp. 334-341.

[24] A. Balachandran, P. Bahl, and G. M. Voelker, "Hot-spot congestion relief in public-area wireless networks," in *Proc. 4th IEEE Workshop on Mobile Computing Systems and Applications*, 2002, pp. 70-82.

[25] Y. Zhu, Q. Ma, C. Bisdikian, and C. Ying, "User-centric management of wireless LANs," *IEEE Trans. on Network and Service Management*, vol. 8, no. 3, pp. 165-175, 2011.

[26] Y. Bejerano and R. S. Bhatia, “MiFi: a framework for fairness and QoS assurance for current IEEE 802.11 networks with multiple access points,” *IEEE/ACM Trans. on Networking*, vol. 14, no. 4, pp. 849-862, Aug. 2006.

[27] M. Abusubaih and A. Wolisz. “An optimal station association policy for multi-rate IEEE 802.11 wireless LANs,” in *Proc. ACM MSWiM*, Oct. 2007, pp. 117-123.

[28] P. Bahl, M. T. Hajiaghayi, K. Jain, V. S. Mirrokni, L. Qiu, and A. Saberi, “Cell breathing in wireless LANs: algorithms and evaluation,” *IEEE Trans. Mobile Computing*, vol. 6, no. 2, pp. 164-178, Feb. 2007.

[29] Y. Bejerano and S.-J. Han, “Cell breathing techniques for load balancing in wireless LANs,” *IEEE Trans. Mobile Comput.*, vol. 8, no. 6, pp. 735-749, Jun. 2009.

[30] H. Ko, J. Shin, D. Kwak, and C. Kim, “A joint approach to bandwidth allocation and AP-client association for WLANs,” in *Proc. 35th IEEE LCN*, Oct. 2010, pp. 576-581.

[31] W. Li, Y. Cui, X. Cheng, M. A. Al-Rodhaan, and A. Al-Dhelaan, "Achieving proportional fairness via AP power control in multi-rate WLANs," *IEEE Trans. Wireless Com.*, vol.10, no.11, pp.3784-3792, Nov. 2011.

[32] Y. Bejerano, S.-J. Han, and L. Li, “Fairness and load balancing in wireless LANs using association control,” in *Proc. 10th ACM MobiCom*, Sep. 2004, pp. 315-329.

[33] Kumar and V. Kumar, “Optimal association of stations and APs in an IEEE 802.11 WLAN,” in *Proc. India NCC*, Jan. 2005, pp. 1-5.

[34] L. Li, M. Pal, and Y. R. Yang, “Proportional fairness in multi-rate wireless LANs,” in *Proc. IEEE INFOCOM*, Apr. 2008, pp. 1004-1012.

[35] W. Li, S. Wang, Y. Cui, X. Cheng, R. Xin, M. A. Al-Rodhaan, and A. Al-Dhelaan, "AP association for proportional fairness in multirate WLANs," *IEEE/ACM Trans. on Networking* , vol. 22, no. 1, pp. 191-202, Feb. 2014.

[36] L. Luo, H. Liu, D. Rarchaudhuri, M. Wu and D. Li, "End-to-end performance aware association in wireless municipal mesh networks," in *Proc. IEEE Globecom Workshops*, Nov. 2007, pp. 1-6.

[37] L. Luo, D. Raychaudhuri, H. Liu, M. Wu, and D. Li, "Improving end-to-end performance of wireless mesh networks through smart association," in *Proc. IEEE WCNC 2008*, Mar. 2008, pp.2087-2092.

[38] G. Athanasiou, T. Korakis, O. Ercetin, and L. Tassiulas, "A cross-layer framework for association control in wireless mesh networks," *IEEE Trans. on Mobile Computing*, vol.8, no.1, pp.65-80, Jan. 2009.

[39] S. Makhlouf, Y. Chen, S. Emeott, and M. Baker, "A network-assisted association scheme for 802.11-based mesh networks," in *Proc. IEEE WCNC 2008*, Mar. 2008, pp. 1339-1343.

[40] H. Wang, W. Wong, W. Soh, and M. Motani, "Dynamic association in IEEE 802.11 based wireless mesh networks," in *Proc. 6th IEEE ISWCS*, Sep. 2009, pp. 81-85.

[41] Y. He, D. Perkins, and S. Velaga, "Design and implementation of class: a cross-layer association scheme for wireless mesh networks," *Ad Hoc Networks*, vol. 9, no. 8, pp. 1476-1488, 2011.

[42] L. Luo, D. Raychaudhuri, H. Liu, M. Wu, and D. Li, "Joint association, routing and bandwidth allocation for wireless mesh networks," in *Proc. IEEE GLOBECOM*, Nov. 2008, pp. 1-6.

[43] Y. Cui, T. Ma, J. Liu, and S. Das, "Load-balanced AP association in multi-hop wireless mesh networks," *The Journal of Supercomputing*, vol. 65, no. 1, pp. 383-409, 2013.

[44] M. Lacage and T. R. Henderson, "Yet another network simulator," in *Proc. ACM WNS2 '06: workshop on ns-2: the IP network simulator*, 2006.

[45] J. Robinson and E. W. Knightly, “A performance study of deployment factors in wmns,” in *Proc. 26th IEEE INFOCOM*, May 2007, pp. 2054-2062.

[46] W. Arbaugh, A. Mishra, and M. Shin, “An empirical analysis of the IEEE 802.11 MAC layer handoff process,” *ACM SIGCOMM Computer Communication Review*, vol. 33, no. 2, pp. 93-102, Apr. 2003.

[47] S. Pack, J. Choi, T. Kwon, and Y. Choi, “Fast-handoff support in IEEE 802.11 wireless networks,” *IEEE Communications Surveys and Tutorials*, vol. 9, no. 1-4, pp. 2-12, 2007.

[48] V. Mhatre and K. Papagiannaki, “Using smart triggers for improved user performance in 802.11 wireless networks,” in *Proc. ACM MobiSys*, Jun. 2006, pp. 246-259.

[49] I. Ramani and S. Savage, “SyncScan: practical fast handoff 802.11 infrastructure networks,” in *Proc. 24th IEEE INFOCOM*, Mar. 2005, pp. 675-684.

[50] M. Kim, Z. Liu, S. Parthasarathy, D. Pendarakis, and H. Yang, “Association control in mobile wireless networks,” in *Proc. of 27th IEEE INFOCOM*, Apr. 2008, pp. 1256-1264.

[51] K. Ramachandran, E. Belding, K. Almeroth, and M. Buddhikot, “Interference-aware channel assignment in multi-radio wireless mesh networks,” in *Proc. of 25th IEEE INFOCOM*, 2006, pp. 1-12.

[52] G. Athanasiou, T. Korakis and L. Tassiulas, “Cooperative handoff in wireless networks”, in *Proc. IEEE PIMRC*, Sep. 2008, pp. 1-6.

[53] R. Raghavendra, E. M. Belding, K. Papagiannaki, and K. C. Almeroth, “Unwanted link layer traffic in large IEEE 802.11 wireless networks,” *IEEE Trans. on Mobile Computing*, vol. 9, no. 9, pp. 1212-1225, 2010.

[54] V. Brik, A. Mishra, and S. Banerjee, “Eliminating handoff latencies in 802.11 wlans using multiple radios: applications, experience, and evaluation,” in *Proc. 5th ACM SIGCOMM conference on Internet Measurement*, Oct. 2005.

[55] J. Ok, P. Morales, A. Darmawan, and H. Morikawa, (2007, April). “Using shared beacon channel for fast handoff in ieee 802.11 wireless networks,” in *Proc. IEEE VTC2007-Spring*, Apr. 2007, pp. 849-853.

[56] C. C. Tseng, K. H. Chi, M. D. Hsieh, and H. H. Chang, “Location-based fast handoff for 802.11 networks,” *IEEE Communications Letters*, vol. 9, no. 4, pp. 304-306, 2005.

[57] B. Radunovic and J. Le Boudec, “Rate performance objectives of multihop wireless networks,” *IEEE Trans. Mob. Comput*. vol. 3, no. 4, pp. 334-349, Oct-Dec 2004.

[58] E. Rodrigues and F. Casadevall, “Control of the trade-off between resource efficiency and user fairness in wireless networks using utility-based adaptive resource allocation,” *IEEE Communications Magazine*, vol. 49, no. 9, pp. 90-98, Sep. 2011.

[59] H. Gong, K. Nahm, and J. Kim, “Access point selection tradeoff for IEEE 802.11 wireless mesh network,” in *Proc. IEEE CCNC*, 2007, pp. 818-822.

[60] A. V. Babu and L. Jacob, “Performance analysis of IEEE 802.11 multirate WLANs: time based fairness vs throughput based fairness,” in *Proc. IEEE Wireless Netw., Commun. Mobile Comput.*, Jun. 2005, pp. 203-208.

[61] D. Bertsekas and R. Gallager, Data Networks. Upper Saddle River, NJ, USA: Prentice-Hall, 1992.

[62] F. P. Kelly, “Charging and rate control for elastic traffic,” *Eur. Trans. Telecommun.*, vol. 8, no. 1, pp. 33-37, 1997.

[63] C. Bron and J. Kerbosch, "Algorithm 457: finding all cliques of an undirected graph," *Commun. of the ACM*, vol. 16, no. 9, pp. 575-577, 1973.

[64] M. R. Garey and D. S. Johnson, “Computers and intractability: a guide to the theory of np-completeness,” W.H. Freeman Publishing Company, 1979.

[65] T. Bu, L. E. Li, and R. Ramjee, “Generalized proportional fair scheduling in third generation wireless data network,” in *Proc. IEEE INFOCOM*, Apr. 2006, pp. 1-12.

[66] D. B. Shmoys and E. Tardos, “An approximation algorithm for the generalized assignment problem,” *Math. Program.*, vol. 62, no. 3, pp. 461-474, Dec. 1993.

[67] D. P. Williamson, and D. B. Shmoys, The Design of Approximation Algorithms, Cambridge University Press, New York, 2011.

[68] Cisco Wireless Mesh Access Points, Design and Deployment Guide Release7-5 http://www.cisco.com/en/US/docs/wireless/technology/mesh/7.5/design/guide/mesh75.html

[69] J. Mo and J. Walrand, “Fair end-to-end window-based congestion control,” *IEEE/ACM Trans. Networking*, vol. 8, no. 5, pp. 556-567, Oct. 2000.

[70] S. Chieochan, E. Hossain, and J. Diamond, “Channel assignment schemes for infrastructure-based 802.11 WLANs: a survey,” *IEEE Communications Surveys & Tutorials*, vol. 12, no. 1, pp. 124-136, 2010.

[71] M. Achanta, “Method and Apparatus for Least Congested Channel Scan for Wireless Access Points,” US Patent No. 20060072602, Apr. 2006.

[72] P. Mahonen, J. Riihijarvi, and M. Petrova, “Automatic channel allocation for small wireless local area networks using graph colouring algorithm approach,” in *Proc. IEEE PIMRC*, Sept. 2004, pp. 536-539.

[73] A. Mishra, V. Brik, S. Banerjee, A. Srinivasan, and W. Arbaugh, "A client-driven approach for channel management in wireless LANs," in *Proc. IEEE INFOCOM*, Apr. 2006, pp. 1-12.

[74] I. Broustis, K. Papagiannaki, S. V. Krishnamurthy, M. Faloutsos, and V. P. Mhatre, "Measurement-driven guidelines for 802.11 WLAN design," *IEEE/ACM Trans. on Networking*, vol. 18, no. 3, pp. 722-735, June 2010.

[75] P. Pathak and Rudra Dutta. "A survey of network design problems and joint design approaches in wireless mesh networks," *IEEE Communications Surveys & Tutorials*, vol. 13, no. 3, pp. 396-428, 2011.

List of Publications

Journal Papers:

1. J. Yu, W.-C. Wong, “Optimal association in wireless mesh networks,” *IEEE Trans. on Vehicular Technology*.
2. J. Yu, W.-C. Wong, “A network resource management framework for wireless mesh networks,” *IEEE Trans. on Mobile Computing*. (submitted)

Conference Papers:

1. J. Yu, W.-C. Wong, "Network resource aware association control in wireless mesh networks," in *Proc. IEEE ICCS*, Nov. 2012, pp.368-372.
2. J. Yu, W.-C. Wong, "Mobility-aware reassociation control in wireless mesh networks," in *Proc. 24th IEEE PIMRC*, Sep. 2013, pp. 3140-3144.
3. J. Yu, W.-C. Wong, “Utility fairness via association control in wireless mesh networks,” in *Proc. IEEE ICCS*, Nov. 2014, pp. 533-537.